This is to certify that the

dissertation entitled

Prostaglandin E2-induced Ca++ mobilization in rabbit cortical collecting tubule cells and swiss 3T3 cells

induced by Prostagla. din E2 in Rabbit

presented by

Ping Shi

has been accepted towards fulfillment
of the requirements for

Ph.D degree in Biochemistry

William L. Smith
Major professor

July, 26, 1993
Date

Ca^{++} MOBILIZATION INDUCED BY PROSTAGLANDIN E_2 IN RABBIT CORTICAL COLLECTING TUBULE CELLS AND SWISS 3T3 CELLS

By

Ping Shi

A DISSERTATION

Submitted to
Michigan State University
in partial fulfillment of the requirements
for the degree of

DOCTOR OF PHILOSOPHY

Department of Biochemistry

1993

ABSTRACTS

Ca^{++} MOBILIZATION INDUCED BY PROSTAGLANDIN E_2 IN RABBIT CORTICAL COLLECTING TUBULE CELLS AND SWISS 3T3 CELLS

By

Ping Shi

Prostaglandin E_2 (PGE_2) produces a broad range of biological actions in diverse tissues through its binding to specific receptors on plasma membranes. PGE receptors are pharmacologically subdivided into three subtypes, EP1, EP2, and EP3, which are suggested to be coupled to different signal transduction pathways. PGE_2 has been shown to mobilize intracellular Ca^{++} through activation of phospholipase C (PLC) in a number of tissues and cells which possess EP1 receptors. Reported here are studies of the effect of PGE_2 on Ca^{++} mobilization in rabbit cortical collecting tubule (RCCT) cells and in Swiss 3T3 cells. Also reported is our attempt to clone a cDNA for the PGE receptor involved in Ca^{++} mobilization using the *Xenopus* oocyte expression system.

PGE_2 plays an important physiological role in transport activities in mammalian kidneys. Our study showed that PGE_2 mobilizes intracellular Ca^{++} in RCCT cells as determined by digital fluorescence imaging. Ca^{++} mobilization by RCCT cells occurs in response to the naturally occurring 15-S-PGE_2 but not 15-R-PGE_2. Moreover, the effect of PGE_2 to mobilize Ca^{++}

is partially desensitized by PGE_2, sulprostone, and $PGF_{2\alpha}$, but not by PGD_2. AH6809, an EP1 PGE receptor antagonist was found to inhibit PGE_2-induced Ca^{++} mobilization. These results suggest that PGE_2 induces Ca^{++} mobilization through an EP1-like PGE receptor. Using digital fluorescence imaging in combination with cell-specific staining, we have found that PGE_2-induced Ca^{++} mobilization occurs in principal cells as well as intercalated cells, suggesting possible roles for PGE_2 in H^+ and/or anion transport in intercalated cells, in addition to their demonstrated roles in water reabsorption and Na^+ flux in principal cells.

In Swiss 3T3 cells where PGE_2 was known to have a synergistic effect on cell proliferation in the presence of low concentrations of insulin, we found that PGE_2 stimulates phosphatidylinositol hydrolysis and intracellular Ca^{++} mobilization through the same receptor that interacts with $PGF_{2\alpha}$. Expression cloning of a cDNA for the PGE receptor involved in Ca^{++} mobilization in 3T3 cells led to the isolation of a protein named GING. A search of GenBank database showed GING is a member of the 14-3-3 protein family. Expression of GING in COS-1 cells potentiates Ca^{++} mobilization occurring in response to PGE_2, but does not result in a corresponding IPs formation. It is not clear if the potentiating effect of GING on Ca^{++} mobilization in oocytes and COS-1 cells has any physiological significance or is an artifact involving overexpression of GING *in vitro*.

ACKNOWLEDGEMENTS

I thank Dr. William L. Smith for his continued professional guidance, his support and his patience during my graduate training.

I thank the members of my thesis committee, Drs. Steve Triezenberg, Shelage Ferguson-Miller, Zachary Burton, and John Linz, for their scientific insight and their encouragement.

Special thanks go to Drs. Dave L. DeWitt, Lois Arend, and Maria Burnadowska-Hledin, to whom I am much indebted for their generous help and coaching during the early years of the journey. It also goes to Dr. Gilad Rimon for his comradeship and friendship when working on the arduous cloning project, whose humor brightened up each of those days.

I thank all the members of our joint lab, whose effort made the lab a dynamic and stimulating place. Among them I thank particularly Teru Shimokawa, Dave McCoy, Dave LeVier, Odette M. S. Laneuville, and Babara Olsen.

I thank people in the department whose technical assistance was indispensable. Among them, John Sell for his time and patience to help me with the ACAS cytometer; Don Herrington for his continued assistance to animal handling.

Above all, I thank those of my special Chinese and American friends, who helped to bring out the best in me, who

sparkled my life along the years (especially during the darkest part of the "tunnel"), who made my experience here a worthwhile one, and without whom I would not have made it.

TABLE OF CONTENTS

LIST OF TABLES

LIST OF FIGURES

ABBREVIATIONS

Abbreviations are: PG, prostaglandin; AVP, arginine vasoppressin; cAMP, adenosine 3′,5′-cyclic monophosphate; RCCT, rabbit cortical collecting tubule; PIP_2, phosphotidylinositol 4,5-phosphate; IP_3, inositol 1,4,5-trisphosphate; IPs, inositol phosphates; PC, phosphatidylcholine; PI, phosphatidylinositol; PE, phosphatidylethanolamine; DAG, diacylglycerol; PLC, phospholipase C; PKC, protein kinase C, TPA, 12-O-tetradecanoylphorbol-13-acetate; PTX, pertussis toxin; ER, endoplasmic reticulum; MT, mitochondria; FITC, fluorescein isothiocyanate; FBP, flurbiprofen; DMEM, Dulbecco's modified Eagle medium; FCS, fetal calf serum; SSS, simplified saline solution; MBS, modified Barth's solution.

CHAPTER ONE

LITERATURE REVIEW

The focus of this review is first, on aspects of the biochemistry of prostaglandins and their physiological actions in the kidney; and second, on the rapidly-expanding family of G-protein coupled receptors and their receptor-mediated signal transduction pathways, especially the inositol trisphosphate(IP_3) /Ca^{++} pathway. The concept has been well developed that prostaglandins function as local hormones to elicit their effect through specific cell surface receptors. I will describe how the collecting tubule of kidney has been used as a model system to study the inhibitory action of prostaglandin E_2 (PGE_2) on water reabsorption occurring in response to arginine vasopressin (AVP). Studies in this system have led to the conclusion that there are two G protein-coupled receptors involved in mediating the action of PGE_2. Since a large body of biochemical evidence indicates that prostaglandin receptors belong to the G protein-coupled receptor family, an overview of the transmembrane signaling system involving these receptors will be given, with an emphasis on the phospholipase C signaling mechanism involving inositol trisphosphate and Ca^{++}.

Prostaglandins and Their Physiological Actions in the Kidney

Prostaglandin Biochemistry. Prostaglandins (PG) are a group of oxygenated derivatives of 20-carbon polyunsaturated fatty acids. These compounds and thromboxane, which are products resulting from the action of prostaglandin endoperoxide H (PGH) synthase (Fig.1), are collectively known as prostanoids. All the prostaglandins contain a cyclopentane ring, with differences in the oxygen-containing substituents giving rise to PGD_2, PGE_2, PGF_{2a}, and PGI_2. The numeric subscript indicates the number of carbon-carbon double bonds present in the molecules (1).

As shown in Fig.1, the prostaglandin biosynthesis occurs in three steps. The first step is the release of the precursor arachidonic acid from glycerophospholipids by phospholipases. This is an important regulatory step since the concentration of free arachidonic acid in the cell is too low (<1 μM) for prostaglandin formation to occur, unless it increases in response to hormonal stimuli (2-4). Arachidonic acid is mainly released from phosphatidylcholine (PC) and phosphatidylethanolamine (PE) via the action of phospholipase A_2, although some arachidonate is also derived from phosphatidylinositol (PI) by the sequential actions of

Figure 1. The biosynthetic pathway of prostaglandins.

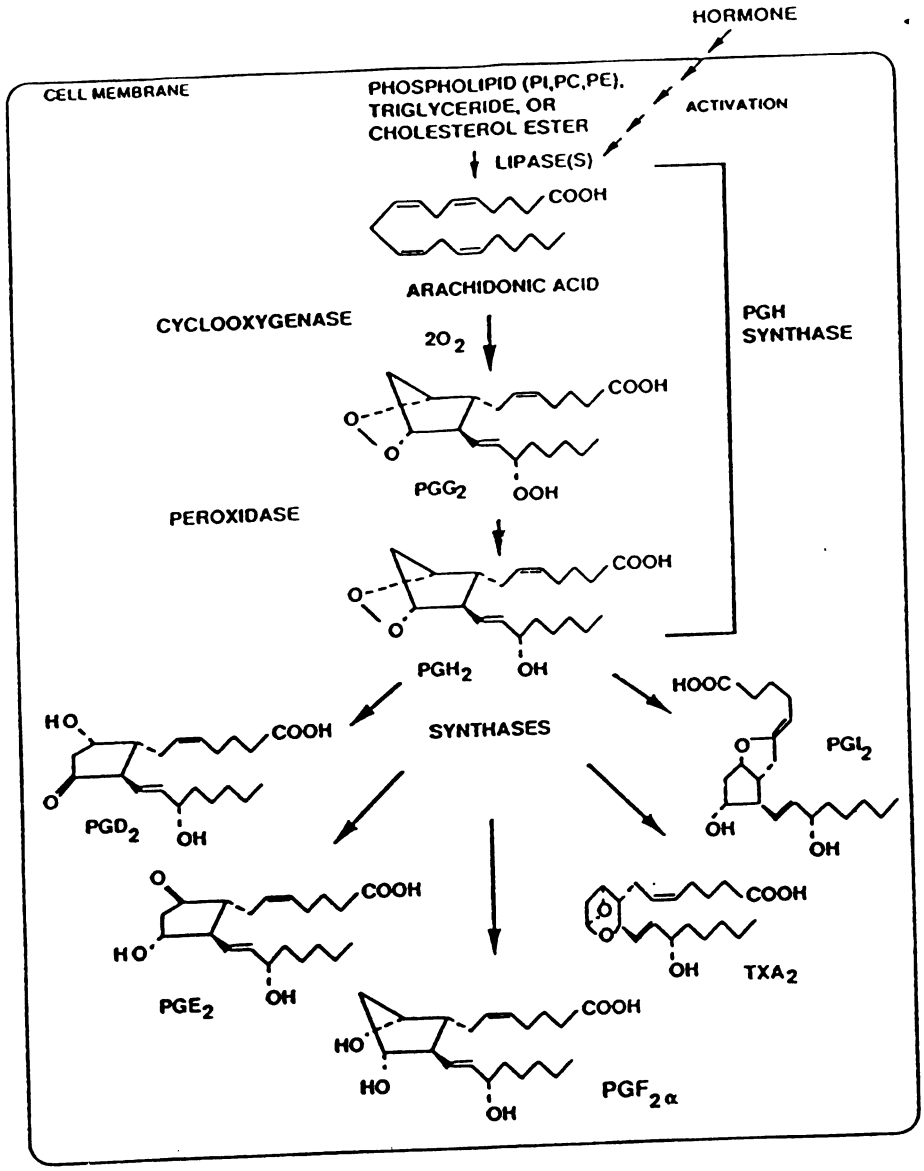
HORMONE
CELL MEMBRANE
PHOSPHOLIPID (PI,PC,PE),
TRIGLYCERIDE, OR
CHOLESTEROL ESTER
ACTIVATION
LIPASE(S)
COOH
ARACHIDONIC ACID
CYCLOOXYGENASE
$2O_2$
PGH
SYNTHASE
COOH
O
O
PGG_2
OOH
PEROXIDASE
COOH
O
O
PGH_2
OH
HOOC
HO
COOH
SYNTHASES
O
PGI_2
O
PGD_2
OH
OH
OH
O
COOH
HO
COOH
O
O
OH
TXA_2
PGE_2
OH
COOH
HO
HO
OH
$PGF_{2\alpha}$

phospholipase C (PLC) and diacylglycerol lipase (5).

The second step in prostanoid biosynthesis is the oxygenation of free arachidonic acid by PGH synthase. PGH synthase is a membrane-bound protein which is associated with the endoplasmic membrane in most cells (6). This enzyme has two catalytic activities: (a) a cyclooxygenase activity which catalyzes a bis-oxygenation reaction, forming the 15-hydroperoxy-prostaglandin endoperoxide PGG_2; and (b) a hydroperoxidase activity which reduces the 15-hydroperoxy moiety of PGG_2 to form PGH_2 (7). Both activities require heme (5). An important characteristic of the cyclooxyenase activity is that it is specifically inhibited by aspirin and a group of related non-steroidal anti-inflammatory drugs including flurbiprofen (FBP) and indomethacin (8).

The third step in prostanoid synthesis is the conversion of PGH_2 to a biologically active endproduct such as PGE_2, $PGF_{2\alpha}$ PGD_2, PGI_2 or thromboxane A_2 (TxA_2). Prostaglandin synthesis is cell-specific. A given cell can only form one particular endproduct (9). The formation of PGD_2 is catalyzed by PGH-PGD isomerase (10). The formation of PGE_2 requires reduced glutathione and is catalyzed by PGH-PGE isomerase (11). In contrast to the isomeration, $PGF_{2\alpha}$ synthesis requires a two-electron reduction of PGH_2 via PGF reductase (12). Information about these enzymes is still limited, although their respective activities have been partially purified. PGI_2 and TxA_2 synthase have been purified to homogeneity (13,14), both

enzymes being membrane-bound hemoproteins of the cytochrome P-450 class.

The concentration of prostanoids in plasma is very low (< 10^{-9} M) (15). Prostaglandins are degraded into inactive forms during a single pass through the circulation (16). On the other hand, prostanoid synthesis is not restricted to a central endocrine organ, but rather occurs in most organs and tissues (9,17). Therefore, the concept has been developed that prostaglandins are local hormones, which act on parent cells or neighboring cells in an autocrine or paracrine fashion, respectively, to coordinate the actions of circulating hormones that stimulate prostaglandin synthesis (7).

Physiological Actions of Prostaglandins in the Kidney. Prostaglandins are involved in the regulation of a wide variety of cellular activities including metabolism, secretion, muscle contraction, and cell differentiation and proliferation (18). One of the model systems in which the role of prostaglandins has been studied in detail is the process of water and sodium transport in collecting tubule cells of mammalian kidney (19).

Fig.2 is a diagram of a nephron. The final segment of the tubule, the collecting tubule, is the critical site where water and sodium reabsorption are regulated. By immunostaining to localize the PGH synthase, and by measuring prostaglandin synthesis in different tubule segments (20,21), it has been found that there are seven different cell types that are

Figure 2. The diagram of a mammalian nephron. (G. glomerulus; EA, efferent artirioles; AA, afferent arterioles; IA, intralobular artery; PCT, proximal convoluted tubule; PR, pars recta; DTL, descending thin limb; ATL, ascending thin limb; MTAL, medullary thick ascending limb; CTAL, cortical thick ascending limb; DCT, distal convoluted tubule; CCT, cortical collecting tubule; PCT, papillary collecting tubule; IC, interstitial cells). The darkened areas represent sites of prostaglandin synthesis.

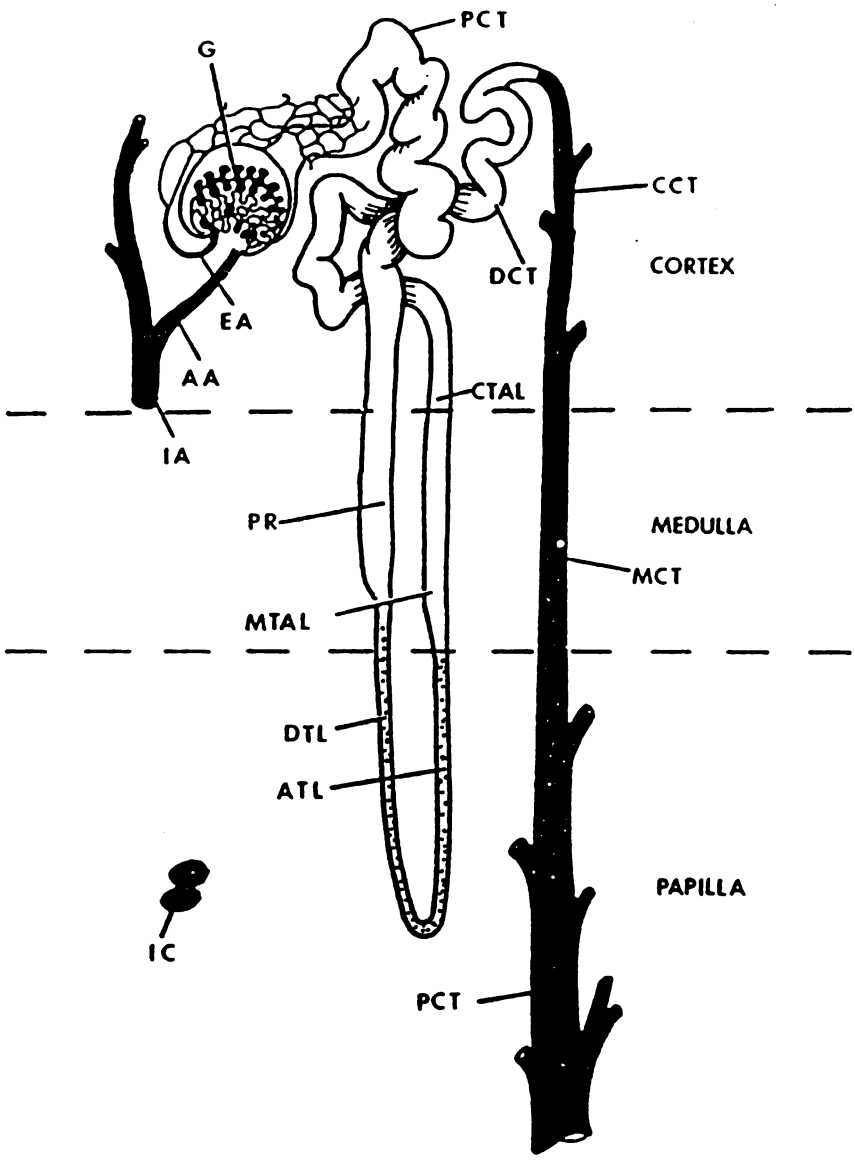
PCT
G
CCT
CORTEX
DCT
EA
AA
CTAL
IA
PR
MEDULLA
MCT
MTAL
DTL
ATL
PAPILLA
IC
PCT

capable of prostaglandin synthesis (darkened areas in Fig.2). Among them, the epithelial cells of the collecting tubule, especially the collecting tubule, have the greatest capacity to form prostaglandins. Moreover, it was shown that PGE_2 was the major form of prostaglandin synthesized by dissected rabbit cortical collecting tubules (22,23).

Grantham and Orloff were the first to demonstrate the effect of PGE on tubular function using perfused microdissected cortical collecting tubules (24). They observed that a low concentration of PGE_1 inhibited water reabsorption stimulated by the circulating hormone arginine vasopressin (AVP), while at higher concentrations, PGE_1, by itself, stimulated water reabsorption. When cAMP or forskolin which stimulates cAMP formation was used to pretreat the tubules, no inhibitory effect of PGE_1 on water flow was seen (24). Since cAMP is believed to be the second messenger that mediates water reabsorption (25), it was postulated that at low concentrations, PGE_1 inhibited AVP-stimulated cAMP accumulation, and at higher concentrations PGE_1 stimulated cAMP formation. This hypothesis was later substantiated by Sonnenberg and Smith (26) who studied the inhibitory regulation by PGE_2 of AVP-induced cAMP formation in immunodissected rabbit cortical collecting tubule (RCCT) cells. They showed that at low concentrations ($\leq 10^{-8}$ M), PGE_2 inhibits AVP-induced cAMP accumulation in pure populations of RCCT cells. The inhibitory effect was blocked by pretreatment

of cells with pertussis toxin, indicating the involvement of the inhibitory guanine nucleotide-binding regulatory protein (G_i). Moreover, PGE_2 was found to inhibit the AVP-stimulated adenylate cyclase activity directly in membranes isolated from RCCT cells. At higher concentrations (above 10^{-7} M) PGE_2 stimulates cAMP synthesis, presumably by activating adenylate cyclase via the stimulatory guanine nucleotide-binding regulatory protein (G_s). Evidence was also obtained that the stimulatory and inhibitory responses are mediated by two subtypes of PGE receptors coupled respectively to G_s and G_i (27). Two binding activities were detected in membranes of isolated cells. The one with high affinity (K_d=10 nM) only existed in fresh cells but disappeared when RCCT cells were cultured for several days. Curiously, the K_d of the higher affinity receptor was decreased in the presence of GTP (although for most G protein coupled receptors K_d values are increased by GTP). The lower affinity PGE receptor could be detected in RCCT cells cultured for several days (27); the K_d value for binding to this receptor was increased in the presence of GTP analog. The dual effects of PGE_2 on cAMP formation are pharmacologically distinct, since sulprostone, a PGE_2 analog, is equipotent to PGE_2 in its inhibitory effect, but fails to stimulate cAMP formation (26). These results obtained with isolated collecting tubule cells demonstrated that the inhibitory and stimulatory effects of PGE_2 on cAMP formation are mediated by two different PGE-specific receptors

that are functionally coupled to G_i and G_s, respectively. The results obtained with RCCT cells agree with the observations Grantham and Orloff made on microdissected collecting tubules.

In addition to cAMP as the major mediator of water reabsorption, Breyer et al. (28) observed with perfused microdissected tubules that PGE_2 releases Ca^{++} from intracellular stores, suggesting that PGE_2 might activate a phospholipase C pathway, resulting in activation of protein kinase C (PKC) (as described below). Indeed, they found that staurosporine, an inhibitor of PKC, relieved the inhibitory effect of PGE_2 on AVP-stimulated water flow (28). Other studies have also indicated that activation of PKC down-regulates AVP-induced cAMP accumulation in cultured rabbit collecting tubule cells (29). Furthermore, when collecting tubules were pretreated with phorbol ester or diacylglycerol that activate PKC, water flow stimulated by both AVP and cAMP analogs was inhibited (30); these findings suggest that activation of PKC can inhibit water flow at a site distal to cAMP accumulation. When collecting tubules were pretreated with PGE_2, results were obtained which were similar to those obtained with phorbol ester or diacylglycerol treatments (28). Therefore, the PGE_2-induced activation of phospholipase C pathway leading to activation of PKC can be another mechanism by which PGE_2 inhibits AVP and cAMP-induced water flow.

Classification of Prostaglandin Receptors. Like other

hormones and growth factors, prostaglandins elicit their effects by interacting with specific cell surface receptors. Coleman et al.(31) developed a system for the classification of prostanoid receptors, by comparing the rank order of potency of agonists, and the affinities of receptor-blocking drugs (antagonists) on smooth muscle preparations. They found evidence for five major types of prostanoid receptors for PGD_2, PGE_2, PGF_{2a}, PGI_2 and TxA_2, designated as DP, EP, FP, IP and TP receptors, respectively. For PGE_2, they proposed three subtypes of receptors, which are defined as EP1, EP2, and EP3, based on their coupling to different signal transduction pathways and on their pharmacological profiles. EP1 receptors are coupled to the inositol trisphosphate/diacylglycerol pathway to mobilize intracellular Ca^{++} and to activate PKC. Its selective agonists include sulprostone and 17-phenyl-ω-trinor-PGE_2; its selective antagonists include SC19220 and AH6809. EP2 receptors are coupled to adenylate cyclase to stimulate cAMP formation. Butaprost is a selective agonist. EP3 receptors are coupled to adenylate cyclase to inhibit the cAMP formation, but may also be coupled to the same pathway as EP1 receptors. EP3 selective agonists include sulprostone, enprostil, GR63799 and MB28767. In smooth muscle preparations, the EP1 receptors mediate muscle contraction, while the EP2 receptors mediate muscle relaxation. A cDNA for an EP3 receptor has been isolated recently from a mouse lung cDNA library. This EP3 receptor cDNA has an open reading frame

encoding 365 amino acid residues (32). As expected, sequence analysis indicates that this receptor belongs to the family of receptors which mediate their actions via G proteins. The *in vitro* expression of the cDNA encoding the EP1 receptor demonstrated that it is solely coupled to the inhibition of cAMP accumulation. Northern blot analysis showed the tissue most highly expressing EP3 mRNA is kidney, in which PGE_2 exerts an inhibitory effect on water reabsoption and sodium reabsorption. Using this cDNA as the probe, a EP2 receptor cDNA was then isolated (33) from a mouse lung cDNA library, encoding a peptide of 513 amino acids. Within the transmembrane domains, EP2 receptor is 36.2% identical to that of the EP3 receptor. In contrast to EP3, EP2 is only marginally expressed in the kidney.

The Family of G Protein-coupled Seven-Transmembrane-Segments Receptors

Transmembrane Signaling System. A transmembrane signaling system which transduces the external stimuli into intracellular signals is very important for intercellular communication in multicellular organisms. Extensive studies in this field since 1960 revealed that one such system consists of three distinct components associated with the plasma membrane: (a) cell surface receptors that recognize and interact with extracellular signals such as light, odorants, hormones (peptide or autacoid), and neurotransmitters (34); (b) a guanine nucleotide-binding regulatory protein, or G protein that is coupled both *p1346Xreceptand effector (35); and (c) effector enzymes exposed to the cytoplasmic surface including adenylate cyclase which generates the second messenger cAMP (36), phospholipase C (PLC) which forms inositol trisphosphate (IP_3) and diacylglycerol (DAG) (37), visual cGMP phosphodiesterase (38) and ion channels (39). To date about 90 kinds of pharmacologically and/or molecularly distinct receptors have been identified as belonging to the family of G protein-coupled receptors (40). The existence of such a transmembrane signaling system makes it possible for an individual cell to adjust its cellular activities to changes

of the extracellular environment, which is essential for a multicellular organism to coordinate and integrate the functions of the various cells it is composed of.

Role of G proteins. G proteins serve as transducers between receptors and effectors. G proteins are so named because they bind and hydrolyze GTP (35). The first evidence for this came from the work of Rodbell who observed that GTP is required for hormonal activation of adenylate cyclase in isolated plasma membranes (41). This discovery led to the purification and eventually the cloning of the first G protein, the adenylate cyclase-stimulatory G protein (G_s) by Gilman et al.(42,43).

The mechanism of G protein signaling is complicated. All G proteins are trimers consisting of three tightly associated subunits: α, β, and γ (1:1:1). Upon interaction with an agonist-occupied receptor, a conformational change in the G protein occurs, which results in the exchange of bound GDP for GTP by the α-subunit. This GTP-bound α-subunit subsequently dissociates from the $\beta\gamma$ dimer, acting as the active form that interacts with and stimulates effector molecules. Bound GTP is slowly hydrolyzed to GDP by the GTPase activity associated with the α-subunit. The resulting α-GDP complex then reassociates with the $\beta\gamma$-subunits to complete the "G protein cycle". The fact that one receptor can activate many G protein molecules and that one activated α-subunit (i.e. α^*-GTP) can stimulate many effector molecules leads to amplification of

the initial signal (35).

Differences in the primary structure of α-subunits distinguish the various G proteins. Among them are G_s, which stimulates adenylate cyclase; G_i, which is involved in inhibiting adenylate cyclase and stimulating ion channels; G_t, the visual G protein which activates cGMP phosphodiesterase; G_0, which stimulates ion channels; and G_p, which activates phospholipases (39). G protein α-subunits can be substrates for ADP-ribosylation by bacterial toxins such as cholera toxin (for G_s) or pertussis toxin (for G_i and G_o). ADP-ribosylation of G_s permanently activates this protein, whereas ADP-ribosylation of G_i or G_o prevents its activation (35).

The Structure of G Protein-coupled Receptors. The first purification of a G protein-coupled hormone receptor, that of the β-adrenergic receptor, was achieved by Lefkowitz et al. in 1981 (44), and subsequent cloning of its gene and cDNA were reported in 1986 (45). Since then, many receptors of this family have been cloned, largely due to the introduction and improvements of expression cloning techniques (46). To date, over 150 receptors have been isolated and identified.

Sequence analysis of these receptors has revealed that they all share sequence homology, and they all have the topography of seven membrane spanning regions, represented by seven stretches of 20-28 highly hydrophobic amino acids (34). This topography is very similar to that of bacterial

rhodopsin, a purple membrane protein of *Halobacterium halobium*, for which the presence of seven α-helical domains spanning the lipid bilayer has been observed by electron microscopy (47). Based on the hydrophobicity profiles and the analogy to bacteria rhodopsin, a model (Fig.3) was proposed by Dixon and Lefkowitz for the orientation of the β-adrenergic receptor within the membrane (45). This unique structure of membrane spanning G protein-coupled receptors reflects their role in transmembrane signaling, which involves interacting with the extracellular stimuli and with a G protein located on the cytoplasmic side of the plasma membrane.

When comparing sequences of receptors within the G protein-coupled receptor family, it is recognized that the transmembrane regions are the most conserved, while the N- and C-terminal regions and the cytoplasmic loop connecting transmembrane segments V and VI are quite divergent (48). By constructing chimeric molecules comprised of portions of the α- and β- adrenergic receptors, it was found that G protein coupling is interchangeable when the intracellular cytoplasmic loop between transmembrane domain V-VI is exchanged (49). This finding suggests that the intracellular loop between V-VI plays functional roles in G protein coupling. The sequence conservation in transmembrane regions suggested that these regions might be involved in the ligand binding. This hypothesis was confirmed by Lefkowitz et al.(34) in studies of receptor chimeras. Ligand binding has been found to depend on critical amino acids present in several of the transmembrane

domains. These domains are thought to form a cluster to accomodate the incoming ligands.

Figure 3. Structure of the hamster β_2-adrenergic receptor as within in the lipid bilayer (boxed). Functionally important amino acids are indicated by different symbols. The seven transmembrane regions are numbered I-IIV from left to right. Abbreviations for the symbols: CHO, N-linked oligosaccharide; PKA, cAMP-dependent protein kinase; βARK, β-adrenergic receptor kinase.

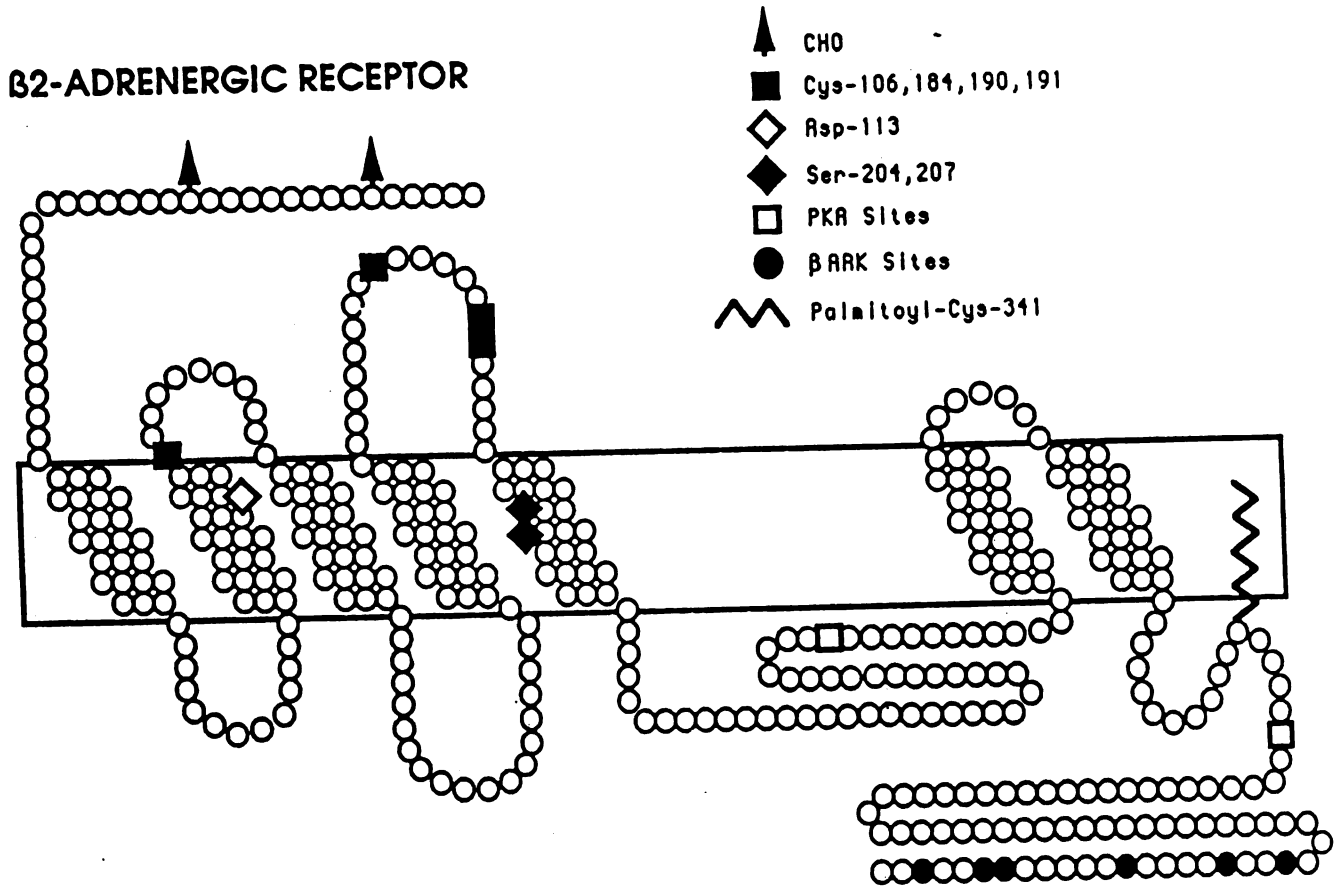
β2-ADRENERGIC RECEPTOR
CHO
Cys-106,184,190,191
Asp-113
Ser-204,207
PKA Sites
βARK Sites
Palmitoyl-Cys-341

Receptor-mediated Inositol Trisphosphate Formation and Subsequent Ca^{++} Mobilization

Hormone-induced Formation of Inositol Trisphosphate. Extracellular signals detected by cell surface receptors are translated and amplified into different intracellular second messengers. One pair of messengers is inositol 1,4,5-trisphosphate (IP_3) plus diacylglycerol (DAG). They form two limbs of a single signaling pathway, with IP_3 mobilizing calcium from intracellular stores and DAG activating protein kinase C (Fig.4). Together IP_3 and DAG initiate a cascade of cellular responses (37).

The key step in this signaling system is a receptor-induced activation of phospholipase C (PLC) which catalyzes hydrolysis of phosphatidylinositol 4,5-bisphosphate (PIP_2) to generate both IP_3 and DAG. Ten years ago, Agranoff et al.(50) found that stimulation of platelets with thrombin resulted in a rapid increase in the level of IP_3, coinciding with a fall in the level of PIP_2. This was the first direct evidence suggesting that a hormone could stimulate the breakdown of polyphosphoinositides via a phospholipase. Many, if not all, cell types are now known to exhibit hormone-induced phosphotidylinositol turnover (51-53). Moreover, there is considerable evidence that a G protein is involved in this

receptor-mediated process. It was demonstrated that IP_3 formation was stimulated by the addition of GTPγS, a non-hydrolyzable GTP analog, to permeablized cells (54). $NaAlF_4$, a compound which persistently activates G protein, also stimulates IP_3 formation (55). In fact, two types of G proteins coupled to PLC have been discovered; these include both pertussis toxin (PTX)-sensitive (56) and PTX-insensitive G proteins (57). Reconstitution experiments with purified PTX-sensitive G proteins G_i and G_o showed that these two G proteins have phospholipase C stimulatory function (58). Molecular cloning has recently yielded a new G protein called G_q. An antibody to this protein was found to inhibit the phospholipase C activity occuring in response to thromboxane A_2 in a PTX-insensitive manner (59). This finding suggested that G_q is the PTX-insensitive G protein involved in PLC activation.

There are several PLCs which hydrolyze phosphatidylinositol derivatives. The PLC isozymes are designated as α, β, γ, δ, ϵ according to their different primary structures (60). All of these PLCs are specific for phosphatidylinositol and/or phosphatidylinositol phosphates (60,61) and do not hydrolyze other phospholipids.

In summary, the hormone-induced IP_3 formation requires three membrane components including a receptor, a PLC responsible for the cleavage of IP_3 from the precursor lipid, and a G protein that couples the receptor to PLC.

Figure 4. The dual signaling pathway of IP_3/Ca^{++} and DAG/PKC. The dashed lines represent the positive and negative feedbacks of PKC on Ca^{++} signaling. Abbreviations: PIP_2, phosphotidylinositol 4,5-bisphosphate; IP_3, inositol 1,4,5-trisphosphate; G_p., the G protein involved in phospholipase C activation; DAG, diacylglycerol.

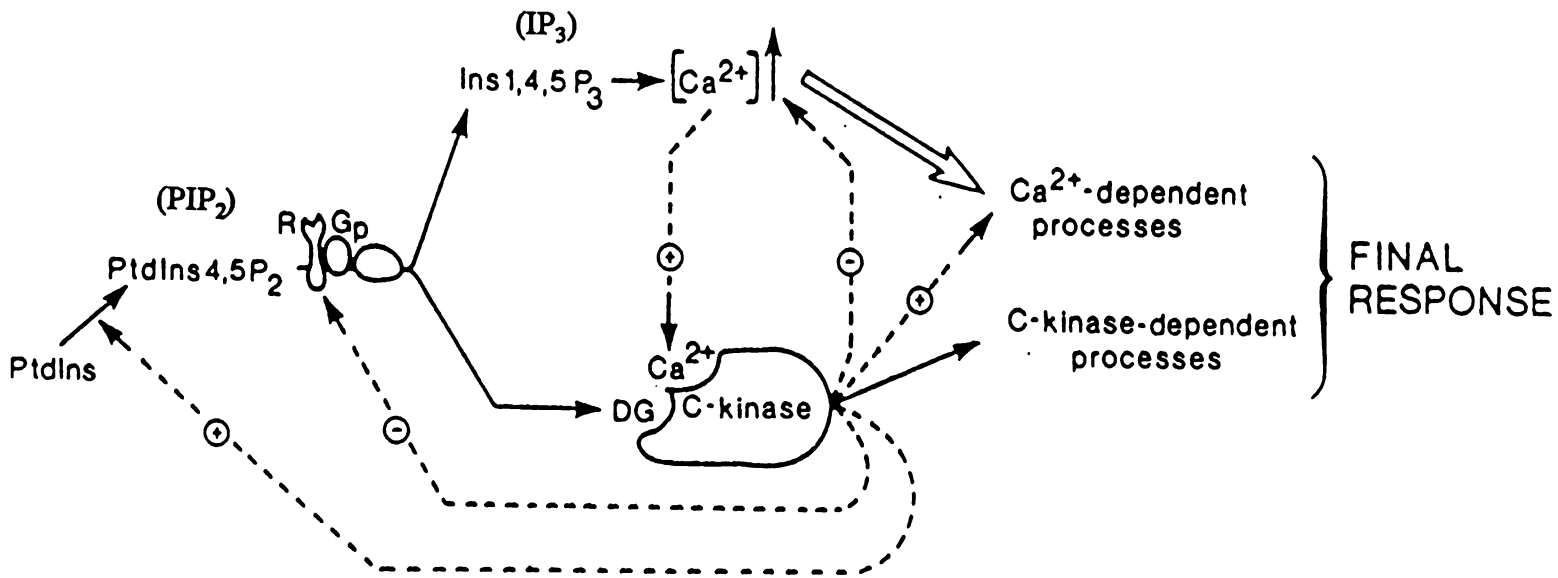
(IP3)
Ins1,4,5 P3
[Ca2+]
(PIP2)
R
Gp
PtdIns4,5P2
PtdIns
Ca2+
DG
C-kinase
Ca2+-dependent processes
C-kinase-dependent processes
FINAL RESPONSE

<u>Ca^{++} Signaling Triggered by Inositol Trisphosphate (IP_3)</u>. The importance of IP_3 as a signaling molecule is mainly due to its role in controlling the level of intracellular calcium, which itself is a major intracellular messenger.

Ca^{++} is a very important ion in biological systems. In higher organisms, the concentration of free Ca^{++} in the extracellular pool ($[Ca^{++}]_o$) is very high (1.0-1.5 mM), while the concentration of free Ca^{++} in the intracellular pool ($[Ca^{++}]_i$) is very low (100-200 nM) (62). For an intracellular messenger like Ca^{++}, this distribution of free Ca^{++} has two advantages. First, the large difference in $[Ca^{++}]$ between the two sides of the plasma membrane results in a large electrochemical force on Ca^{++}. Under such conditions, small changes in the permeability of the plasma membrane to Ca^{++} induced by extracellular stimuli will cause a significant change in $[Ca^{++}]_i$. Secondly, the very low level of $[Ca^{++}]_i$ in resting cells makes it possible to achieve a large fluctuation in $[Ca^{++}]_i$ rapidly.

The $[Ca^{++}]_i$ is controlled by Ca^{++}-transporting systems in the plasma membrane and membranes of intracellular organelles including the mitochondria and endoplasmic reticulum. The plasma membrane contains three general systems responsible for Ca^{++} exchange between extracellular and intracellular pools. They are Ca^{++} channels (63), Na^+/Ca^{++} exchangers (64), and Ca^{++}-ATPases (65). The major mechanism

for Ca^{++} entry is the opening of Ca^{++} channels. There are several types of these channels which can be operated by changes in membrane potential, by receptors upon binding of ligands, or by second messengers (66). The extrusion of intracellular Ca^{++} is achieved by Ca^{++} ATPases, whose pumping activity is subject to regulation by calmodulin- and cAMP-dependent protein kinases (67). In addition to the extracellular source of Ca^{++}, cells also use intracellular sources. The two major calcium stores within mammalian cells are the endoplasmic reticulum (ER) and mitochondria (MT). It is clear now that the ER plays an active role in regulating the intracellular pool of Ca^{++}. As will be described below, part of the ER pool of calcium is sensitive to IP_3, while the remaining pool of Ca^{++} can be released by Ca^{++} ionophores. Ca^{++} accumulation by the ER is achieved by transport of Ca^{++} via a Ca^{++}-pumping ATPase. This enzyme has a high Ca^{++} affinity (K_m=1 μM), and can load relatively large amounts of Ca^{++} into the isolated reticular vesicles in the presence of the trapping anion oxalate (68). Calmodulin- and cAMP-dependent protein kinases (70) have been suggested to be involved in the regulating of the process of Ca^{++} pumping. Thus, by refilling and releasing the stored Ca^{++} efficiently, the ER "fine-tunes" cytosolic [Ca^{++}] from 100 to 200 nM in the resting state, to the millimolar range when stimulated by Ca^{++}-mobilizing agonists. This wide range of change in $[Ca^{++}]_i$ permits Ca^{++} to act as an intracellular regulator. In

contrast to the ER, the MT is a low-affinity Ca^{++} uptake organelle (K_m about 10 μM) (71), but it has a large capacity for Ca^{++} accumulation (72) since it can coaccumulate phosphate and Ca^{++} leading to formation of hydroxyapatite deposits in the matrix space. So it has been suggested that the main role of the MT is to absorb and store away the cytosolic Ca^{++} when there is excess Ca^{++} influx through the plasma membrane.

Evidence has long been accumulated that hydrolysis of phosphoinositides and formation of IP_3 always occur with so called calcium-mobilizing agonists which bind to receptors that induce calcium release from internal stores. Included in this group are muscarinic cholinergic receptors, α_1-adrenergic receptors and V_1-vasopressin receptors (73). The response to the calcium-mobilizing agonists involves initially a release of sequestered Ca^{++} from the internal stores, which results in a rapid (10-30 sec) increase in $[Ca^{++}]_i$ to some maximal value that soon declines. This initial Ca^{++} transient is then followed by entry of Ca^{++} from the extracellular medium through the plasma membrane, which keeps the $[Ca^{++}]_i$ at a level above the resting level for several minutes.

The initial observation that the release of Ca^{++} from non-mitochondrial calcium stores could be triggered by IP_3 was made by Berridge et al. (74) about ten years ago, using permeabilized pancreatic cells monitored with a calcium electrode. Similar observations were obtained in many other

permeabilized cells. It was shown subsequently that the non-mitochondrial IP_3-sensitive calcium pool resides in ER (75); this latter pool accounts for 30-50% of the total non-mitochondrial pool of calcium. A variety of tissues have a high affinity stereospecific binding site for IP_3, but how IP_3 interacts with receptors that mediate intracellular Ca^{++} release remained unclear until recently, when Supattapone et al (76). isolated an IP_3-binding protein from cerebellar Purkinje cells which shows abundant IP_3 binding sites. This protein is a tetramer of about 260 Kd subunits. When reconstituted into lipid vesicles, the purified IP_3 receptor protein binds with IP_3 and its derivatives and mediates Ca^{++} fluxes (77). A corresponding pharmacological profile of agonist binding and agonist-induced Ca^{++} release was observed, providing compelling evidence that IP_3 binding site and Ca^{++} channel reside in the same protein. Immunostaining using a specific antibody against this receptor on Purkinje cells revealed that it is localized on the nuclear envelope and on parts of the ER, particularly near the nucleus (78). Eventually, the entire cDNA sequence was obtained from a mouse cerebellum library screened with the monoclonal antibody of this receptor (79), revealing an open reading frame encoding 2,749 amino acids. Comparison of immunolocalization and hydropathy profile suggest that the receptor possesses a very large N-terminal region on the cytoplasmic face of the ER, and a cluster of up to seven transmembrane domains close to the C

terminal.

As a universal intracellular messenger, Ca^{++} is involved in the stimulation of a variety of physiological processes, including the contraction of smooth muscle, the breakdown of glycogen in liver, the secretion of enzymes from pancreas, the opening of ion channels in a number of cells, some early events of fertilization; growth factor-induced gene transcription; and information storage by nervous system. Many of these events are short-term responses that are switched off rapidly; but some are long-term events such as cell growth and information storage. Ca^{++} plays its role in these processes either by directly activating the enzymes involved or by binding to calmodulin, the most abundant high-affinity Ca^{++}-binding protein in most eukaryotic cells. Calmodulin is known to interact with a number of cellular enzymes including adenylate cyclase, cyclic nucleotide phosphodiesterase, phosphorylase b kinase, and Ca^{++} ATPase of plasma membranes (37,73).

One aspect of Ca^{++} signaling that has attracted considerable attention in recent years is Ca^{++} oscillations. When cells challenged with Ca^{++}-mobilizing agonists are monitored at the single cell level, oscillatory patterns of response are frequently observed (80). The oscillatory patterns are usually in the form of a constant baseline which is interrupted periodically by calcium spikes. Most oscillations have a period of between 5 and 60 seconds,

dependant or independent of the concentration of agonists (81). Each individual cell has a unique pattern and frequency of response, which remains constant after repeated application of a specific agonist; this pattern serves as a cell "fingerprint" (82). In Ca^{++} oscillations, the Ca^{++} transient often initiates at a specific subcellular location and then spreads throughout the cells in waves which propagate at a rate of 10-100 μm/s (83). These spatial and temporal features of Ca^{++} mobilization imply that Ca^{++} may act as an intracellular messenger in a very complex way.

The Modulatory Function of Diacylglycerol and Protein Kinase C. Another product of the hydrolysis of PIP_2 is diacylglycerol (DAG), which functions as a second messenger to activate protein kinase C (PKC) (37), forming the second limb of the signaling system (Fig.4).

The stimulation of PKC requires the synergistic action of DAG and Ca^{++}. Upon cell activation, cytosolic Ca^{++} increases, which mediates the translocation of PKC from the cytosol to the membrane (84). PKC thus gains access to and binds DAG which remains in the membrane after hydrolysis of PIP_2.

Activated PKC exerts its function by phosphorylating specific proteins. Its substrates include receptors, G proteins, phospholipases, Ca^{++} channels and glycogen synthase. It is proposed that of the two limbs of the PLC signaling pathways resulting from PIP_2 hydrolysis, the

IP_3/Ca^{++} pathway plays a major role in initiating cellular responses, while the DAG/PKC pathway mainly serves to modulate the IP_3/Ca^{++} pathway, though in some cases it may also contribute directly and synergistically to the responses initiated by IP_3/Ca^{++} (37,85).

PKC is at the center of positive and negative controls, exerting duel actions over various steps of IP_3/Ca^{++} signaling (86). As cytosolic Ca^{++} increases, PKC begins to exert a negative feedback by activating the Ca^{++}-transport ATPase and Na^+/Ca^{++} exchange protein, both of which remove Ca^{++} from the cytosol (87), so that the $[Ca^{++}]_i$ will not rise too much. PKC also causes inhibition of receptor-mediated PIP_2 hydrolysis, blocking further activation of the IP_3/Ca^{++} pathway. There are a number of targets of PKC-mediated phosphorylation. For instance, in liver, activation of PKC selectively inhibits α_1-adrenergic receptor-mediated PIP_2 hydrolysis, but not vasopressin and angiotensin II receptor-mediated PIP_2 hydrolysis; this finding suggests that PKC can phosphorylate the α_1-receptor (88). There is also evidence that G proteins and PLC are phosphorylated by PKC (89). On the other hand, PKC can also have positive feedback effects on the IP_3/Ca^{++} pathway. PKC activation leads to the increased formation of PIP_2, which is the substrate for IP_3 formation. The net effect of the feedback effects of PKC on Ca^{++} signaling probably depends on the degree to which those feedback mechanism are

expressed in each cell.

Experimentally PKC can be activated by treating cells with tumor-promoting phorbol esters, which mimick the stimulatory effect of the DAG normally only generated from receptor activation (90). One of the most commonly used phorbol esters is 12-O-tetradecanoylphorbol-13-acetate (TPA). TPA induces persistent activation of PKC because it is very stable to metabolism. With short treatments, TPA elicits a positive effect on PKC by binding to its DAG binding site and immediately activating it. Chronic treatment with TPA, however, depletes cells of PKC, since the persistent activation of this enzyme makes it sensitive to proteolysis which leads to its subsequent degradation (91). The TPA-induced depletion of PKC, termed down-regulation of PKC, has been observed in many cell types (92, 93). Thus, one way to study the function of PKC is to down-regulate the enzyme by chronic treatment of cells with TPA. It has been shown in a number of cell lines that depletion of PKC results in potentiation of IP_3 formation occurring in response to Ca^{++}-mobilizing agonists (94), probably due to withdrawal of the normal negative feedback effects that PKC exerts on the IP_3/Ca^{++} limb of the PLC signaling pathway.

REFERENCE

1. Hinman, J.W. (1972) Ann. Rev. Biochem. 41, 161.
2. Rittenhouse-Simmons, S. (1981) J. Biol. Chem. 256, 4153-4155.
3. Schwartzman, M., Liberman, E., Raz, A. (1981) J. Biol. Chem. (1981) 256, 2329-2333.
4. Garcia,-Perez, A., Smith, W. L. (1984) J. Clin. Invest. 74, 63-74.
5. Smith, W.L. (1992) Am. J. Physiol. 263, F181-F191.
6. Rollins, T. E., Smith, W. L. (1980) J. BIol. Chem. 255, 4872-4875.
7. Smith, W.L. (1989) Biochem. J. 259, 315-324.
8. Ferreira, S.H., Vane, J.R. (1974) Ann. Rev. Pharmacol. 14, 57.
9. Smith W.L. (1986) Ann. Rev. Physiol. 48, 251-262.
10. Pace-Asciak, C.R., Smith, W.L. (1983) In: The Enzymes (Boyer, P.D., ed.) Vol.16, pp 543-603.
11. Moonen, P., Buytenhek, M., Nugteren, D.H. (1982) Methods Enzymol. 86, 84-91.
12. Watanabe, K., Iguchi, Y., Iguchi, S., Arai, Y., Hayaishi, O., Roberts, L.J. (1987) Adv. Prostaglandin Thromboxane Leukotriene Res. 17A, 44-49.
13. DeWitt, D.L., Smith, W.L. (1983) J. Biol. Chem. 258, 3285-

3293.

14. Shen, R.-F., Tai, H.-H. (1986) J. B. Chem. 261, 11592-11599.

15. Christ-Hazelhof, E., Nugteren, D.H. (1981) Prostaglandins 22, 739-746.

16. Ferreira, S.H., Vane, J.R. (1967) Nature (London) 216, 868-873.

17. Smith, W.L. (1985) In: Biochemistry of Arachidonic Acid Metabolism (Lands, W.E.M., ed),pp. 77-94, Martinus Nijoff, Boston.

18. Samuelssson, B., Granstrom, E., Green, K., Hamberg, M., Hammarstrom, S. (1975) Ann. Rev. Biochem. 44, 669-689.

19. Smith, W.L., Sonnenberg, W.K., Allen, M.L., Watanabe, T., Zhu, J. El-Harith, E.A. In: Renal Eicosanoids (Patrono, C. and Dunn, M.J., eds.), Plenum, New York.

20. Currie, M.G., Needleman, P. (1984) Ann. Rev. Physiol. 46, 327-341.

21. Smith, W.L., Bell, T.G. (1978) Am. J. Physiol. 235, F451-F457.

22. Grenier,F.C., Smith, W.L. (1978) Prostaglandins 16, 759-772.

23. Kirschenbaum, M.A., Lowe, A.G., Trizna, W., Fine, L.G. (1982) J. Clin. Invest. 70, 63-74.

24. Grantham, J.J., Orloff, J. (1968) J. Clin. Invest. 47, 1154-1161.

25. Handler, J.S., Orloff, J. (1981) Ann. Rev. Physiol. 43,

611-624.

26. Sonnenberg, W.K., Smith, W.L. (1988) J. Biol. Chem. 263, 6155-6160.
27. Sonnenburg, W.K., Zhu, J. Smith, W.L. (1990) J. Biol. Chem. 265, 8479-8483.
28. Breyer, M.D., Jacobson, H.R., Hebert, R.L. (1990) Kidney International 38, 618-624.
29. Dixon, B.S., Breckon, R., Burke,C., Anserson, R.J. (1988) Am. J. Physiol. 254, C183-C191.
30. Ando, Y., Jacobson, H.R., Breyer, M.D. (1987) J. Clin. Invest. 80, 590-593.
31. Coleman,R.A., Kennedy, I., Humprey, P.P.A., Bunce, K., Lumley, P. (1990) In: Comprehensive Medicinal Chemistry, edited by Transch, C., Sammes, P.G., taylor, J. Oxford: Pergamon, 1990, Vol.3, pp 643-714.
32. Sugimoto, Y., Namba, T., Honda, A., Hayashi, Y., Negishi, M., Ichikawa, A., Narumiya, S. (1992) J. Biol. Chem. 267, 6463-6465.
33. Honda, A., Sugimoto, Y., Namba, T., Watabe, A., Irie, A., Negishi, M., Narumiya, S., Ichikawa, A. (1993) J. Biol. Chem. 268, 7759-7762.
34. Dohlman, H.G., Thorner, J., Caron, M.G., Lefkowitz, R.J. (1991) Ann. Rev. Biochem. 60, 653-688.
35. Gilman, A. G. (1987) Ann. Rev. Biochem. (1987) 56, 615-649.
36. Iyengar, R., Abramowitz, J., Bordelon,-Riser, M.E.,

Birnbaumer, L. (1980) J. Biol. Chem. 255, 3558-3564.

37. Berridge, M.J.A. (1987) Ann. Rev. Biochem. 56, 159-193.
38. Stryer, L. (1986) Ann. Rev. Neurosci. 9, 87-119.
39. Birnbaumer, L., Brown, A.M. (1990) Ann. Rev. Pharmacol. Toxicol. 30, 675-705.
40. Birnbaumer, L. (1990) FASEB J. 4, 3068-3078.
41. Rodbell, M., Birnbaumer, L., Pohl, S., Krans, H.M.J. (1971) J. Biol. Chem. 246, 1877-1812.
42. Northup,J.K., Sternwise, P.C., Smigel, M.D., Schleifer, L.S., Ross, E.M., Gilman, A.G. (1980) Proc. Natl. Acad. Sci. USA 77, 6516-6520.
43. Harris, B.A., Robishaw, J.D., Mumby, S.M., Gilman, A.G. (1985) Science 229, 96-99.
44. Shorr, R.G.L., Lefkowitz, R.J., Caron, M.G. (1981) J. Biol. Chem. 256, 5820-5826.
45. Dixon, R.A., Caron, M.G., Lefkowitz, R.J., Strader, C.D. et al. (1986) Nature 321, 75-79.
46. Masu. Y., Nakayama, K., Tamaki, H., Harada, Y., Kuno, M., Nakanishi, S. (1986) Nature 329, 836-838.
47. Henderson, R., Unwin, P.N.T. (1975) Nature 257, 28-32.
48. Dohlman, H.G., Caron, M.G., Lefkowitz, R. J. (1988) Biochemistry 26, 2657-2664.
49. Wong, S.K., Parker, E.M., Ross, E.M. (1990) J. Biol. Chem. 265, 6219-6224.
50. Agranoff, B.W., Murthy, P., Seguin, E.B. (1983) J. Biol. Chem. 258, 2076-2078.

51. Berridge, M.J. (1983) Biochem J. 212, 849-858.

52. Martin, T.F.J. (1983) J. Biol. Chem. 258, 14816-14822.

53. Rebecchi, M.J., Gershengorn, M.C. (1983) Biochem J. 216, 299-308.

54. Smith, C.D., Lane, B.C., Kusaka, I., Verghese, M.W., Snyderman, R. (1985) J. Biol. Chem. 260, 5875-5878.

55. Strnad, C.F., Parente, J.E., Wong, K. (1986) FEBS Lett. 206, 20-24.

56. Nakamura, T., Ui, M. (1985) J. Biol. Chem. 260, 3584-3593.

57. Taylor, C.W., Blakeley, D.M., Corps, A.N., Berridge, M.J., Brown, K.D. (1988) Biochem J. 249, 917-920.

58. Kikuchi, A., Kozawa, O., Kaibuchi, K., Katada, T., Ui, M., Takai, Y. (1986) J. Biol. Chem. 261, 11558-11562.

59. Gutowski, S., Smrcka, A., Nowak, L., Wu, D., Simon, M., Sternwise, P.C. (1991) J. Biol. Chem. 266, 20519-20524.

60. Rhee, S.G., Suh, P.-G., Ryu, S.-H., Lee, S.Y. (1989) Science 244, 546-550.

61. Ryu, S.H., Suh, K.S., Cho, K.Y., Lee, S.Y., Rhee, S.G. (1987) Proc. natl. Acad. Sci. USA 84, 6659.

62. Carafoli, E. (1987) Ann. rev. Biom. 56, 395-433.

63. Reuter, H. (1984) Ann. Rev. Physiol. 46, 473-484.

64. Reuter, H., Seitz, N. (1968) J. Physiol. 198, 46-48.

65. Kostyuk, P.G. (1982) In: Membrane Transport of Calcium, ed. E. Carafoli, pp 41-108.

66. Tsien, R.W. Tsien, R.Y. (1990) Ann. Rev. Cell Biol. 6,

715-760.

67. Reuter, H., Stevens, C.F., Tsien, R. W., Yellen, G. (1982) Nature 297, 501-504.
68. Constantin, L.L. Franzini-Armstrong, C., Podolsky, R.J. (1965) Science 147, 158-160.
69. Moore, P.B., Kraus-Friedmann, N. (1983) Biochem J. 214, 69-75.
70. Bygrave, F.L., Tranter, C.J. (1978) Biochem. J. 174, 1021-1030.
71. Crompton, M., Sigel, E., Salzmann, M., Carafoli, E. (1976) Eur. J. Biochem. 69, 429-434.
72. Carafoli, E. (1974) Biochem. Soc. Symp. 39, 89-113.
73. Berridge, M.J. (1982) In: Calcium and Cell Function (Cheung, W.Y., ed), Vol. 3, pp 1-36. Academic Press, New York.
74. Streb, H., Irvine, R.F., Berridge, M.J., Schulz, I. (1983) Nature, 306, 67-69.
75. Streb, H., Bayerdorffer, E., Hasse, W., Irvine, R.F., (1984) Schultz I. J. Membrane Biol. 81, 241-253.
76. Supattapone, S., Worley, P.F., Baraban, J.M., Snyder, S.H. (1988) J. Biol. Chem. 263, 1530-1534.
77. Ferris, C.D., Huganir, R.L., Supattapone, S., Snyder, S.H. (1989) Nature 342, 87-89.
78. Ross, C.A. et al. (1989) Nature 339, 468-470.
79. Furuichi, T., Yoshidawa, S., Miyawaki, A., Wada, K., Meada, N., Mikoshiba, K. (1989) Nature 342, 32-38.

80. Berridge, M.J., Galione, A. (1988) FASEB J. 2, 3074-3082.

81. Rink, T.J., Jacob, R. (1989) Trends Neurosci. 12, 43-46.

82. Prentki, M. et al. (1988) J. Biol. Chem. 263, 11044-11047.

83. Takamatsu, T., Wier, W.G. (1990) FASEB J. 4, 1519-1525.

84. Kosaka, Y. et al. (1988) Biochem. biophys. Res. Commun. 149, 946-952.

85. Berridge, M.J. (1984) Biochem. J. 220, 345-360.

86. Nishizuka, Y. (1988) Nature 334, 661-665.

87. Kikkawa, U., Nishizuka, Y. (1986) Ann. Rev. Cell Biol. 2, 149-178.

88. Sibley, D.R., Benovic, J.L., Cron, M.G., Lefkowitz, R.J. (1988) Endocr. Rev. 9, 38-56.

89. O'Brien, R.M., Houslay, M.D., Milligan, G., siddle, K. (1987) FEBS Lett. 212, 281-288.

90. Sando, J.J., Young, M.C. (1983) Proc. Natl. Acad. Sci. USA 80, 2642-2646.

91. Kishimoto, A., Kajikawa, N., Shiota, M., Nishzuka, Y. (1983) J. Biol. Chem. 258, 1156-1164.

92. Young, S., Parker, P.J., Ullrich, A., Stabel, S. (1987) Biochem. J. 244, 775-779.

93. Helper, J.R., Earp, H.S., Harden, T.K. (1988) J. Biol. Chem. 263, 7610-7619.

94. Brown, K.D., Littlewood, C.J., Blakeley, D.M. (1990) Biochem. J. 270, 557-560.

CHAPTER TWO

PROSTAGLANDIN E_2-INDUCED Ca^{++} MOBILIZATION IN SUBTYPES OF RABBIT CORTICAL COLLECTING TUBULE CELLS

The renal collecting tubule is importantly involved in regulating water and electrolyte balance. PGE_2, the major prostanoid formed by collecting tubule cells (1), plays a key role in the modulation of this process. In immunodissected rabbit cortical collecting tubule (RCCT) cells, PGE_2 acting at relatively low concentrations (ca.10^{-8} M) inhibits arginine vasopressin (AVP)-induced cAMP accumulation; at higher concentrations ($\geq 10^{-7}$ M), PGE_2 by itself stimulates cAMP formation (2). These effects appear to be mediated through inhibitory EP3 and stimulatory EP2 receptors, coupled to an inhibitory G protein (G_i) and a stimulatory G protein (G_s), respectively (3). These *in vitro* studies with isolated RCCT cells provide a biochemical basis for the dual actions of PGE_2 on water reabsorption observed in perfused collecting tubules (4).

In addition to the well-studied cAMP inhibitory and stimulatory pathways, some evidence suggests that PGE_2 regulates water and salt transport through a third signaling

pathway involving increases in the concentration of intracellular Ca^{++} ($[Ca^{++}]_i$) and the activation of protein kinase C (PKC) (5,6). However, there is no direct evidence for a third PGE receptor coupled to Ca^{++} mobilization in the mammalian collecting tubule. The purpose of the present study was to characterize PGE_2-induced Ca^{++} mobilization in RCCT cells. It was demonstrated that PGE_2 induced Ca^{++} mobilization and that this effect was mediated via a receptor with properties resembling those of an EP1 PGE receptor and differing those of EP2 and EP3 PGE receptors. The combination of Ca^{++} measurements and immunostaining at the single cell level using fluorescence digital imaging enabled us to establish that this putative EP_1 PGE receptor is distributed in both principal and type B intercalated collecting tubule cells.

MATERIALS AND METHODS

Materials. Dulbecco's modified Eagle medium (DMEM), collagenase, fetal calf serum (FCS) and trypsin were purchased from GIBCO. Bovine calf serum (CS) was from Hyclone Laboratories. PGE_2, $PGF_{2\alpha}$, PGD_2, and 15-(R)-PGE_2 were from Cayman Chemical Company. Arginine vasopressin (AVP), fluorescein isothiocyanate-labeled peanut lectin (FITC-PNA), and fluorescein isothiocyanate (FITC)-labeled goat anti-mouse IgG were from Sigma. Fluo-3/AM was from Molecular Probes, Inc. Pertussis toxin was from List Biological Laboratories. A hybridoma line producing a monoclonal antibody (DT.17) specifically reactive with a cell surface determinant of principal cells was a gift from Dr. Geza Fejes-Toth, Dartmouth Medical School (7). Other reagents were from common commercial sources.

Purification of mouse IgG_3(rct-30) from hybridoma culture medium. The monoclonal antibody IgG_3(rct-30), which interacts specifically with a cell surface antigen of RCCT cells, was isolated as follows. The rct-30 hybridoma line was grown in HT-complete medium containing DMEM, 10% FCS, 10% NCTC-135 medium, 2 mM glutamine, 13.6 μg of hypoxanthine/ml and 3.9 μg of thymidine/ml. Before harvest, this medium was replaced by IgG free medium (8) in which cells were allowed to incubate

for several days to secrete the antibody. This latter medium was collected, filter-sterilized and adjusted to pH 8.0 before being applied to a Protein A-Sepharose column. The column was eluted stepwise with 0.1 M buffers of pH 8.0 (sodium phosphate), and pH 4.5 and pH 3.5 (sodium citrate). IgG_3(rct-30) was eluted at pH 4.5. The eluant was collected and immediately neutralized with 100 μl of 1M Tris (pH 9.5) contained in each collection tube. Fractions containing IgG_3(rct-30) were pooled, sterilized by filtration, and diluted with phosphate-buffered saline (PBS: 137 mM NaCl, 8.1 mM Na_2HPO_4, 1.5 mM KCl, pH 7.3). The protein concentration was estimated by measuring the absorbance at 280 nm.

Immunofluorescence staining of rabbit kidney sections. Fresh rabbit kidneys were cut into small cubes (ca. 1 cm^3) which were frozen rapidly. The frozen pieces were sectioned into thin slices (ca.8 μm) and were adhered onto glass slides. After vacuum-drying, these slices were subject to immunostaining. Diluted purified IgG_3(rct-30) or medium from DT.17 hybridoma growth were applied to the sections. After a 15 min incubation, the sections were rinsed with simplified saline solution (SSS: 145 mM NaCl, 5 mM KCl, 1 mM Na_2HPO_4, 0.5 mM $MgCl_2$, 5 mM glucose, 10 mM Hepes, 1 mM $CaCl_2$, pH 7.4). and then incubated with a 1:10 diluted FITC-labeled anti-mouse IgG for another 15 min. The stained sections were rinsed with SSS, mounted on glass slides and examined under a fluorescent

microscope.

Preparation of culture wells coated with IgG_3(rct-30). Each well of a 24 well culture plate was incubated for 2-4 hours at room temperature with 0.25 ml of IgG_3(rct-30)(100-400 μg/ml). Immediately before use, the antibody solution was aspirated from the wells, which were then washed twice with 1% bovine serum albumin in PBS.

Isolation and culture of RCCT cells. Homogeneous populations of RCCT cells were isolated by immunodissection using IgG_3(rct-30) (9). For each isolation, two kidneys were removed from a 8-16 week old male or female New Zealand White rabbit, which had been sacrificed with an overdose of 7.5% sodium pentobarbital injected through the marginal ear vein. The renal cortex was dissected, minced into a fine paste, and transferred into a tube containing 30-40 ml of 0.1% collagenase in SSS. After a 30-40 min incubation at 37°C, the cells were filtered through a 250-μm Gelman wire mesh, and resuspended in PBS. The cell suspension was overlayed onto IgG_3(rct-30)-coated 24-well culture dishes, which, after a few minutes of incubation, were washed gently with PBS to remove nonadherent cells. The RCCT cells absorbed to the wells were ready for culture in DMEM containing 10% bovine calf serum in a water-saturated 7% CO_2 atmosphere. Flurbiprofen (FBP), a PGH synthase inhibitor was included at a concentration of 5 μM in all isolating solutions and in the culture medium.

Measurement of Ca^{++} mobilization in individual RCCT

cells. One day-cultured RCCT cells were incubated with 10 μM fluo-3/AM at 37°C for 40 min in SSS containing 0.1% BSA. The cells were then washed three times with SSS. The fluo-3 loaded cells remained responsive for two or three hours at 24°C without significant loss of the dye. Loaded cells that were immobilized in the culture wells were treated with agonist and scanned using an ACAS 570 interactive laser cytometer with an excitation wavelength of 488 nm and an emission wavelength of 505 nm. The change in fluorescence intensity in the cells was monitored during scanning. The basal and the peak $[Ca^{++}]_i$ of responding cells were calculated as described previously (10) with the formula:

$$[Ca^{++}]=(F-F_{min}/F_{max}-F)xK_d.$$

K_d is 400 nM, the dissociation constant for Ca^{++}-bound fluo-3; F represents the fluorescence at a given time point; F_{max} represents the maximum fluorescence observed when 10 μM of ionomycin was added to permeabilize fluo-3 loaded cells. $MnCl_2$ (2mM) was added to the permeabilized cells to obtain a value for F_{Mn}, which was used to calculate the F_{min} using the formula:

$$F_{min}=(1.25xF_{Mn})-(0.25xF_{max}).$$

In the analysis of the fluorescence digital image, the fluorescence within a cell at each time point was normalized to the fluorescence of the first scan. Responding cells were defined as RCCT cells which exhibited an increase in

fluorescence intensity of ≥10% following challenge with an agonist.

Identification of principal and intercalated cells. To determine the identity of responsive cells among different types of RCCT cells, cell populations were (a) stained with FITC-PNA which binds type B intercalated cells or (b) subjected to indirect immunofluorescence staining using a monoclonal antibody (DT.17) reactive with principal cells (7). Since fluorescein falls into the same range of excitation and emission wavelengths as fluo-3, it was not feasible to stain the fluo-3 loaded cells in the same scanned field with fluorescein. Therefore, after imaging the cells challenged with agonists, the fluorescence of fluo-3 was quenched with 2 mM $MnCl_2$, plus 10 μM ionomycin which permibilizes the cells to allow the entry of divalent ion. The quenched cells were then subjected to staining with FITC-labeled lectin or antibody. For staining of intercalated cells, cells were incubated with FITC-PNA (1:10 dilution in SSS) for 5 min, then washed extensively with SSS. For staining of principal cells, medium from the growth medium of DT.17 hybridoma cells, which secrete an anti-principal cell antibody (7), was added to the cells and the incubation continued for 10 min. Excess antibody was removed by washing with SSS. The cells were then incubated for 10 min with FITC-labeled anti-mouse IgG (1:10 dilution in SSS). The stained cells were rinsed with SSS and then scanned for fluorescein fluorescence.

Pertussis toxin treatments. One-day cultures of RCCT cells in DMEM containing 10% calf serum (CS) were incubated with pertussis toxin (2.5 μg/ml) at 37°C for 12-16 hours. Control cells were cultured in the absence of pertussis toxin. 28A cells, which are a line derived from RCCT cells (11), were grown under the same conditions as the RCCT cells and treated in parallel with or without pertussis toxin (2.5 μg/ml) at 37°C.

Measurement of inositol phosphates (IPs). Immunodissected RCCT cells were cultured in 24 well dishes for 4-5 days until the cells were confluent. Cells in each well were labeled with 10 μCi [^{3}H]inositol/ml in medium 199 containing 200 mM glutamine for 12-16 hours. The labeled cells were washed and then incubated in 0.5 ml of Hepes/Li buffer (4.7 mM KCl, 0.5 mM EDTA, 13 mM glucose, 20 mM Hepes, 1.2 mM KH_2PO_4, 1.2 mM $MgSO_4$, 58 mM NaCl, 60 mM LiCl, 1.5 mM $CaCl_2$) for 30 min. Then the Hepes/Li buffer was removed and replaced by 0.5 ml SSS containing 10 μM agonist, and the samples incubated for various times. The reactions were stopped by adding 0.5 ml of ice-cold 12% trichloroacetic acid. Cells were then frozen at -70°C. After defrosting, medium was collected and centrifuged; 0.85 ml of the supernatant was loaded onto AG-1X8 resin columns to determine IPs using the method of Berridge et al. (12).

RESULTS

Heterogeneity of RCCT cells. The monoclonal antibody IgG_3(rct-30), which is specifically against collecting tubules, was harvested from the culture medium of the hybridoma line rct-30 and purified by selective elution from a Protein A-Sepharose column. The affinity-purified IgG_3(rct-30) was used to isolate rabbit cortical collecting tubule (RCCT) epithelia cells.

Sections of rabbit kidney were examined after immunofluorescence staining with IgG_3(rct-30) (Fig.1). As expected, IgG_3(rct-30) stained the surfaces of all cells of the collecting tubules, and therefore, did not discriminate between principal (PC) and intercalated cells (ICC).

Another monoclonal antibody DT.17 (an IgG_3) that is directed against principal cells (10) was also used to stain kidney sections (Fig.2A). Only some cells in the collecting tubule were reactive to IgG_3(DT.17), as shown in the cross section of a collecting tubule at higher magnification in Fig.2B.

The freshly isolated RCCT cell populations was examined for their subtype compositions (Table 1). As expected, all cells were stained with IgG_3(rct-30). About 60% of the RCCT

cells were identified as principal cells based on their reactivity with IgG_3(DT.17); About 28% of these cells were peanut lectin (PNA) positive, and are defined as type B intercalated cells; the remaining 12% of these cells presumably represent type A intercalated cells. Similar results were obtained with one-day old primary cultures, which were used for measurements of Ca^{++} mobilization in response to hormones. The immunofluorescence digital images of RCCT cells stained with IgG_3(rct-30), IgG_3(DT.17) and PNA are shown in Fig.3, Fig.4, and Fig.5.

PGE_2- and AVP-induced Ca^{++} mobilization by RCCT cells. Changes in $[Ca^{++}]_i$ occurring in response to PGE_2 and AVP were studied at the single cell level using fluorescence digital imaging in one-day old primary cultures of RCCT cells loaded with fluo-3. Shown in Fig.6 are sequential digital images of six cells challenged consecutively with 10^{-5} M PGE_2 and 10^{-5} M AVP. Changes in $[Ca^{++}]_i$ were reflected by changes in fluorescence intensity, as indicated by the color bar in the figure. Fig.7 is the tracings of eight cells from one scanning field challenged with 10^{-5} M PGE_2 and then 10^{-5} M AVP. As shown in this time couse, maximal responses to PGE_2 or AVP were observed 25-50 sec following the addition of agonists, fluorescence then declined gradually to near basal levels over a 2-3 min period. AVP appears to be a more potent agonist than PGE_2; it evoked responses more rapidly and to a larger

magnitude. Clearly, not all RCCT cells responded to either PGE_2 and/or AVP. In a series of isolates PGE_2-responsiveness was observed in an average of about 40% of the cells (Fig.8) (percentage of responses to AVP was similar). The majority of cells remained their vitality under such a condition, as indicated by the fact that about 80% of cells are responsive to PGE_2 or AVP or to the Ca^{++} ionophore ionomycin.

Absolute $[Ca^{++}]_i$ was quantitated as described in the Methods. In response to PGE_2, $[Ca^{++}]_i$ increased from an average resting value of 220±62 nM to an average peak value of 700±330 nM (n=21). Thus, at the single cell level, PGE_2-evoked changes in $[Ca^{++}]_i$ were about two to five fold, which is what typically observed in many cell types and with numerous agonists. The basal level of $[Ca^{++}]_i$ was slightly higher than expected. For most cells basal $[Ca^{++}]_i$ ranges from 100-200 nM.

Distribution of PGE_2- and AVP-responsive cells among subtypes of RCCT cells. Since PGE_2 and AVP responses were only observed in subpopulations of RCCT cells, experiments were formulated to examine whether the responding subpopulations corresponded to specific subtype of RCCT cells.

The strategy of associating a responding cell with a specific cell type is illustrated in Fig.9. Agonists-induced changes of fluorescence intensity were determined for the cells, which were then classified based on their binding reactivity with either the principal cell-specific antibody

IgG_3(DT.17) or type B intercalated cell marker FITC-PNA. Interestingly, both principal cells and type B intercalated cells were found to respond to both PGE_2 and AVP (Table 2 and 3). As shown in Table 2, PGE_2-induced Ca^{++} mobilization occurred in about 43% of principal cells and 32% of intercalated cells, and AVP-induced response occurred in about 35% of both the principal cells and intercalated cells. A smaller population of 15-20% of both cell types responded to both PGE_2 and AVP. In these and other experiments described above, about 20% of RCCT cells failed to respond to any agonist or ionomycin. As shown in Table 3, PGE_2 induced Ca^{++} mobilization in about 40% of type B intercalated cells; about 60% of these type B intercalated cells were also responsive to AVP. Taken together, the results indicate that PGE_2- and AVP-responsive cells are distributed somewhat indiscriminately among all subtypes of RCCT cells.

It is not known if the heterogeneity of responses to PGE_2 and AVP within our RCCT cell populations reflects the *in vivo* situation with collecting tubule epithelia or simply represents loss of responses occurring as a result of RCCT isolation and manipulation.

<u>PGE_2-induced Ca^{++} mobilization is mediated by a PGE receptor</u>. As shown in Fig.10 for a representative RCCT cell isolate, the ability of PGE_2 to induced changes in $[Ca^{++}]_i$ is dose-dependent. The size of the responding population

increased with dose (Fig.10A). With 10^{-8} M PGE_2 only 21% of the RCCT cells responded while with 10^{-5} M PGE 48% of the cells responded. Half-maximal percentages of cells responded at about $5x10^{-6}$ M PGE_2. Not only the size of responding population but also the magnitude of response of each cell increased with dose. This is reflected in Fig.10B where the number of responding cells is plotted versus the magnitude of response to each dose of PGE_2.

Importantly, the Ca^{++} mobilizing effect of PGE_2 is stereospecific. In the experiment depicted in Fig.11, PGE_2 induced responses in 40±2% of the RCCT cells, but the 15R enantiomer of PGE_2 induced changes in only 8.6±1% of the RCCT cells in the same preparations (n=2); this latter value was not significantly different from the background responses observed with vehicle alone. The orientation of the hydroxyl group at C-15 is important for the biological activities of prostaglandins (13). The fact that the naturally occurring 15S enantiomer of PGE_2 but not 15R-PGE_2 causes Ca^{++} mobilization in RCCT cells suggests that PGE_2-induced Ca^{++} mobilization is a receptor-mediated event.

Another piece of evidence that supports the view that PGE_2-induced Ca^{++} mobilization is receptor mediated is the finding that flubiprofen (FBP), a non-steroid PGs synthesis inhibitor, up-regulated PGE_2-induced Ca^{++} mobilization. It has been reported that inhibition of PGE_2 synthesis up-regulates

PGE receptors, as indicated either by ligand binding or by receptor-mediated responses (14,15). When $5x10^{-6}$ M FBP was included in the isolation solutions and culture media, the percentage of responding cells increased from 22% to 43% (n=2), while the responsiveness to AVP were not significantly affected (Fig.12).

Further support for the concept PGE_2 mobilizes Ca^{++} through a receptor(s) and that the receptor shows a preference for the PGE class of prostaglandins came from examining the desensitization of the Ca^{++} mobilization process. As shown in Fig.13, PGE_2 as well as a PGE_2 analog, sulprostone were the most effective prostaglandins in desensitizing RCCT cells to subsequent PGE_2-induced Ca^{++} mobilization. $PGF_{2\alpha}$ caused desensitization to a level somewhat less than that observed with PGE_2 while sulprostone was more effective than PGE_2. PGD_2 and AVP did not cause desensitization. Sulprostone and $PGF_{2\alpha}$, however, were not as potent as PGE_2 in stimulating Ca^{++} mobilization. For sulprostone(10^{-5} M), the percentage of total RCCT cells population responding was 23 ± 2% versus 49 ± 6% for PGE_2 (n=2). $PGF_{2\alpha}$ (10^{-5}) caused an increase in Ca^{++} mobilization in 23 ± 3% of RCCT cells versus 47 ± 8% for PGE_2 (n=2). Taken together, these results suggest that Ca^{++} mobilization occurring in response to PGE_2 is due to interaction of PGE_2 with a PGE receptor. However, we cannot rule out the possibility the some of the response to PGE_2

occurred via its interaction with receptors for $PGF_{2\alpha}$.

There are three known pharmacological subclasses of PGE receptors designated EP1, EP2, and EP3 receptors. As described in chapter one (16), EP1 receptors are involved in smooth muscle contraction possibly via Ca^{++} mobilization and responses mediated via EP1 receptor are blocked by AH6809. We found that 5 min pretreatment of 10^{-5} M AH6809 decreased the percentage of RCCT cells responding to 10^{-5} M PGE_2 by approximately 50% (48% versus 25%, Fig.14A). Studies in 28A cells, a RCCT-derived cell line (11), showed similar results. A 10 min of pretreatment with 10^{-4} M AH6809 decreased the percentage of 28A cells responding to 10^{-5} M PGE_2 from 80% to 42%; in contrast, the responsiveness to adenosine A1 receptor agonist CHA was unaffected by AH6809 (96% vs 97%, Fig.14B).

<u>PGE_2-induced Ca^{++} mobilization and activation of PLC</u>. It was found that the effect of PGE_2 on Ca^{++} mobilization was independent of extracellular Ca^{++}. Neither the percentage of responding cells nor the magnitude of the response to PGE_2 was significantly affected when 2.5 mM EDTA was included in the medium to deplete extracellular Ca^{++} (Fig.15). This is characteristic of Ca^{++}-mobilizing agonists that release Ca^{++} from IP_3-sensitive intracellular stores.

Phorbol ester TPA activates PKC which has a negative feedback on the PLC pathway. The effect of TPA was first examined using AVP, which has previously been characterized to

mediate Ca^{++} mobilization by activating PLC. As shown in Fig.16, TPA decreased the percentage of cells responding to AVP in a dose-dependent manner. The inhibitory effect of TPA was also observed on the PGE_2-induced response. A 10 min of incubation with 10^{-6} M TPA decreased the percentage of cells responding to PGE_2 from 40% to 21% (Fig.16B). To determine if PGE_2 acts through a pertussis toxin (PTX) sensitive G_i or G_o to cause Ca^{++} mobilization, RCCT cells were pretreated with pertussis toxin (2.5 μg/ml) for 16 hours prior to stimulation with PGE_2. No significant change was observed in the size of the subpopulation responding to PGE_2 in the treated cells compared to the non-treated cells (Fig.17A). The presence of G_i in cultured RCCT cells was established previously by the finding that α_2-adrenergic receptor induced inhibition of cAMP accumulation is abolished by PTX treatment (3). To verify that PTX was acting on G_i in RCCT cells under conditions used in our experiment, a parallel treatment of the RCCT-derived line 28A cells was performed. As expected, Ca^{++} mobilization induced by the A1 adenosine receptor agonist CHA was substantially inhibited (>85%) by treatment of 28A cells with PTX. There was no significant effect of PTX to block Ca^{++} mobilization by PGE_2 in 28A cells (Fig.17B).

Finally, the effect of PGE_2 on the formation of inositol phosphates was examined in confluent (4-5 day old) RCCT cells and in 28A cells. Stimulation with 10^{-5} M PGE_2 for 30 min had

no significant effect on the production of inositol phosphates in RCCT cells (12±2.8%, n=2). In contrast, bradykinin, a potent Ca^{++}-mobilizing agonist in RCCT cells, caused a 50% increase in those cells under the same condition. Similar results were obtained using 28A cells.

Figure 1. Indirect immunofluorescence staining of a section of rabbit renal cortex with IgG_3(rct-30). The staining was performed as described in the text. The upper figure is a phase contrast photomicrograph (X100) of the stained section shown in the lower photomicrograph.

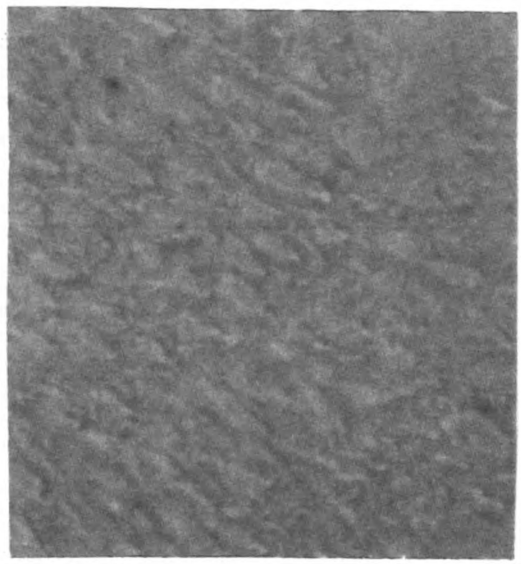

Figure 2. Indirect immunofluorescence staining of a section of rabbit renal cortex with an anti-principal cell antibody IgG_3(DT.17). (A). Phase contrast and fluorescence photomicrographs at low magnifications (X100). (B). phase contrast and fluorescence photomicrographs at higher magnification (X400), showing the cross section of one collecting tubule, in which two cells were not stained with IgG_3(DT.17).

A

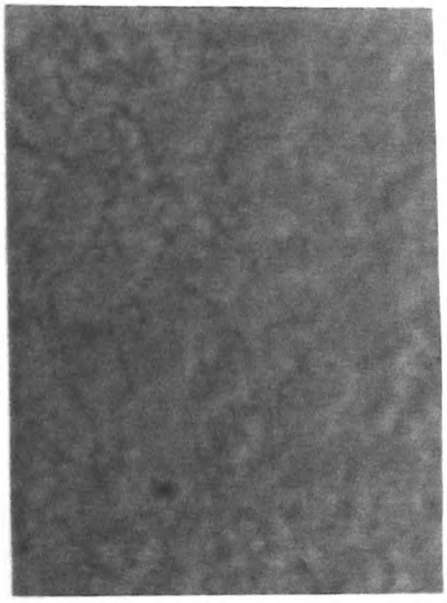

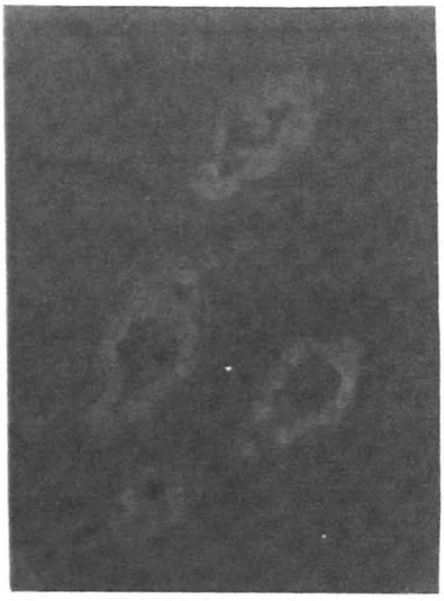

B

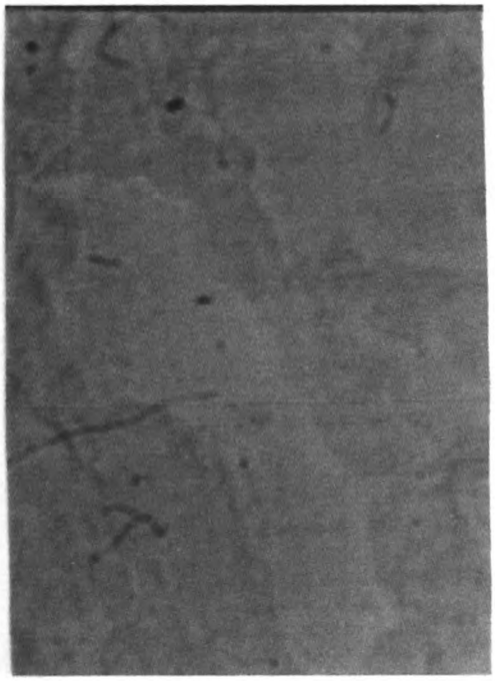

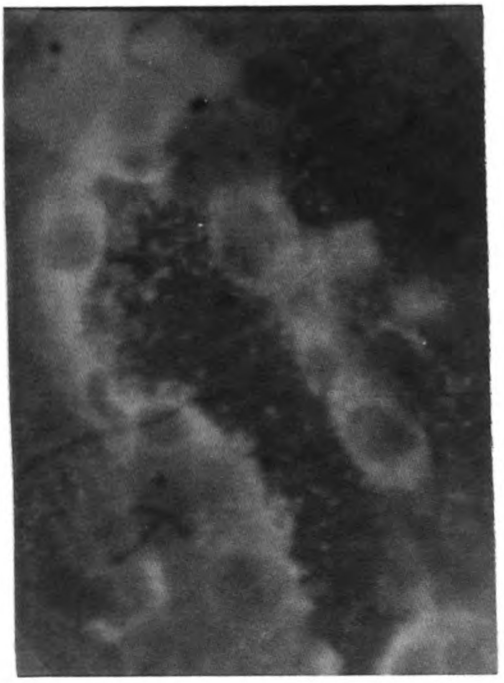

Table 1. Immunostaining and lectin staining of freshly isolated RCCT cells. RCCT cells were tested for staining with IgG_3(rct-30), principal antibody IgG_3(DT.17), and intercalated cell marker FITC-PNA. The cells counted are from one isolation, similar results were obtained from another similar isolation.

	reactive cells	cell number
IgG_3(rct-30)	246 (100%)	247
DT.17	162 (60%)	268
FITC-PNA	76 (28%)	271

Figure 3. Fluorescence digital image of freshly isolated RCCT cells stained with IgG_3(rct-30). Cells were immunodissected and stained as described in the text. The ring-like staining is typically observed for cell surface antigens. The fluorescence value of pseudo colors are indicated by the color bar on the right.

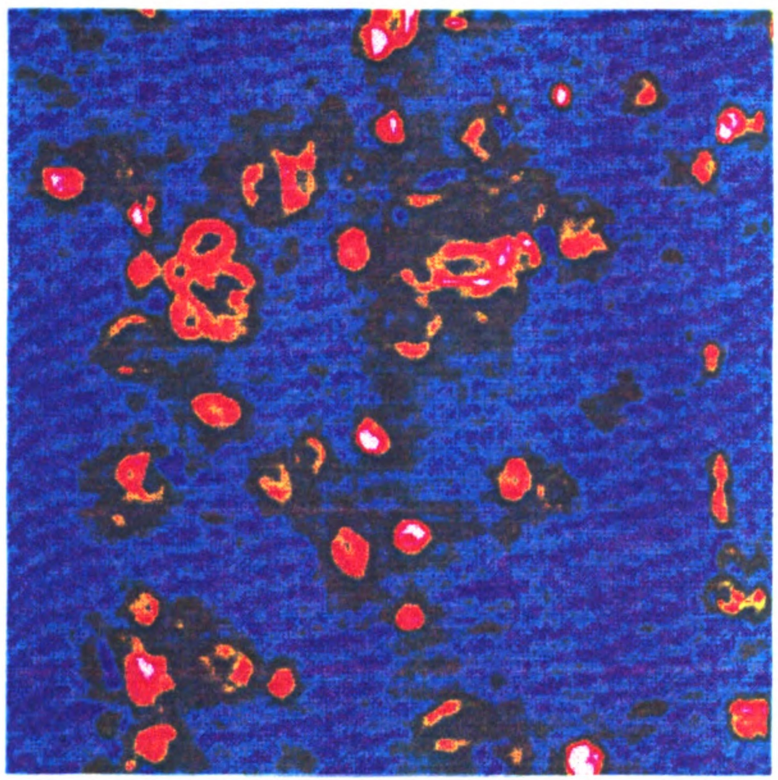
Color Values
3000↑
2859
2718
2577
2437
2296
2155
2015
1874
1733
1593
1452
1311
1171
1030
889
749↓

Figure 4. Fluorescence digital images of freshly isolated RCCT cells stained with an anti-principal cell antibody IgG_3(DT.17). (A). The basolateral surface of a piece of undigested tubule, showing a mosaic staining pattern for IgG_3(DT.17). (B). Individual cells stained with IgG_3(DT.17). The dark shades in between the stained cells were unstained cells, whose fluorescence was lower than that of the background of the well.

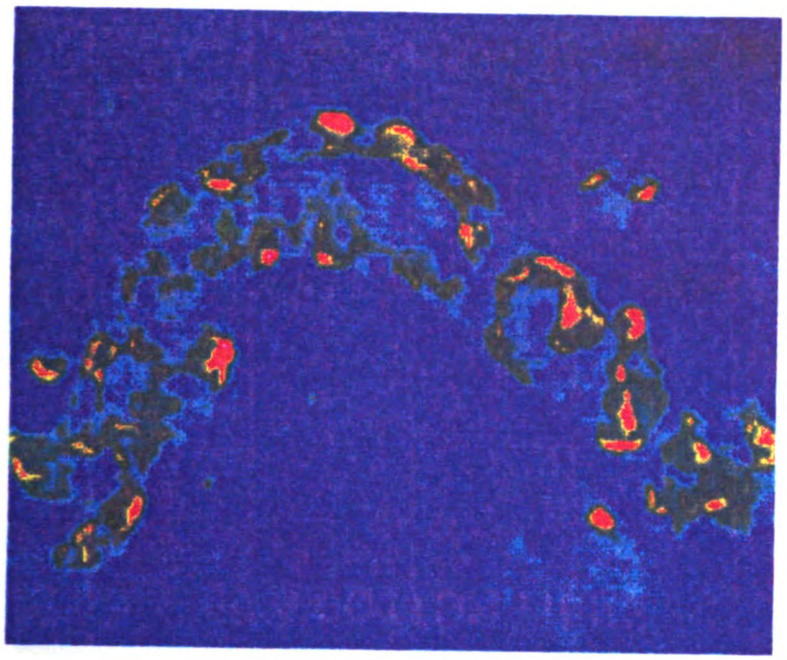
Color Values
1900↑
1796
1693
1590
1487
1384
1280
1177
1074
971
868
764
661
558
455
352
249↓

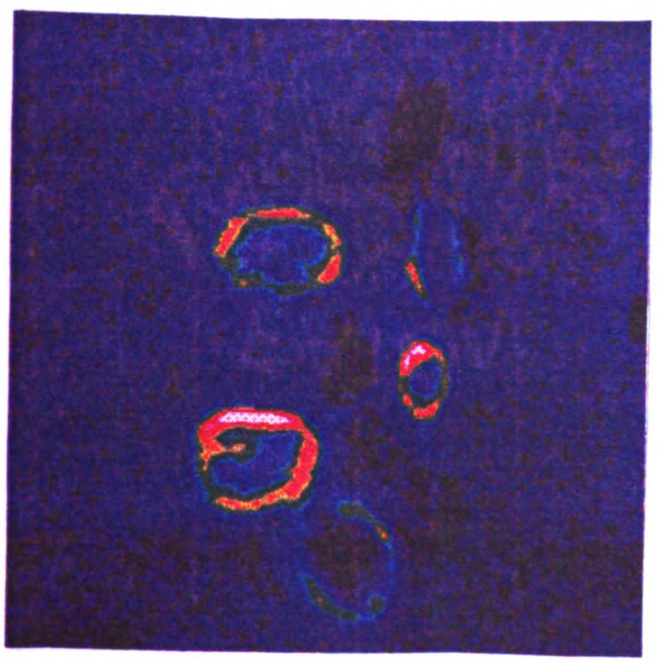
Color Values
1900↑
1856
1812
1768
1724
1680
1637
1593
1549
1505
1461
1418
1374
1330
1286
1242
1199↓

Figure 5. Fluorescence digital image of freshly isolated RCCT cells stained with intercalated cell marker FITC-labeled peanut lectin (PNA).Staining was performed as described in the text. In stained cells, FITC-PNA aggregated on membrane. This "capping" phenomenon is typically observed with lectin staining.

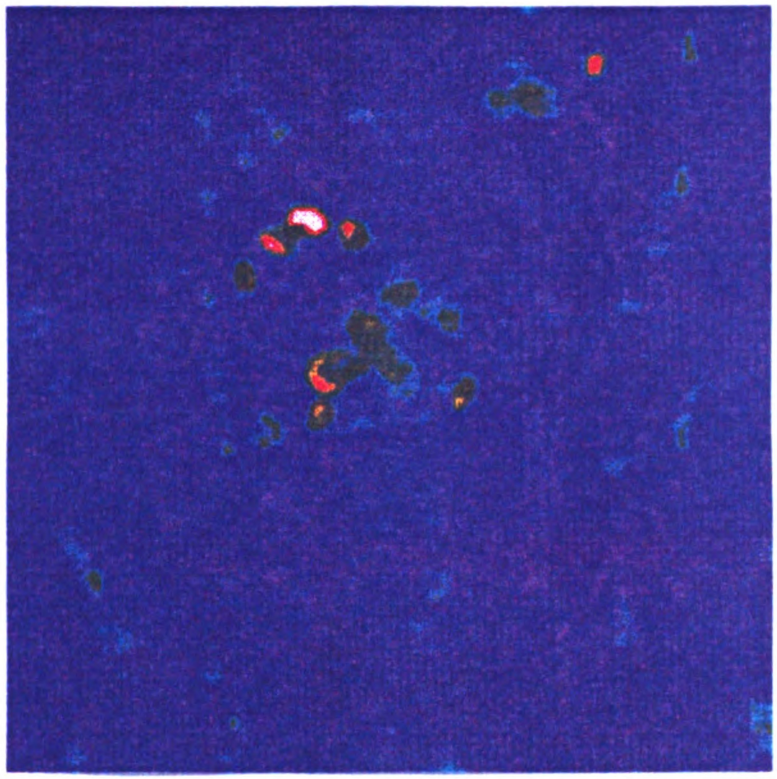
Color Values
- 2700↑
- 2578
- 2456
- 2334
- 2212
- 2090
- 1968
- 1846
- 1724
- 1602
- 1480
- 1358
- 1236
- 1114
- 992
- 870
- 749↓

Figure 6. Ca^{++} mobilization in RCCT cells in response to agonists as observed by fluorescence digital imaging. One-day cultured RCCT cells were loaded with fluo-3 and stimulated with 10^{-5} M PGE_2 and 10^{-5} M AVP consecutively. A. Cells in the buffer. B. cells 10 s after addition of PGE_2. C,D: cells 36 s and 52 s after addition of PGE_2. E: cells 78 s after addition of PGE_2 and before addition of AVP. F: cells 10 s after addition of AVP. G,H: cells 36 s and 52 s after addition of AVP.

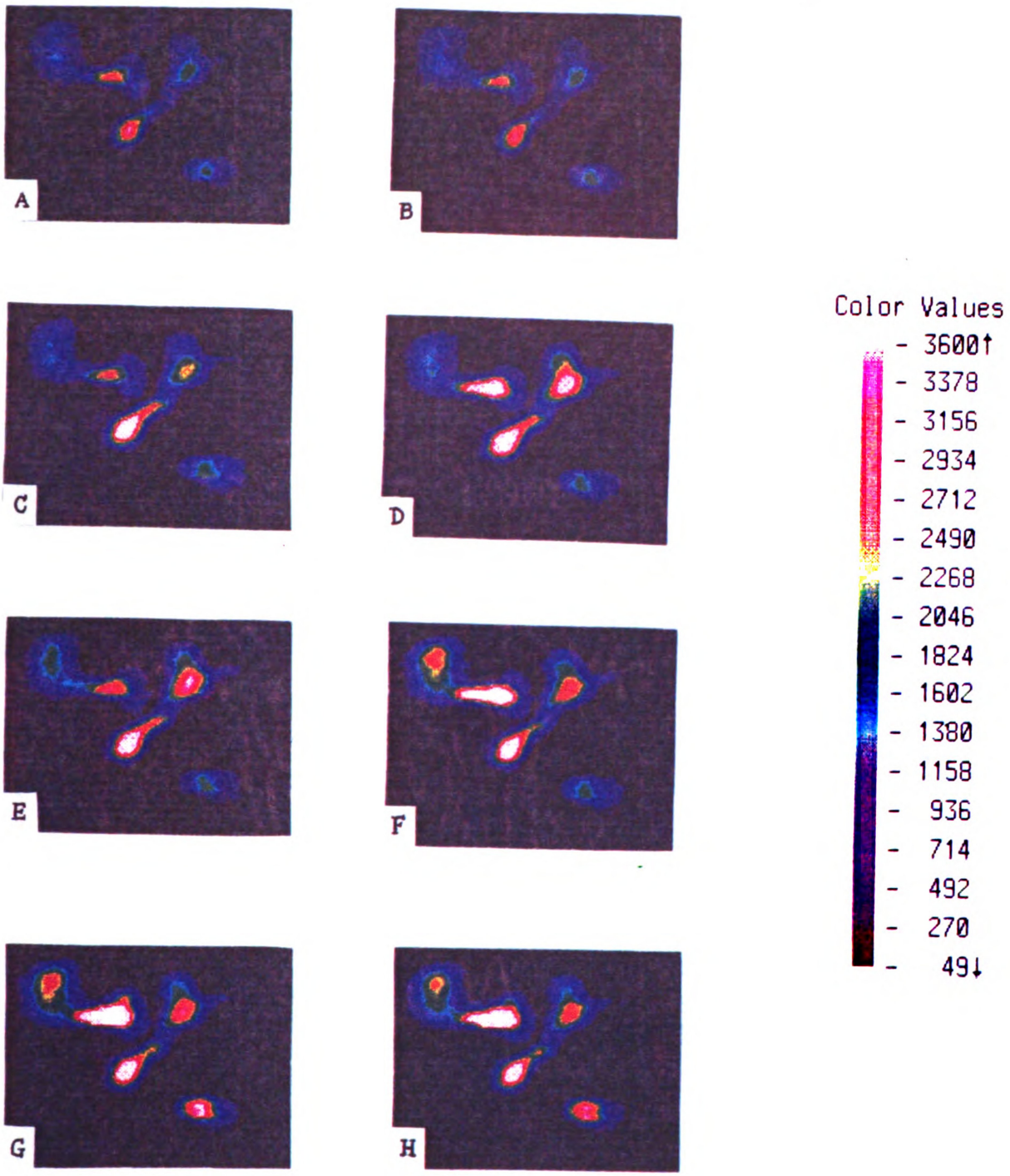
A
B
C
D
E
F
G
H
Color Values
- 3600↑
- 3378
- 3156
- 2934
- 2712
- 2490
- 2268
- 2046
- 1824
- 1602
- 1380
- 1158
- 936
- 714
- 492
- 270
- 49↓

Figure 7. Representative tracings of individual RCCT cells challenged with 10^{-5} M PGE_2 and 10^{-5} M AVP. Cells loaded with fluo-3 were scanned for their fluorescence using an interactive laser cytometer. The eight cells were from one scanned field. Changes in $[Ca^{++}]_i$ were indicated by the changes in fluorescence within each cell. The values on the Y axis are the fluorescence intensity normalized by that of the first scan within each cell. Heterogeneity in responses was shown from this group of cells.+···+···+···+ : cells responding neither to PGE_2 or AVP.■···■···■···■ : cells responding to both PGE_2 and AVP. o···o···o ·o: cells responding only to AVP.●···● ·●···● : cells responding only to PGE_2.

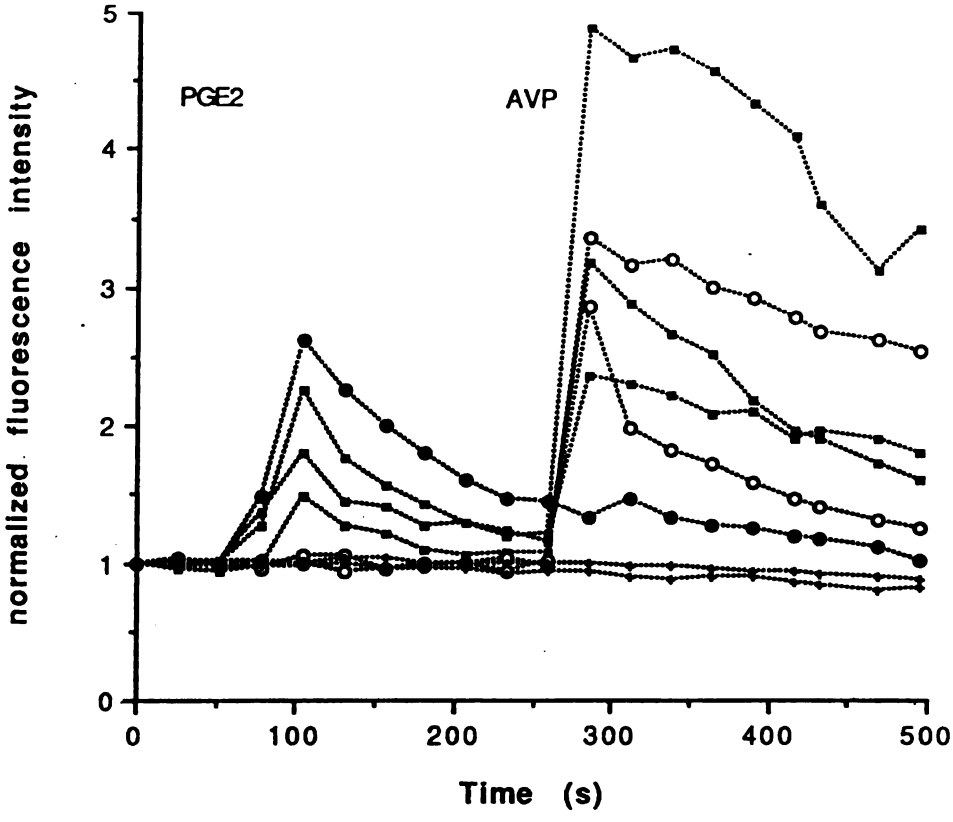
normalized fluorescence intensity
PGE2
AVP
0
1
2
3
4
5
0
100
200
300
400
500
Time (s)

Figure 8. Subpopulations of RCCT cells which mobilize Ca^{++} in response to PGE_2. One-day cultured RCCT cells were loaded with fluo-3 and analyzed for the changes in $[Ca^{++}]_i$ in response to PGE_2. Cells exhibiting an increase in fluorescence intensity of greater than 10% after challenge with agonist were counted as responding cells. Shown in the figure are the percentage of cells responding to PGE_2 (10^{-5} M) in eight representative isolations with 100-150 cells analyzed in each isolation. The size of the subpopulation that responded ranged between about 20% to 60%.

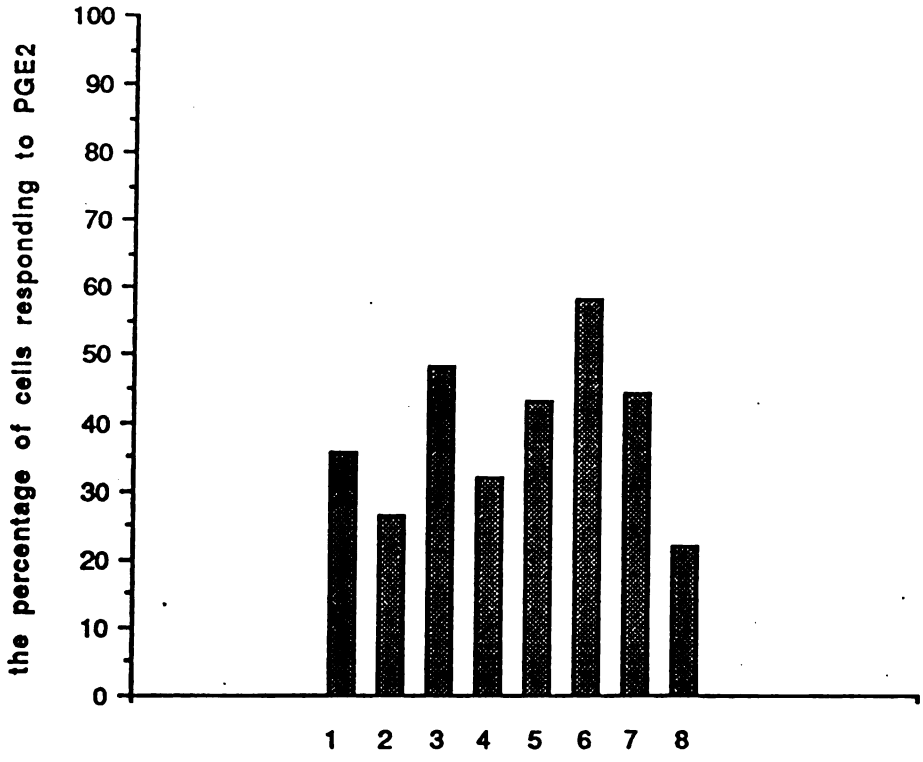
the percentage of cells responding to PGE2
100
90
80
70
60
50
40
30
20
10
0
1
2
3
4
5
6
7
8

Figure 9. Strategy of identifying subtypes of RCCT cells which mobilize Ca^{++} in response to agonists. Cells in grey shades are those loaded with fluo-3. Cells with "*" are responsive cells. Cells in white are those whose fluorescence are quenched by treatement of ionomycin and $MnCl_2$. Cells in dark shades are those which bind with FITC labeled antibody or peanut lectin.

IDENTIFICATION OF SUBTYPE OF RCCT CELLS THAT RESPOND

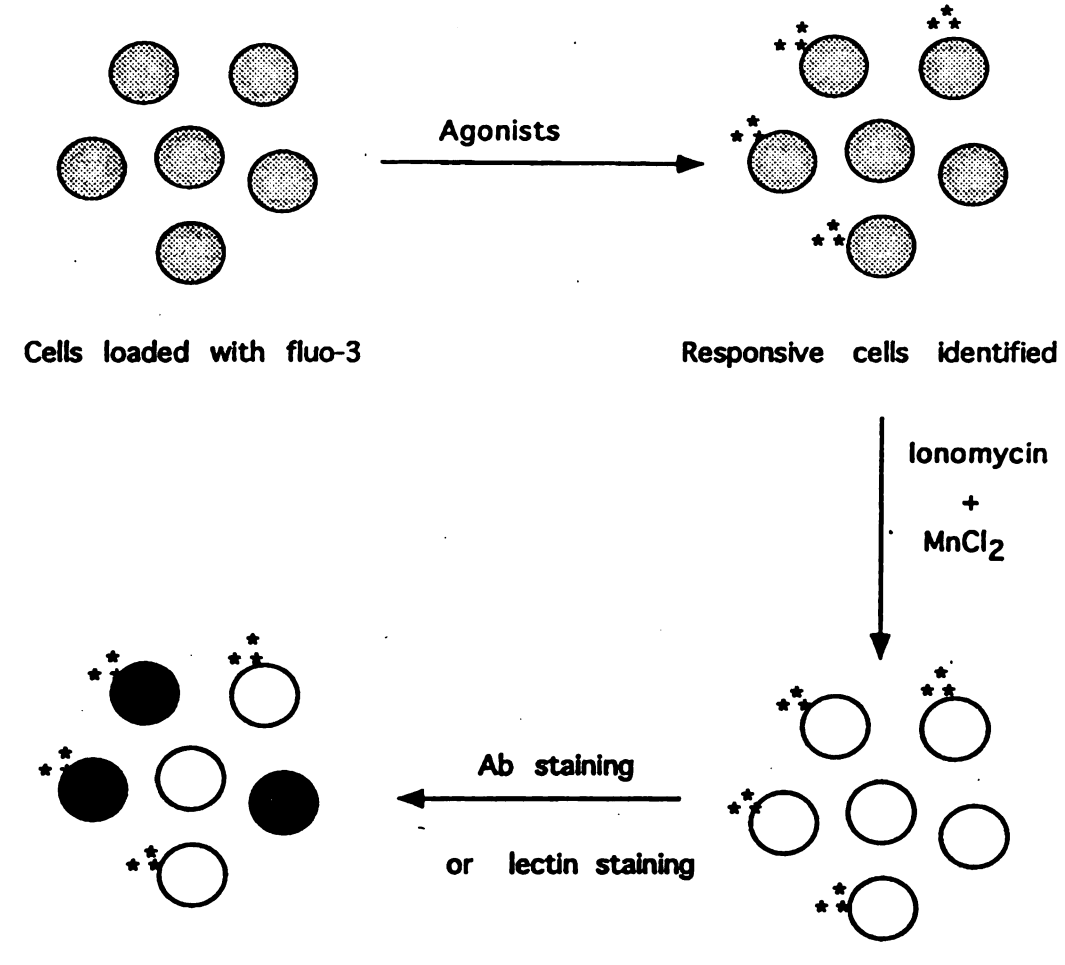

Table 2. PGE_2 and AVP responses in both the principal and intercalated cell. After each tracing of cells challenged with 10^{-5} M PGE_2 and 10^{-5} M AVP, 2 mM $MnCl_2$ was added to cells that were permeabilized with 10^{-5} M ionomycin to quench the fluorescence of fluo-3. Then the cells were stained with hybridoma media of principal cell antibody DT.17 for 10 min, washed, and stained with anti-mouse IgG-FITC (1:10 dilution in SSS) for another 10 min.

	PGE_2(+)	AVP(+)	PGE_2(+)/AVP(+)	n
DT.17(+)	58 (43%)	45 (34%)	28 (21%)	134
DT.17(-)	29 (32%)	32 (35%)	13 (14%)	92
Total	87 (39%)	77 (34%)	41 (18%)	226

Table 3. PGE_2 and AVP responses in subtype B of intercalated cells. After each tracing of cells challenged with 10^{-5} M PGE_2 and 10^{-5} M AVP, 2 mM of $MnCl_2$ was added to the cells that were permeabilized with 10^{-5} M ionomycin to quench the fluorescence of fluo-3. Then FITC-PNA (1:10 dilution in SSS) was added to stain the cells for 5 min. n is the number of cells examined in two isolations.

	PGE_2(+)	AVP(+)	PGE_2(+)/AVP(+)	n
FITC-PNA(-)	85 (40%)	107 (50%)	69 (32%)	213
FITC-PNA(+)	25 (43%)	35 (60%)	20 (35%)	58
Total	110 (41%)	142 (52%)	89 (33%)	271

Figure 10. Dose-response to PGE_2 in RCCT cells. The dose effect was examined by challenging groups of cells with different concentrations of PGE_2. About 100 cells were examined in each group. (A). Dose dependence of the size of responding population. (B). Dose dependence of magnitude of responses in responding cells.

A

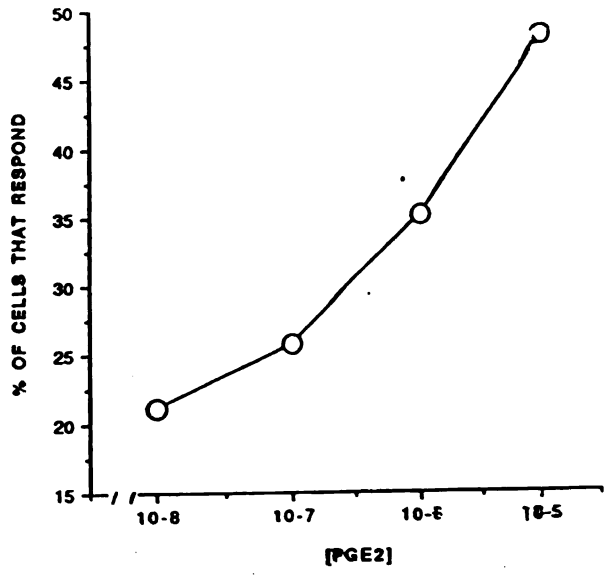
% OF CELLS THAT RESPOND
50
45
40
35
30
25
20
15
10-8
10-7
[PGE2]

B

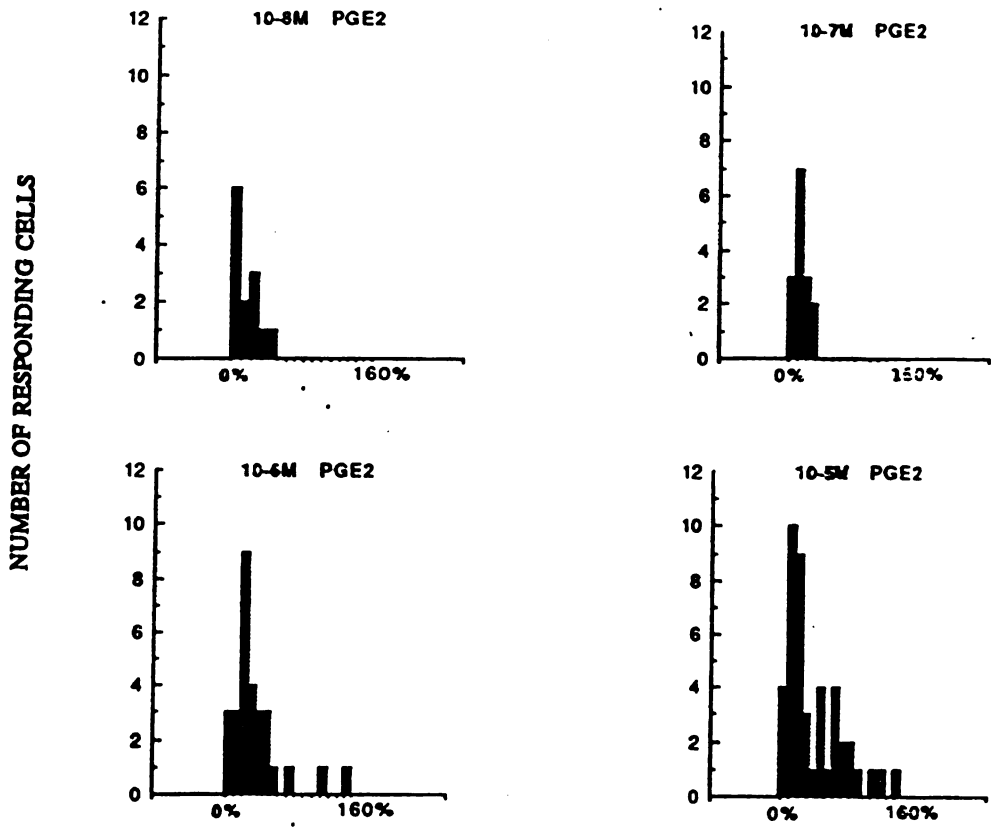
NUMBER OF RESPONDING CELLS
10-8M PGE2
10-7M PGE2
10-6M PGE2
10-5M PGE2
0%
160%
MAGNITUDE OF RESPONDE
(PERCENT INCREASE OF FLUORESCENCE)

Figure 11. The stereospecificity of PGE_2-induced Ca^{++} mobilization. RCCT cells were challenged with 10^{-5} M PGE_2 or 15-(R)-PGE_2. The percentage of cells responding to PGE_2 was significantly higher than that to 15-(R)-PGE_2. ($p<0.02$). The results are from three separate experiments, with about 100 cells examined for each group in each experiment.

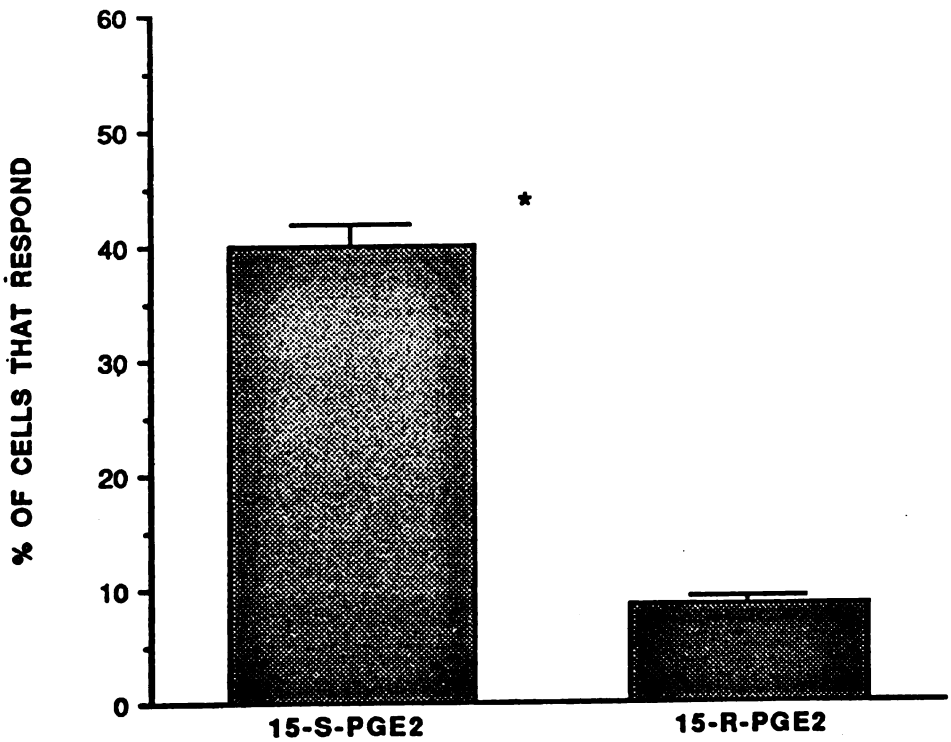
% OF CELLS THAT RESPOND
60
50
40
30
20
10
0
*
15-S-PGE2
15-R-PGE2

Figure 12. The effect of flurbiprofen (FBP) on PGE_2-induced Ca^{++} mobilization by RCCT cells. FBP ($5x10^{-5}$ M) was included in all the isolation solution media and culture media, and the percentage of RCCT cells responding to 10^{-5} M PGE_2 and 10^{-5} M AVP was measured in parallel with RCCT cells isolated and cultured in the absence of FBP. *, significantly increased compared with control (non-treated cells) ($p<0.02$). The results are from two experiments, with about 100 cells examined for each group in each experiment.

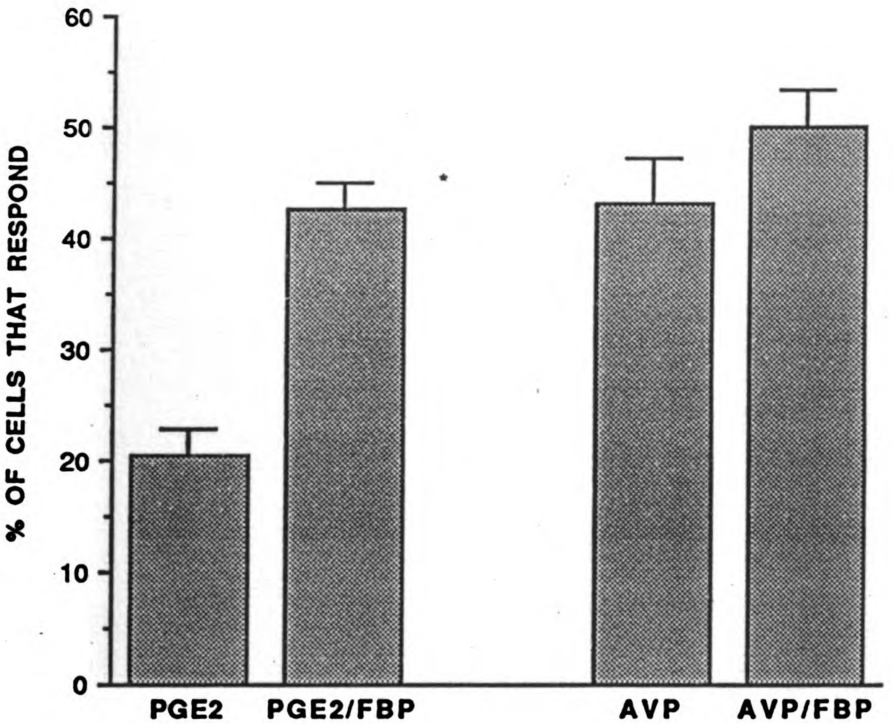
% OF CELLS THAT RESPOND
60
50
40
30
20
10
0
PGE2
PGE2/FBP
AVP
AVP/FBP

Figure 13. Desensitization of PGE_2-induced Ca^{++} mobilization by various prostaglandins and AVP. In all the groups except the control, RCCT cells were treated with desensitizing agonists (10^{-5} M) for 30 min, then rinsed and challenged with 10^{-5} M PGE_2. The size of the responding population in control cells was taken as 100%, to which the response from other groups were compared. *, significantly different from control value (shown by ANOVA analysis).The result are from three experiments, with about 100 cells examined for each group in each experiment.

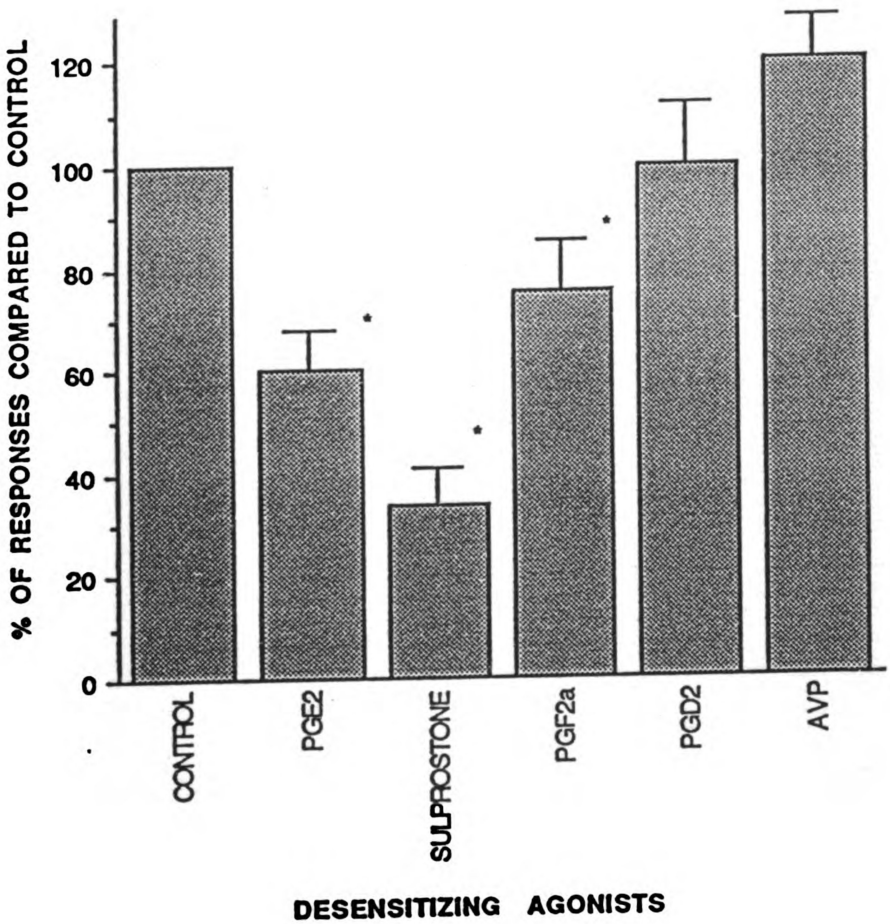
% OF RESPONSES COMPARED TO CONTROL
120
100
80
60
40
20
0
CONTROL
PGE2
SULPROSTONE
PGF2a
PGD2
AVP
DESENSITIZING AGONISTS

Figure 14. The effect of AH6809 on PGE_2-induced Ca^{++} mobilization by RCCT cells and 28A cells. (A). RCCT cells were pretreated with 10^{-5} M AH6809 for 5 min, then rinsed and challenged with 10^{-5} M PGE_2. (B). 28A cells were pretreated with 10^{-4} M AH6809 for 10 min, then rinsed and challenged with 10^{-5} M PGE_2 and CHA consecutively.

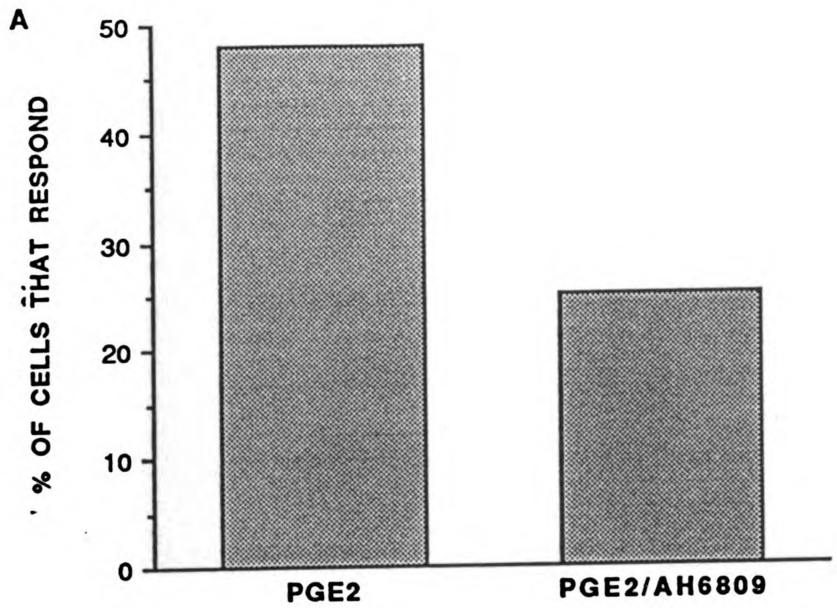
A
% OF CELLS THAT RESPOND
50
40
30
20
10
0
PGE2
PGE2/AH6809

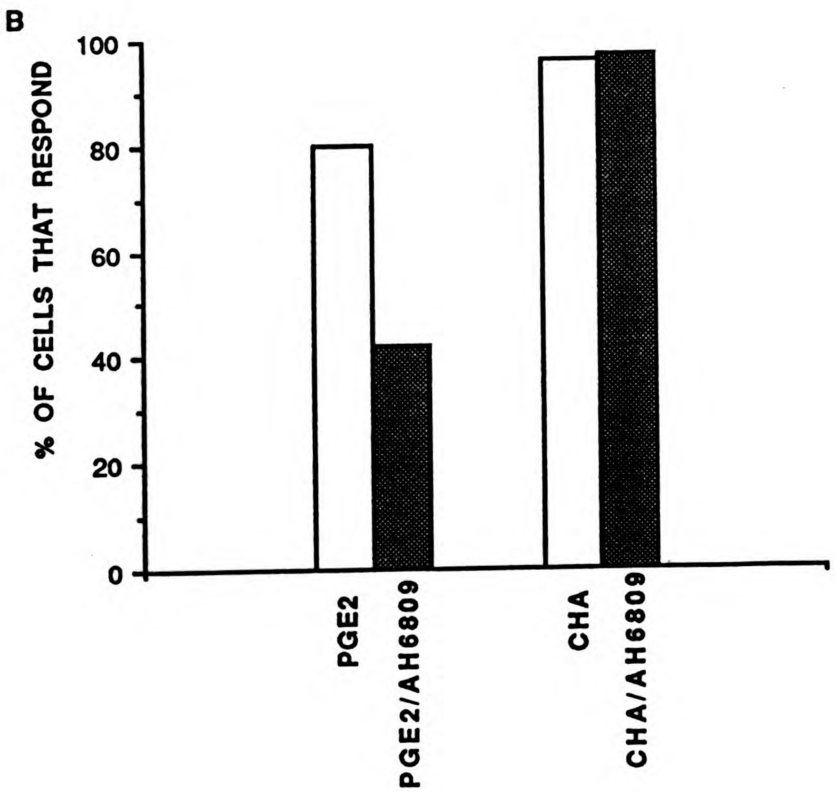
B
% OF CELLS THAT RESPOND
100
80
60
40
20
0
PGE2
PGE2/AH6809
CHA
CHA/AH6809

Figure 15. The effect of depletion of extracellular Ca^{++} on PGE_2-induced Ca^{++} mobilization by RCCT cells. The representative traces of responding cells are shown as (A). in the presence of 1.0 mM extracellular Ca^{++}; B, in the media where 2.5 mM of EDTA was added to chelate the extracellular Ca^{++}.

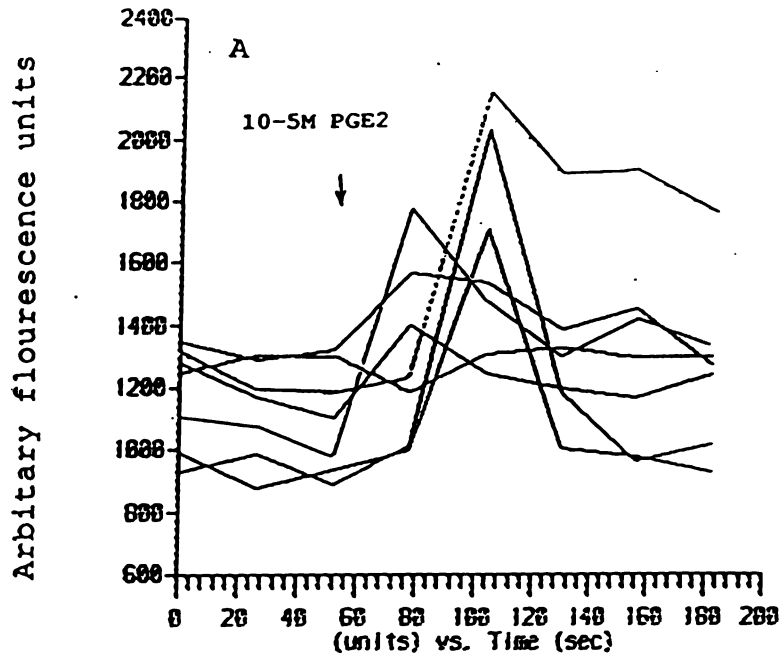
A
10-5M PGE2
Arbitary flourescence units
2400
2200
2000
1800
1600
1400
1200
1000
800
600
0 20 40 60 80 100 120 140 160 180 200
(units) vs. Time (sec)

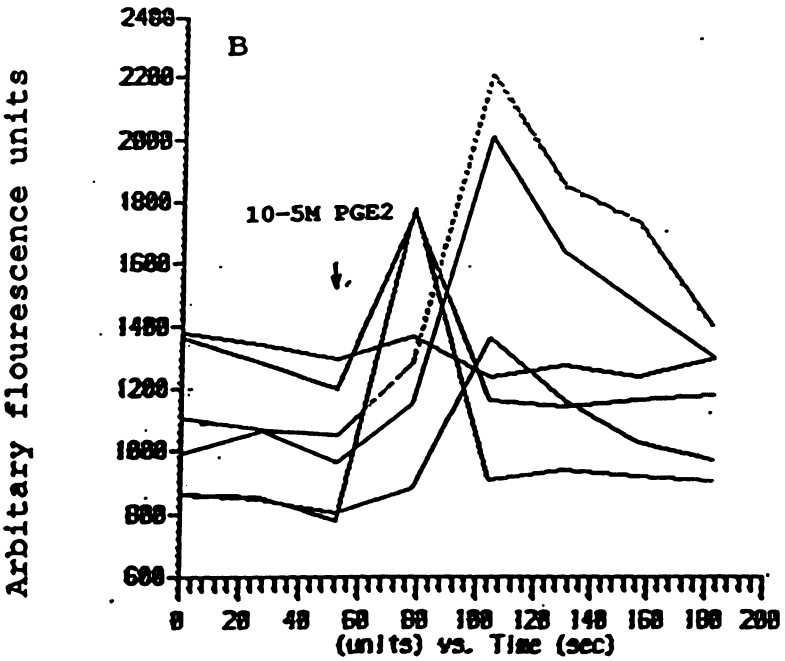
B
10-5M PGE2
Arbitary flourescence units
2400
2200
2000
1800
1600
1400
1200
1000
800
600
0 20 40 60 80 100 120 140 160 180 200
(units) vs. Time (sec)

Figure 16. The effect of TPA on PGE_2- and AVP-induced Ca^{++} mobilization by RCCT cells. (A). The dose effect of TPA on the AVP-induced response. RCCT cells were incubated with the indicated concentration of TPA for 10 min, and were challenged with 10^{-5} M AVP. (B). Cells were incubated with 10^{-6} M TPA and then challenged with 10^{-5} M PGE_2 and then 10^{-5} M AVP.

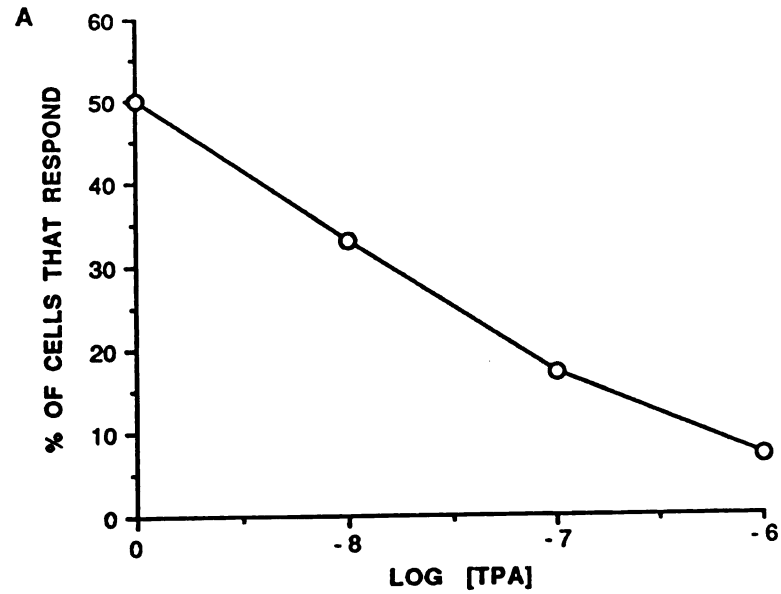
A
% OF CELLS THAT RESPOND
60
50
40
30
20
10
0
0
-8
-7
-6
LOG [TPA]

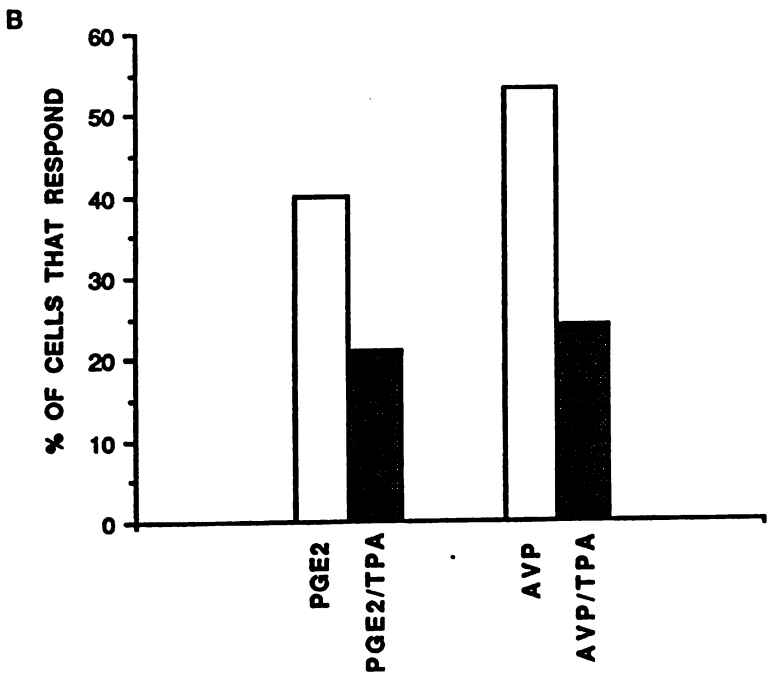
B
% OF CELLS THAT RESPOND
60
50
40
30
20
10
0
PGE2
PGE2/TPA
AVP
AVP/TPA

Figure 17. The effect of PTX on PGE_2-induced Ca^{++} mobilization by RCCT cells and 28A cells. (A). RCCT cells were treated with PTX (2.5 μg/ml) for 12-16 hours, and then the response to 10^{-5} M PGE_2 was examined. The result are from three experiments, with about 100 cells examined for each group in each experiment. (B). 28A cells were treated under the same condition used to treat RCCT cells, and the responses to 10^{-5} M PGE_2, CHA and AVP was examined.

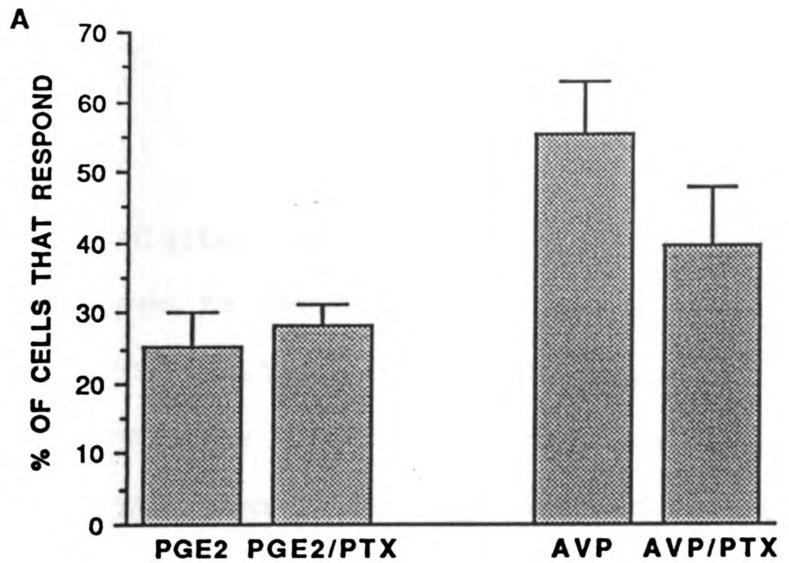
A
% OF CELLS THAT RESPOND
70
60
50
40
30
20
10
0
PGE2
PGE2/PTX
AVP
AVP/PTX

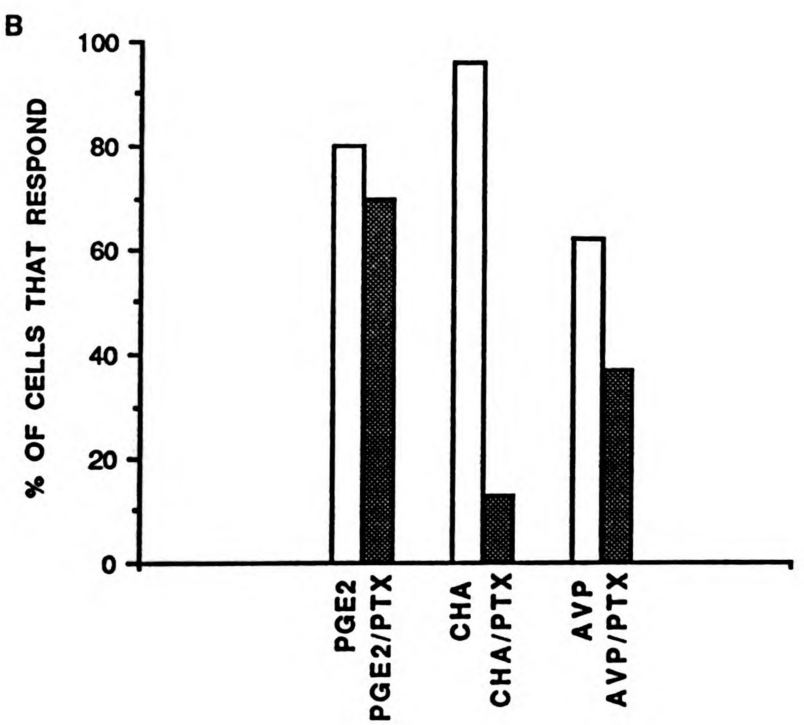
B
% OF CELLS THAT RESPOND
100
80
60
40
20
0
PGE2
PGE2/PTX
CHA
CHA/PTX
AVP
AVP/PTX

DISCUSSION

Digital imaging analysis of fluo-3 fluorescence was employed to examine the effect of PGE_2 on Ca^{++} mobilization in RCCT cells at the single cell level. This study demonstrates that PGE_2 evokes an increase in $[Ca^{++}]_i$ in a subpopulation of one-day cultured RCCT cells. A heterogeneity in the responses to PGE_2 and AVP in those cells was observed. The responsive cells were indiscriminately distributed among all subtypes of RCCT cells. Several observations suggest that PGE_2 acts via a receptor to induce Ca^{++} mobilization. For example, the effect of PGE_2 is dose dependent, stereospecific, agonist specific, and upregulated by the inhibition of prostaglandin synthesis.

The receptor mediating PGE_2-induced Ca^{++} mobilization is pharmacologically distinct from the previously characterized adenylate cyclase stimulatory EP2 receptor and the inhibitory EP3 receptor in RCCT cells (2). EP2 receptors are unresponsive to sulprostone, the agonist for EP1 and EP3 receptors; EP3 receptors are insensitive to the PGE receptor antagonist AH6809 (17). PGE_2 induced Ca^{++} mobilization in RCCT cells, however, was found to be moderately responsive to and potently desensitized by sulprostone. Moreover, it was blocked by

AH6809. This pharmacological profile resembles that of EP1 receptors, the subtype of PGE receptors involved in smooth muscle contraction possibly via Ca^{++} mobilization. Unlike the EP3 receptor, this EP1-like receptor of RCCT cells was not coupled to a PTX-sensitive G protein.

The collecting tubule system is well known for its structural and functional heterogeneity (18,19). Different subtypes of cells are engaged in different transport activities, and considerable effort has been made to associate specific tubule functions with specific cell types. Principal cells are the most abundant cell type and function primarily to modulate AVP-induced water reabsorption, to reabsorb Na^+, and to secrete K^+ (7). Intercalated cells are interspersed between principal cells, and make up about 35-40% of the total cell population in the cortical collecting tubule (20). Two subtypes of intercalated cells are present. Type A intercalated cells, which are H^+-ATPase and band 3 protein positive, secrete H^+ and reabsorb luminal HCO_3^-; Type B intercalated cells, which can be identified by their staining by FITC-labeled PNA, are responsible for HCO_3^- secretion (21). The observation in our studies that PGE_2 induces Ca^{++} mobilization in principal cells is consistent with the role of cytosolic Ca^{++} Breyer et. al. demonstrated in inhibiting water reabsorption and sodium transport in collecting tubules perfused with PGE_2 (5,6). The simultaneous presence of this

PGE_2-induced response in intercalated cells suggested the possible involvement of Ca^{++} in other functions, such as acid or bicarbonate secretion. The approach applied in our study enabled us to associate the Ca^{++} mobilization with a specific cell type at the single cell level. This approach should also be feasible for other ion transport studies in RCCT cells, including Na^+, Cl^-, HCO_3^-, H^+, where appropriate fluorescence indicators are available.

There is always a constant concern whether the freshly isolated cells would undergo phenotypic changes during culture. We tried to use fresh cells in our experiment, but we found that the vitality of cells was largely lost after the isolating procedure. In freshly isolated RCCT cells, only 20-40% of the total population would respond to Ca^{++} ionophore ionomycin, compared to 60-80% in one-day cultured cells. To examine if the immuno-specificity and the composition of cultured cells remained unchanged compared to fresh cells, these cells were stained with Ig_3(rct-30), principal-specific antibody IgG_3(DT.17), and FITC-PNA. It was found that all cells were stained with IgG_3(rct-30); 59% of them were reactive to IgG_3(DT.17); and 21% of them were reactive to FITC-PNA. This result was comparable with that in freshly isolated cells (Table 1), indicating that the cultured cells did not change their phenotypes during the one-day culture.

To date, the product of PIP_2 hydrolysis, IP_3, is the best-

defined mediator involved in the release of Ca^{++} from intracellular stores. In the case of RCCT cells, no significant inositol phosphates production was observed in response to PGE_2. It is not known if there exists another mediator for Ca^{++} release in these cells, or if the amount of inositol phosphates produced in the subpopulation of responding RCCT cells were simply too low to be detected. No significant inositol phosphates formation in response to PGE_2 was detected in 28A cells, either, although the size of subpopulation of responding cells is larger than that in RCCT cells.

REFERENCES

1. Grenier, F.C., Smith, W.L. (1978) Prostaglandins 16, 759-772.
2. Sonnenburg, W.K., Smith, W.L. (1988) J. Biol. Chem. 236, 6155-6160.
3. Sonnenburg, W.K., Zhu, J., Smith, W.L. (1990) J. Biol. Chem. 265, 8479-8483.
4. Grantham, J.J., Orloff, J. (1968) J. Clin. Invest. 47, 1154-1161.
5. Breyer, M.D., Jacobson, H.R., Hebert, R.L. (1990) Kidney International 38, 618-624.
6. Hebert, R.L., Jacobson, H.R., Breyer, M.D. (1991) J. Clin. Invest. 87, 1992-1998.
7. Fejes-Toth, G., Fejes-Toth, A.N. (1989) Am. J. Physiol. 256, F742-F750.
8. Garcia-Perez. A., Smith, W.L. (1984) Clin. Invest. 74, 63-74.
9. Spielman, W.S., Sonnenburg, W.K., Allen, M.L., Arend, J.L., Gerozissis, K., Smith, W.L. (1986) Am. J. Physiol. 251, F348-F367.
10. Vandenberghe, P.A., Ceuppens, J.L. (1990) J. Immun. Method 127, 197-205.
11. Arend, L.J., Handler, J.S., Rhim, J.S., Gusovsky, F.,

Spielman, W.S. (1989) Am. J. Physiol. 256, F1067-F1074.

12. Berridge, M.J., Dawson, R.M.C. et.al. (1983) Biochem. J. 212, 473-482.
13. De Asua, L.J., Otto, A.M., Lindgren, J.A., Hammarstrom, S. (1983) J. Biol. Chem. 258, 8774-8780.
14. Limas, C., Limas, C. (1984) Arch. Biochem. and Biophy. 233, 32-42.
15. Rice, M.G., Mcrae, J.R., Storm, D.R., Robertson, R.P. (1981) Am. J. Physiol. 241, E291-E297.
16. Coleman, R.A., Kennedy, I., Humphrey, P.P.A., Bunce, K., and Lumley, P. (1990) Prostanoids and their receptors. In: Comprehensive Medicinal Chemistry, Oxford:Pergamon, Vol.3, p643-714.
17. Coleman R.A., Humphrey, P.P.A., Kennedy I. (1985) In Trends in Autonomic Pharmacology. Kalsner S (ed.), Taylor and Francis, London and Philiadelphia, vol. p.35
18. Lefurgey, A., Tisher, C.C. (1979) Am J. Anat. 155, 111-124.
19. Madsen, K.M., Tisher, C.C. (1986) Am. J. Physiol. 250, F1-F15.
20. Brown, D., Roth, J., Orci, L. (1985) Am J. Physiol. 248, C348-C356.
21. Alper, S.L., Natale, J., Gluck, S., Lodish, H.F., Brown, D. (1989) Proc. Natl. Acad. Sci. USA 86, 5429-5433.

CHAPTER THREE

PROSTAGLANDIN E_2 ACTIVATES THE PHOSPHOLIPASE C PATHWAY IN SWISS 3T3 CELLS THROUGH THE SAME RECEPTOR THAT INTERACTS WITH PROSTAGLANDIN $F_{2\alpha}$

Prostaglandins can modulate differentiation and proliferation of a variety of mammalian cells (1-3). Prostaglandin $F_{2\alpha}$, in particular, acts as a potent mitogen in fibroblast-like Swiss mouse 3T3 cells (4,5). As with other mitogens such as bombesin, bradykinin and vasopressin, $PGF_{2\alpha}$ stimulates cell growth by turning on the phospholipase C (PLC) pathway. PLC-mediated phosphotidylinositol-4,5-bisphosphate (PIP_2) hydrolysis leads to activation of protein kinase C (PKC) and mobilization of intracellular Ca^{++}, both of which are involved in various steps of cell proliferation (10).

The prostaglandin E series, PGE_1 and PGE_2, do not by themselves have as potent mitogenic effects as $PGF_{2\alpha}$. However, in the presence of submaximal levels of insulin, PGE_1 and PGE_2 remarkably stimulate DNA synthesis in quiescent Swiss mouse 3T3 cells (4). It has been reported that PGE_1 induces cAMP formation (6) in these cells, without eliciting the PIP_2 hydrolysis. Increased levels of cAMP are thought to act

synergistically with second messengers induced by insulin to initiate DNA synthesis and cell division.

In this study, we demonstrated that PGE_2 can activate the PLC pathway in Swiss 3T3 cells. PGE_2 stimulated PIP_2 hydrolysis and subsequent Ca^{++} release from internal stores. Depletion of PKC in 3T3 cells by chronic treatment of TPA potentiates both the production of inositol phosphates (IPs) and Ca^{++} mobilization, suggesting a negative regulatory role of PKC in this pathway. Our study indicates that PGE_2 and $PGF_{2\alpha}$ share the same receptor that mediates activation of PLC.

MATERIALS AND METHODS

Materials. Dulbecco's modified Eagle medium (DMEM) was purchased from GIBCO. Bovine calf serum (CS) was from Hyclone Laboratories. Fura-2/AM was from Molecular Probe Inc. Myo-[^{3}H]inositol was from New England Nuclear. Medium 199, trypsin, bombesin and 12-O-tetradecanoyl-phorbol-13-acetate (TPA) were from Sigma. PGE_2, $PGF_{2\alpha}$, 15-(R)-PGE_2 were from Cayman Chemical Company. Pertussis toxin (PTX) was from List Biological Laboratories. Sulprostone was a gift from Schering AG, Berlin. AH6809 was a gift from Glaxo Group Research Limited, UK. Swiss 3T3 mouse fibroblasts were from the American Type Culture Collection.

Treatments and labeling of cells. Swiss 3T3 cells were seeded onto 24-well tissue culture plates (for measurement of IPs) or 100-mm tissue culture dishes (for measurement of Ca^{++} mobilization) in DMEM containing 10% CS. After the cells reached confluence and became quiescent, they were subjected to various treatments. For TPA treatment, the cells were incubated with medium containing TPA (300 ng/ml) for 48 hours. For pertussis toxin treatments, the cells were incubated with medium containing PTX (100 ng/ml) for 18 hours. For labeling of cells with myo-[^{3}H]inositol, confluent cells after a one day treatment of TPA were incubated in medium 199^+ (medium 199

supplemented with 200 mM Glutamine) containing myo-[^{3}H]inositol (10 μCi/ml) and TPA (300 ng/ml) for 12-18 hours.

Measurement of IPs formation. Cells labeled with myo-[^{3}H]inositol labeled cells in each well of a 24-well plate were washed and then incubated with 0.5 ml of Hepes/lithium buffer (4.7 mM KCl, 0.5 mM EDTA, 13 mM glucose, 20 mM Hepes, 1.2 mM KH_2PO_4, 1.2 mM $MgSO_4$, 58 mM NaCl, 60 mM LiCl, 1.5 mM $CaCl_2$) for 30 min. The Hepes/Li buffer was replaced by simplified saline solution (SSS: 145 mM NaCl, 5 mM KCl, 1 mM Na_2HPO_4, 0.5 mM $MgCl_2$, 5 mM glucose, 10 mM Hepes, 1 mM $CaCl_2$, pH7.4) containing vehicle as control or different agonists, and incubated for various lengths of times. The incubations were stopped by adding 0.5 ml of 12% ice-cold trichloroacetic acid to each well. Cells were then frozen at -70°C. After defrosting, the media were collected and centrifuged; 0.85 ml of the supernant from each sample was loaded onto an AG-1x8 resin column (0.7 ml bed volume) pre-equilibrated with deionized water and washed with 3x 3 ml of water and 2x 3 ml of 100 mM ammonium formate/sodium borate. To collect pooled IPs, columns were washed with 3x 2ml of 1 M ammonium formate/formic acid. To separate IP_1, IP_2, and IP_3, columns were washed stepwise with 1x 2 ml of 200 mM, 400 mM and 1 M ammonium formate/formic acid. The eluates were collected in scintillation vials and quantitated by liquid scintillation counting.

Measurement of intracellular calcium concentration

$([Ca^{++}]_i)$. Confluent Swiss mouse 3T3 cells in 100-mm dish were loaded with fura-2 by incubating in DMEM containing 1.3 μM fura-2/AM at 37°C for 40 min. The dye-loaded cells on the culture dish were then rinsed with PBS, detatched by treatment with 0.25% trypsin, and collected and resuspended in SSS. For each measurement, about $5x10^5$ cells were suspended in 1.5 ml of SSS in a temperature-controlled cuvette. Fluorescence (F) was measured with a SPEX dual excitation wavelength spectrofluorometer. Cells were excited at 340 nm and 380 nm, and the emission was monitored at 505 nm. The fluorescence ratio R was obtained by dividing the fluorescence excited at 340 nm by the fluorescence excited at 380 nm. The intracellular Ca^{++} ($[Ca^{++}]_i$) was calculated as described by Grynkiewitz et al.(7), using the formula:

$$[Ca^{++}]_i=(R-R_0/R_s-R) \times (F_0/F_s)_{380} \times K_d.$$

The R_0 is the ratio at zero $[Ca^{++}]_i$ and the R_s is the ratio at saturating $[Ca^{++}]_i$; a value of 224 nM was used as the dissociation constant K_d for the fura-2-Ca^{++} complex (7).

RESULTS

Effect of PGE_2 and $PGF_{2\alpha}$ on Ca^{++} mobilization and IPs formation in Swiss mouse 3T3 cells. Treatment of confluent quiescent 3T3 cells with PGE_2 or $PGF_{2\alpha}$ induces an increase in intracellular Ca^{++} concentrations. As shown by the representative tracings in Fig.1, in response to PGE_2 and $PGF_{2\alpha}$, there were rapid increases of $[Ca^{++}]_i$ from a resting value of around 100 nM to a maximal value, which then gradually declined towards the basal level. As shown in Fig.2, the response is dose-dependent. $PGF_{2\alpha}$ is a more potent effector than PGE_2. The concentrations necessary to produce 50% of the maximal effect (EC_{50}) were detected at $5x10^{-8}$ M $PGF_{2\alpha}$ and at $2x10^{-6}$ M PGE_2. The maximal response to $PGF_{2\alpha}$ (320%) is also somewhat larger than that to PGE_2 (230%). This profile agrees well with the effects of these two compounds on the initiation of DNA synthesis by these cells in the presence of insulin (4).

Since in many cell types, Ca^{++} mobilization is mediated by the second messenger IP_3, the effects of PGE_2 and $PGF_{2\alpha}$ on inositol phosphate formation were examined. Confluent quiescent cells were labeled with myo-[^{3}H]inositol, and the radiolabeled inositol phosphates were measured in cells

stimulated by PGE_2 and $PGF_{2\alpha}$. Indeed, 10 μM of PGE_2 and $PGF_{2\alpha}$ increased IPs 250±50% and 300±50% (n=2) respectively, over the basal levels (Fig.3).

Down-regulation of PKC potentiates IPs formation and Ca^{++} mobilization. When confluent quiescent cells were incubated with TPA (300 ng/ml) for 48 hours, PKC in these cells is depleted (8). To determine the impact of PKC on the IP_3/Ca^{++} pathway activated by PGE_2 and $PGF_{2\alpha}$, TPA was used to treat confluent quiescent 3T3 cells. After 40-48 hours treatment, we observed that the round-shaped quiescent cells became spindle-shaped as if they resumed to proliferative mode. Ca^{++} mobilization in response to PGE_2 and $PGF_{2\alpha}$ were measured in cells treated with or without TPA for 40-48 hours. As shown in Fig.4, TPA did not significantly change the level of IPs in control wells treated with vehicle (680±20 cpm vs 790±30 cpm); however, TPA treatment potentiated the effect of 10 μM of both PGE_2 (3220±130 cpm vs 1730±100 cpm) and $PGF_{2\alpha}$ (4480±50 cpm vs 2230±60 cpm). Similarly, the effects of both PGE_2 and $PGF_{2\alpha}$ on Ca^{++} mobilization were potentiated in TPA-treated cells. In non-treated cells, 10 μM PGE_2 and $PGF_{2\alpha}$ raised $[Ca^{++}]_i$ by 310±50% and 390±20% (n=3) (Fig.5), respectively; while in TPA-treated cells, the values were increased to 630±70% and 660±60% (n=3), respectively. These results suggest that in normal cells, PKC is activated upon PGE_2 and $PGF_{2\alpha}$ stimulation, and that PKC then exerts its

typical negative feedback effect leading to inhibition of both IPs formation and Ca^{++} mobilization. Depletion of PKC by chronic treatment with TPA appeared to diminish the IP_3/Ca^{++} pathway from the inhibitory effect of PKC.

Characterization of the responses to PGE_2 in PKC-depleted cells. The responses of IPs and Ca^{++} occurring to PGE_2 were studied in PKC-depleted cells. Formation of IPs in response to PGE_2 was dose-dependent. Fig.6 shows the effects of increasing doses of PGE_2 and $PGF_{2\alpha}$ on IPs level after a 30 min treatment. The half-maximum stimulation occurred at $9x10^{-9}$ M for $PGF_{2\alpha}$, and at $2x10^{-6}$ M for PGE_2. The time course of IP_1, IP_2 and IP_3 following the addition of 10 μM of PGE_2 is shown in Fig.7. IP_3 formation could be detected as early as 30 seconds and appeared to reach a plateau after 1 min. Formation of IP_1 and IP_2 increased more slowly than IP_3.

PGE_2 stimulates IPs formation by acting through a specific receptor. This is supported by the finding that the effect of PGE_2 is stereospecific (Fig.8). The naturally occurring 15-S-PGE_2 increased IPs formation by 470$\pm$40% (n=2); its enantiomer, 15-R-PGE_2, increased IPs formation by only 250$\pm$10% (n=2). Sulprostone, an acylsulphonamide analog of PGE_2 which is used as an agonist for the EP_1 receptor, was found to be equipotent to PGE_2 (Fig.9). However, AH6809, an EP_1-specific antagonist, did not inhibit PGE_2-stimulated IPs formation (Fig.10).

To test whether a pertussis toxin (PTX)-sensitive or a PTX-insensitive G protein is involved in PGE_2-dependent IPs formation, cells were treated with 100 ng PTX /ml and 1000 ng PTX/ml for 12-18 hours. As shown in Fig.11, the lower concentration (100 ng/ml) of PTX had no effect on PGE_2-induced IPs formation, whereas in cells treated with higher concentration (1000 ng/ml) of PTX, there was a 20% loss of the responsiveness compared to control cells.

The PGE_2-induced IP_3 would be expected to trigger the release of Ca^{++} from intracellular stores. That this is the case is demonstrated in Fig.12. When extracellular Ca^{++} was removed by adding 1 mM EGTA to Ca^{++}-free SSS, the basal $[Ca^{++}]_i$ dropped from 100 nM to 40 nM. PGE_2 (10 μM) raised the $[Ca^{++}]_i$ from 40 nM to 230 nM--a 530% increase.

The dose response (Fig.13) of PGE_2-induced Ca^{++} mobilization in PKC-depleted 3T3 cells revealed a EC_{50} of $2x10^{-6}$ M, which is the same as that for the effect of PGE_2 on Ca^{++} mobilzation in normal 3T3 cells. The maximal response, however, was significantly higher in PKC-depleted cells than normal cells (530% vs 230%). The situation was similar with $PGF_{2\alpha}$ (EC_{50} of $9x10^{-8}$ vs $5x10^{-8}$; maximal response of 710% vs 320% for TPA-treated and untreated cells, respectively). Possibly, the negative modulation of PKC targets on components downstream the receptor in the pathway, so that PKC inhibits the agonist-induced response without changing the affinity of

the receptor for its ligands, as indicated by the unchanged EC_{50} in treated and non-treated cells. Furthermore, EC_{50} of PGE_2 for mobilizing Ca^{++} in PKC-depleted cells was the same as its EC_{50} in stimulating IPs formation in those cells (EC_{50}=2 μM). This correlation between IPs formation and Ca^{++} mobilization are consistent with the concept that PGE_2-induced IPs formation mediates subsequent Ca^{++} mobilization.

<u>PGE_2 and $PGF_{2\alpha}$ activate PLC through the same receptor</u>. Experiments were formulated to test whether PGE_2 and $PGF_{2\alpha}$ interact with the same receptor or separate receptors. In PKC-depleted cells, a maximal dose of PGE_2 ($5x10^{-5}$ M) or $PGF_{2\alpha}$ (10^{-6} M) increased IPs formation by 456% and 492%, respectively (Fig.14 A). No additive effect was observed when $5x10^{-5}$ M of PGE_2 and 10^{-6} M of $PGF_{2\alpha}$ were combined to stimulate cells, which together increased IPs formation by 506%. Similarly, no additive effect of maximal doses of PGE_2 and $PGF_{2\alpha}$ was observed in stimulating Ca^{++} mobilization (Fig.14B). PGE_2 ($5x10^{-5}$ M) increased $[Ca^{++}]_i$ from 130 nM to 1310 nM. $PGF_{2\alpha}$ (10^{-5} M) increased $[Ca^{++}]_i$ from 120 nM to 1250 nM. Combined doses of PGE_2 and $PGF_{2\alpha}$ increased $[Ca^{++}]_i$ from 140 nM to 1120 nM.

Desensitization experiments in normal cells are shown in Fig.15. Cells pre-stimulated with 10^{-5} M of $PGF_{2\alpha}$ were desensitized to subsequent addition of 10^{-5} M $PGF_{2\alpha}$ or 10^{-5} M PGE_2, but the cells remained responsive to a challenge by 10^{-5} M bombesin after the $PGF_{2\alpha}$ treatment.

Figure 1. Representative tracings of Ca^{++} mobilization in confluent quiescent Swiss 3T3 cells in response to (A). 10^{-5} M PGE_2 and (B). 10^{-5} M $PGF_{2\alpha}$. Agonists were added as indicated by the arrow. Spikes were caused by opening of the shutter.

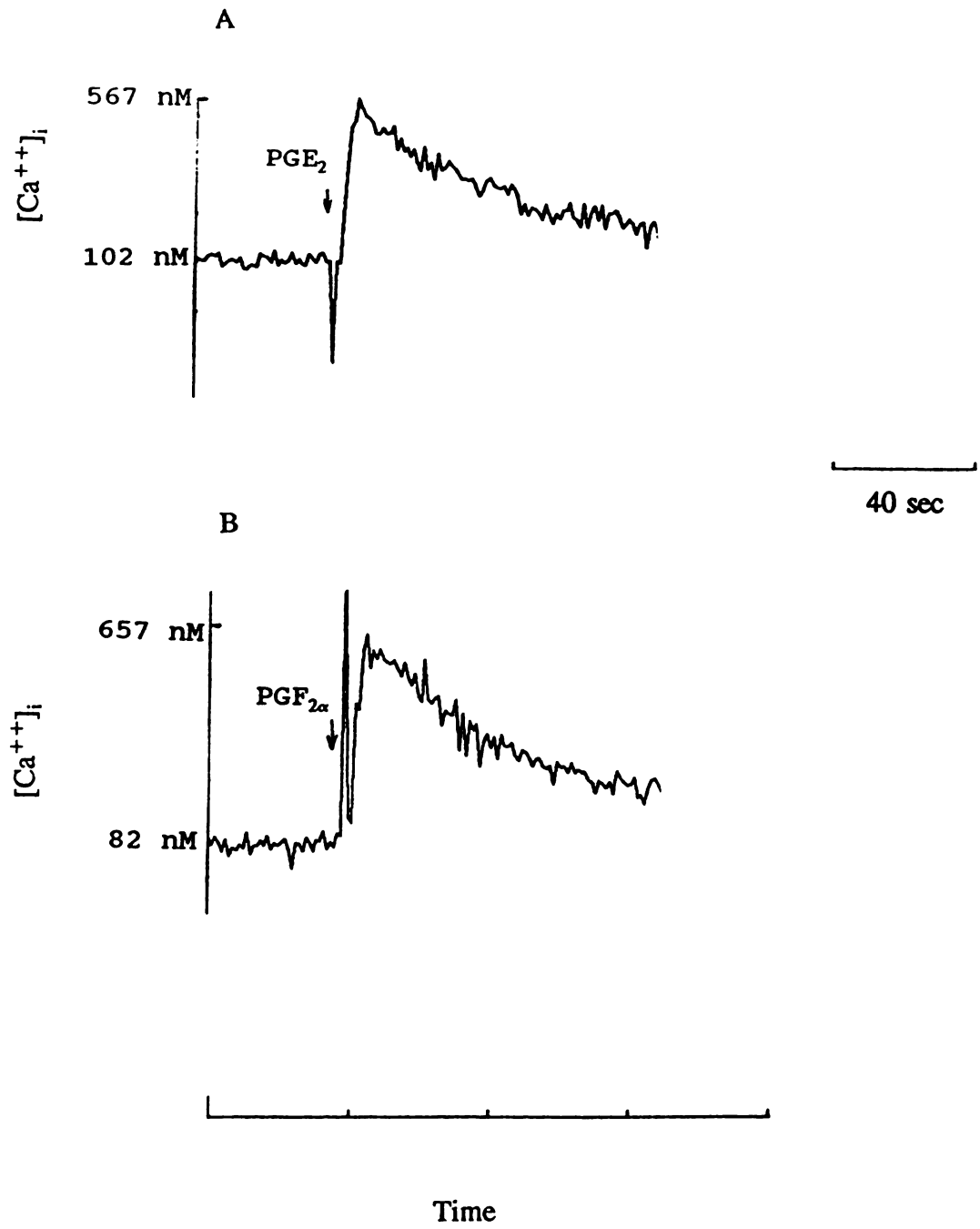
A
567 nM
102 nM
PGE2
[Ca++]i
40 sec
B
657 nM
82 nM
PGF2α
[Ca++]i
Time

Figure 2. Dose dependence of the responses to PGE_2 and $PGF_{2\alpha}$ that induce Ca^{++} mobilization in confluent quiescent Swiss 3T3 cells. The results are expressed as the percent increase over the resting level of $[Ca^{++}]_i$.

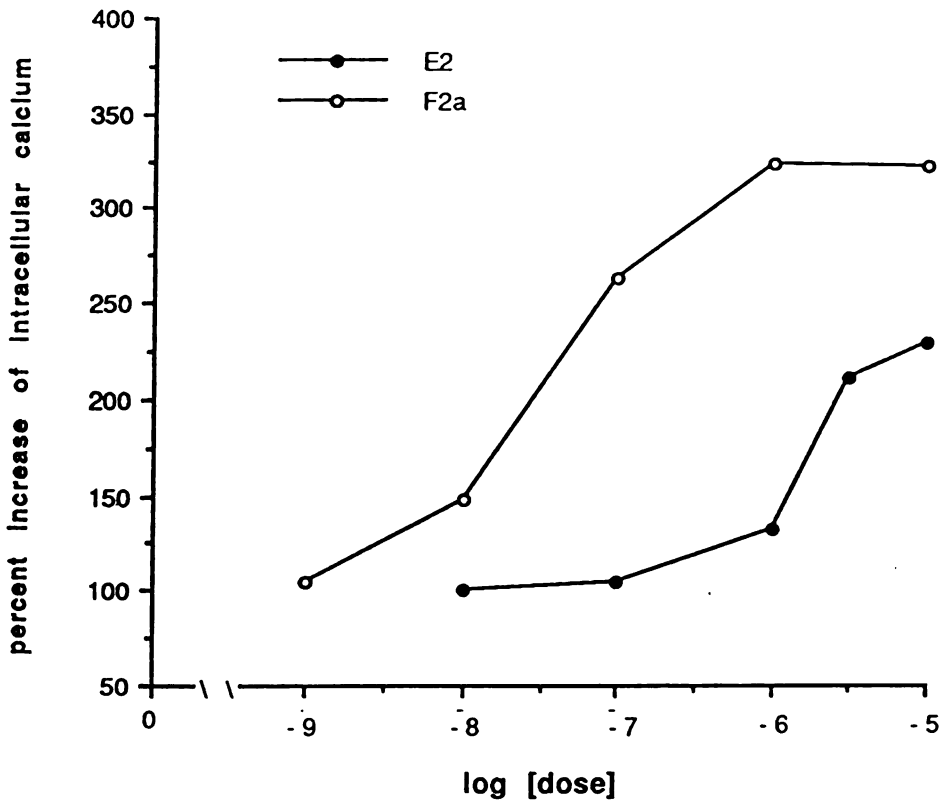
E2
F2a
400
350
300
250
200
150
100
50
0
-9
-8
-7
-6
-5
percent increase of intracellular calcium
log [dose]

Figure 3. PGE_2- and $PGF_{2\alpha}$-induced IPs formation in confluent quiescent Swiss 3T3 cells. Cells were incubated with vehicle or 10^{-5} M agonists for 30 min and the ^3H-labeled IPs were measured as described in the text. Results are expressed as the percent increase over the basal value observed with cells treated with vehicle alone and represent the mean$\pm$ S.E.(n=2).

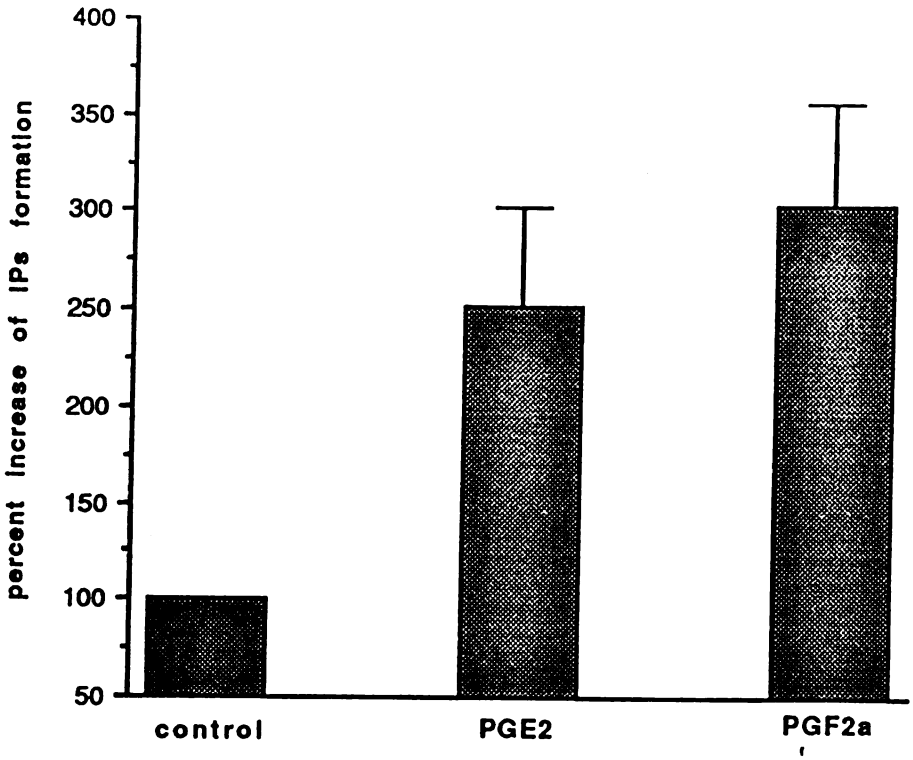
400
350
300
250
200
150
100
50
percent increase of IPs formation
control
PGE2
PGF2a

Figure 4. The effect of depletion of PKC on PGE_2- and $PGF_{2\alpha}$-induced IPs formation. Confluent Swiss 3T3 cells were treated with or without TPA (300 ng/ml) for 40-48 hours. The total ^3H-labeled IPs were measured as described in the text after a 30 min incubation with vehicle or 10^{-5} M agonists. Results were expressed ascounts from each culture well and represent mean$\pm$ S.E. of triplicate determinations.

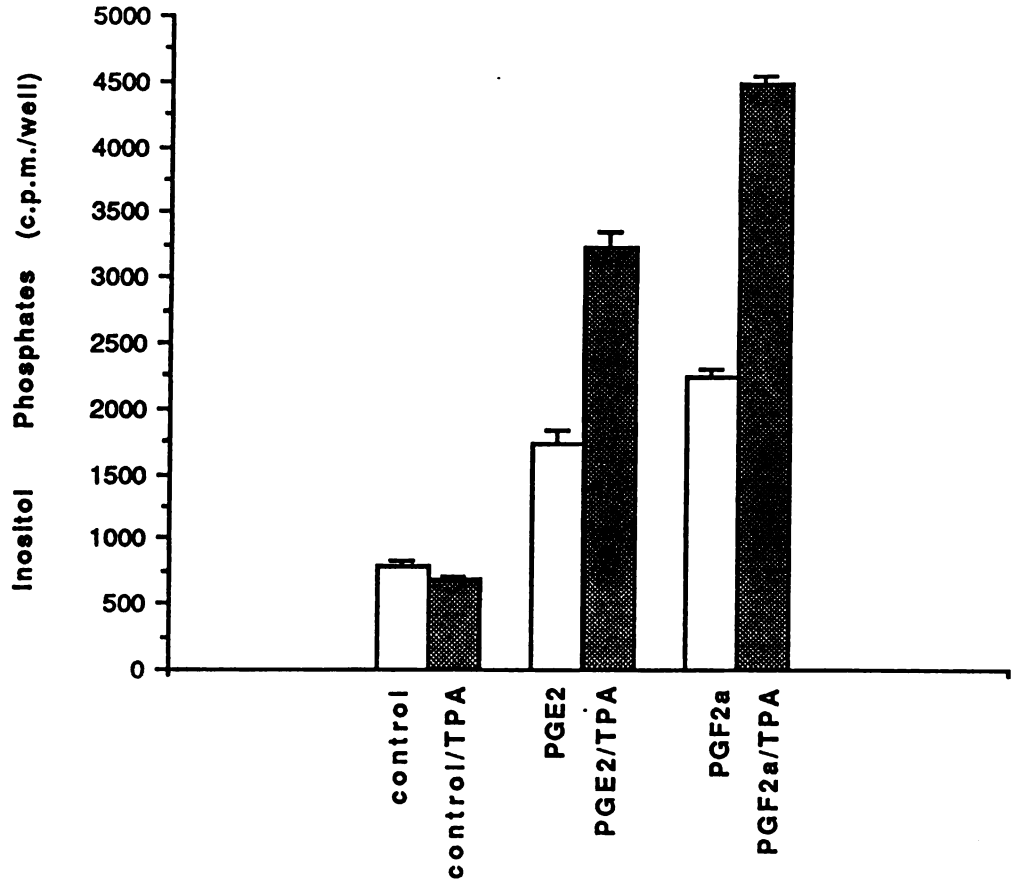
Inositol Phosphates (c.p.m./well)
5000
4500
4000
3500
3000
2500
2000
1500
1000
500
0
control
control/TPA
PGE2
PGE2/TPA
PGF2a
PGF2a/TPA

Figure 5. The effect of depletion of PKC on PGE_2- and $PGF_{2\alpha}$-induced Ca^{++} mobilization. Confluent Swiss 3T3 cells were treated with or without TPA (300 ng/ml) for 40-48 hours. Increases in $[Ca^{++}]_i$ in response to 10^{-5} M agonists were then determined fluorometrically as described in the text. The results are expressed as the percent increase over the resting level of $[Ca^{++}]_i$ and represent mean$\pm$ S.E. (n=3).

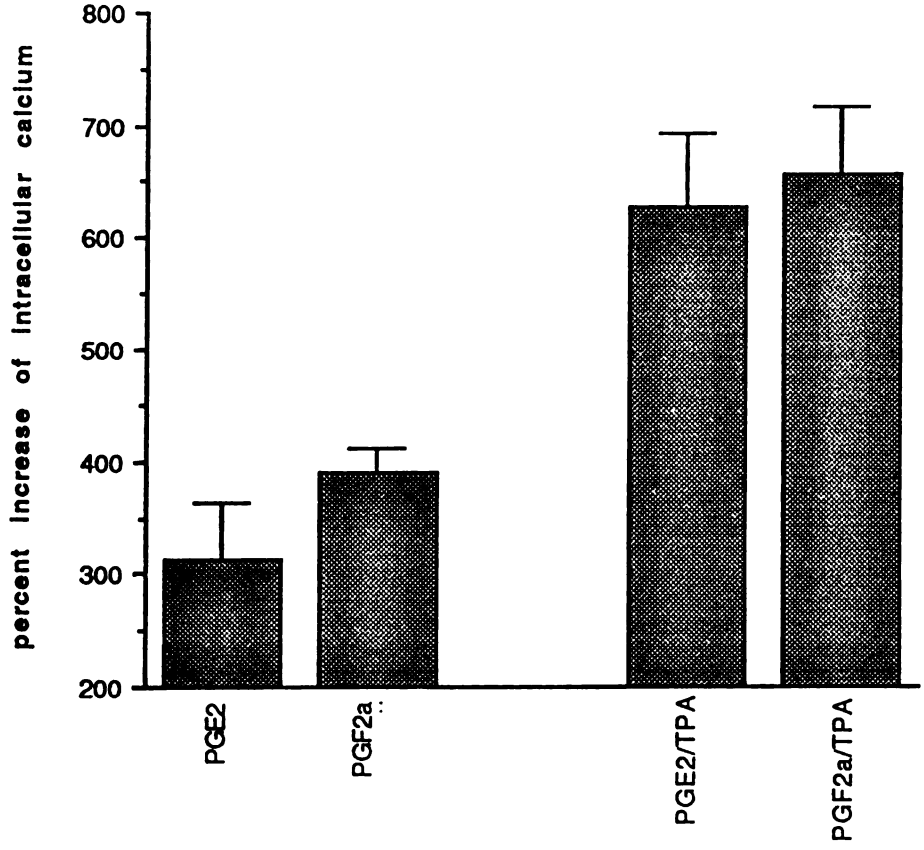
percent increase of intracellular calcium
800
700
600
500
400
300
200
PGE2
PGF2a
PGE2/TPA
PGF2a/TPA

Figure 6. Dose dependence of PGE_2- and $PGF_{2\alpha}$-induced IPs formation in PKC-depleted Swiss 3T3 cells. PKC-depleted cells were incubated with the indicated concentrations of PGE_2 and $PGF_{2\alpha}$ for 30 min, and the total ^3H-labeled IPs were measured as described in the text.

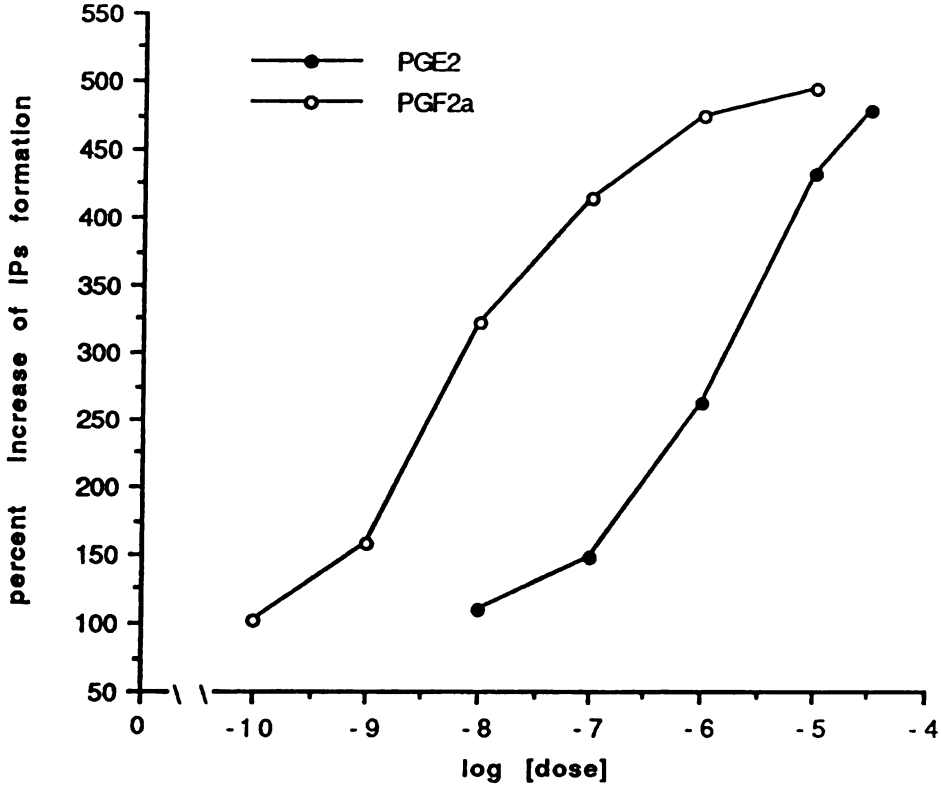
550
500
450
400
350
300
250
200
150
100
50
0
-10
-9
-8
-7
-6
-5
-4
PGE2
PGF2a
percent Increase of IPs formation
log [dose]

Figure 7. Time course of PGE_2-induced formation of various inositol phosphates in PKC-depleted Swiss 3T3 cells. ^3H-labeled IP_1, IP_2 and IP_3 fractions were measured as described in the text in PKC-depleted cells at the indicated times after incubation with 10^{-5} M PGE_2. The results represent mean$\pm$S.E.(n=2).

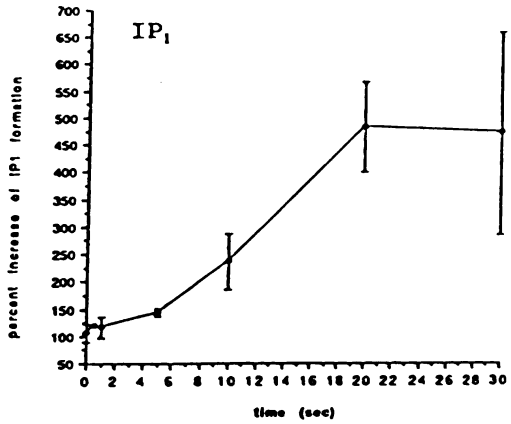
IP1
percent increase of IP1 formation
time (sec)

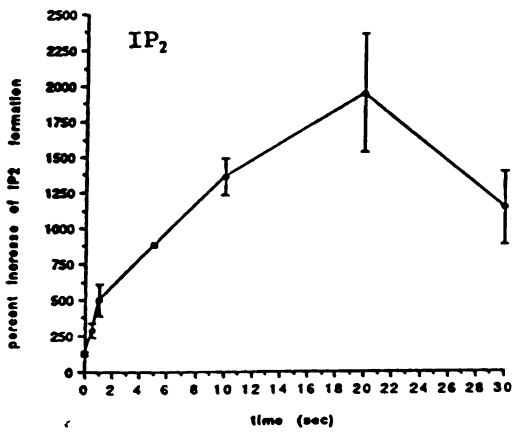
IP2
percent increase of IP2 formation
time (sec)

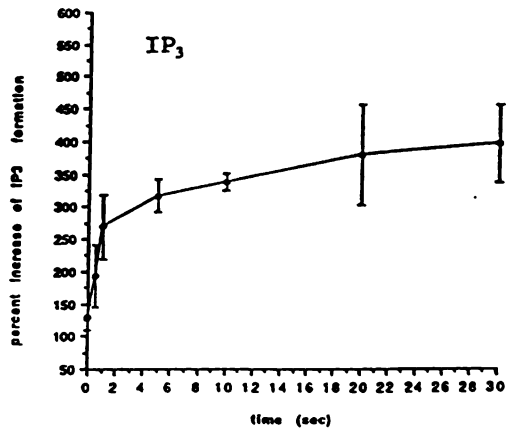
IP3
percent increase of IP3 formation
time (sec)

Figure 8. Stimulation of IPs formation by 15-S-PGE_2 and 15-R-PGE_2 in PKC-depleted Swiss 3T3 cells. The PKC-depleted cells were incubated with 10^{-5} M of 15-S-PGE_2 or 15-R-PGE_2 for 30 min, and the total ^3H-labeled IPs were measured as described in the text. The results represent mean$\pm$S.E.(n=2).

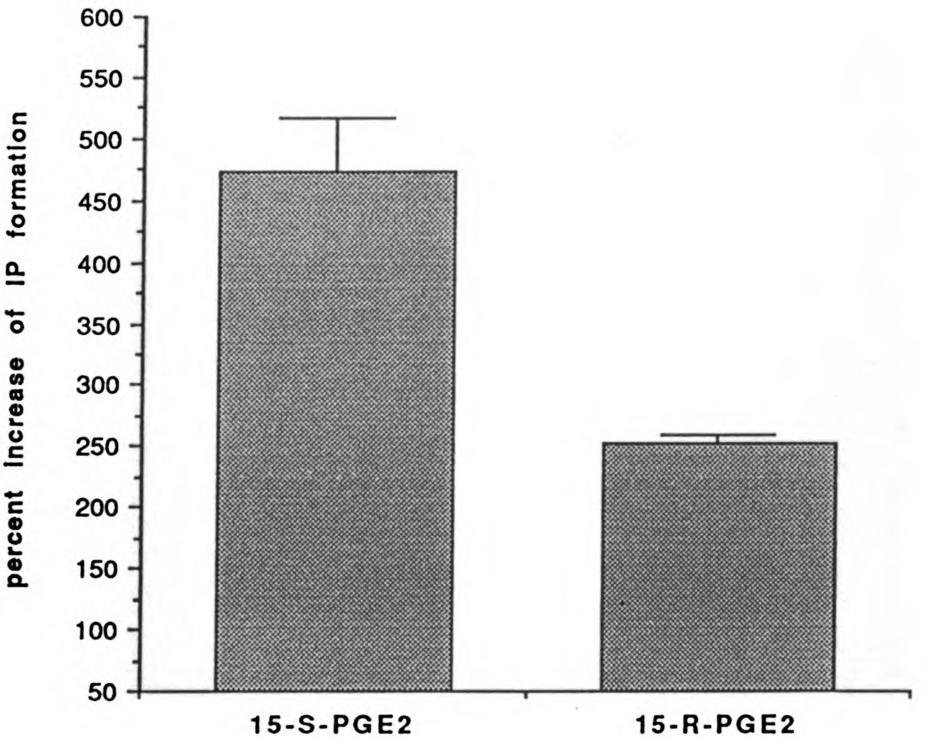
percent increase of IP formation
600
550
500
450
400
350
300
250
200
150
100
50
15-S-PGE2
15-R-PGE2

Figure 9. The effect of sulprostone on IPs formation in PKC-depleted Swiss 3T3 cells. The indicated concentrations of sulprostone (open symbol) and PGE_2 (closed symbol) were added to PKC-depleted cells and the total ^3H-labeled IPs were measured after 30 min incubation as described in the text.

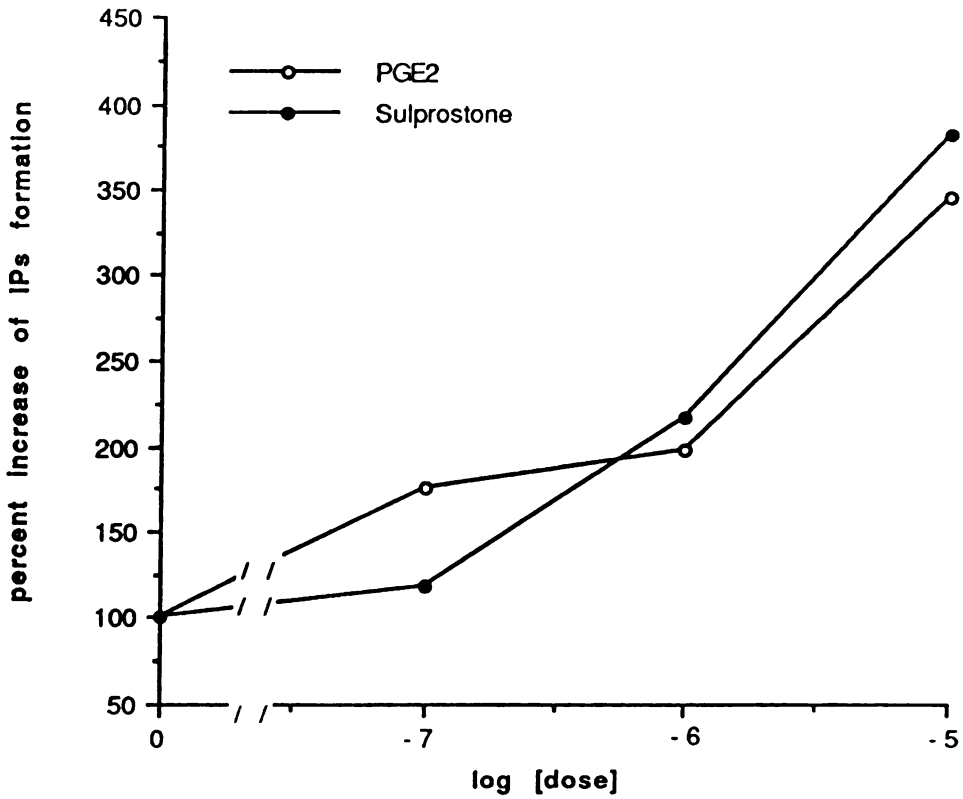
450
400
350
300
250
200
150
100
50
PGE2
Sulprostone
percent increase of IPs formation
0
- 7
- 6
- 5
log [dose]

Figure 10. The effect of AH6809 on PGE_2-induced IPs formation in PKC-depleted Swiss 3T3 cells. PKC-depleted cells were incubated with $5x10^{-7}$ M PGE_2 for 30 min in the absence or presence of the indicated concentrations of AH6809. The total ^3H-labeled IPs were measured as described in the text.

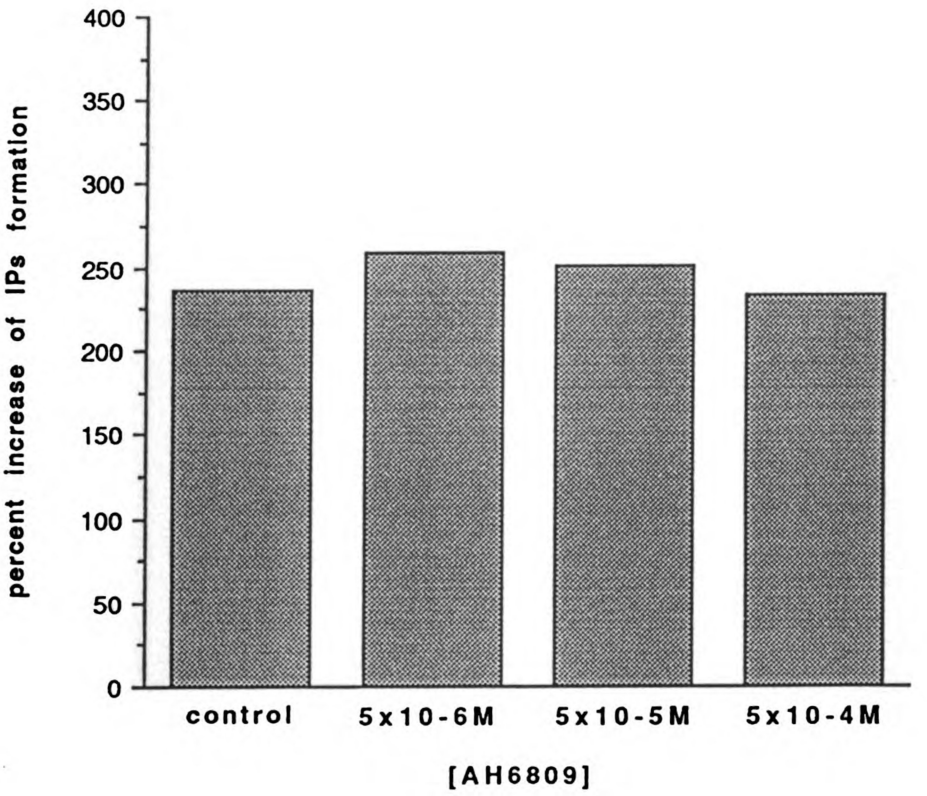
400
350
300
250
200
150
100
50
0
percent increase of IPs formation
control
5x10-6M
5x10-5M
5x10-4M
[AH6809]

Figure 11. The effect of pertussis toxin on PGE_2-induced IPs formation in PKC-depleted Swiss 3T3 cells. PKC-depleted cells were treated with pertussistoxin (100 ng/ml or 1000 ng/ml) for 12-18 hours. The control cells and treated cells were incubated with 10^{-5} M PGE_2 for 30 min and the total ^3H- labeled IPs were measured as described in the text.

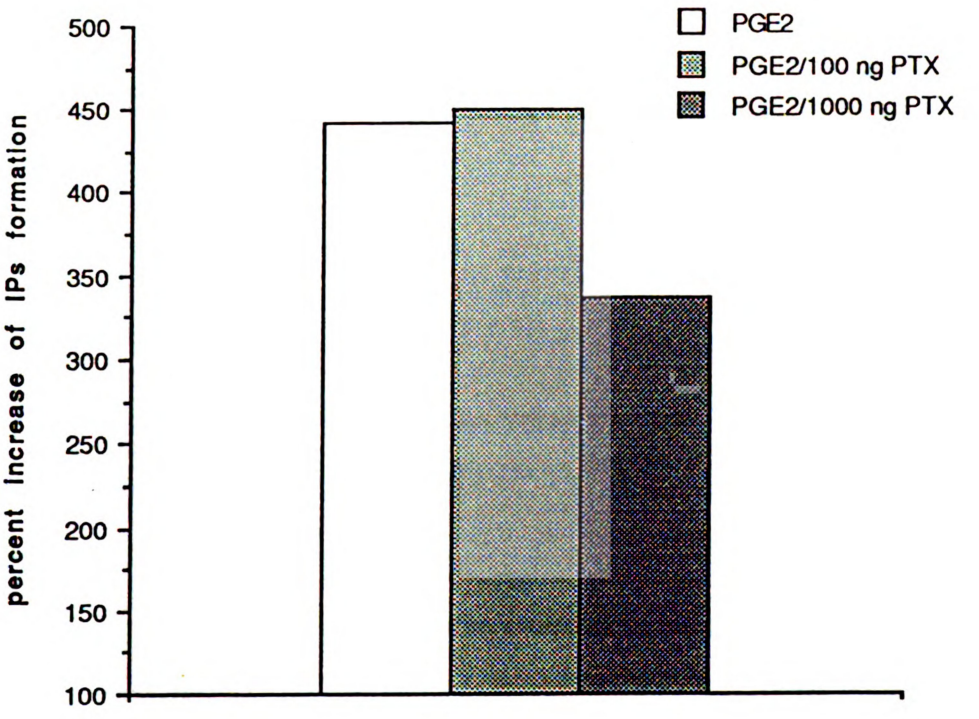
PGE2
PGE2/100 ng PTX
PGE2/1000 ng PTX
percent increase of IPs formation
500
450
400
350
300
250
200
150
100

Figure 12. The effect of extracellular Ca^{++} on PGE_2-induced Ca^{++} mobilization in PKC-depleted cells. PKC-depleted Swiss 3T3 cells were suspended in Ca^{++} free simplified saline solution. 1 mM of EGTA was added to the media before the cells were challenged with 10^{-5} M of PGE_2. The spikes were caused by opening of the shutter.

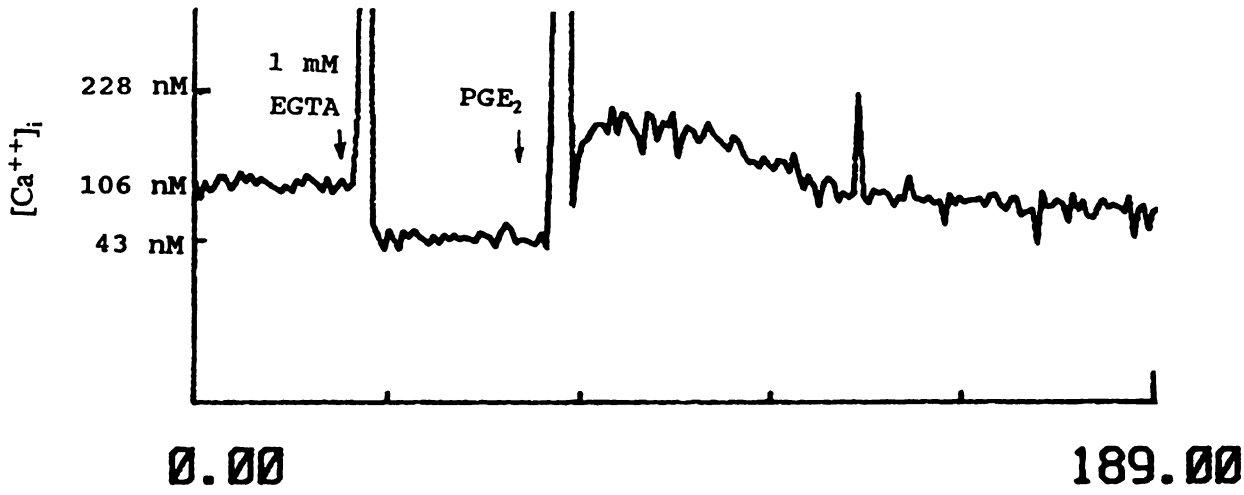

Time (sec)

Figure 13. Dose dependence of PGE_2- and $PGF_{2\alpha}$-induced Ca^{++} mobilization in PKC-depleted Swiss 3T3 cells. The results are expressed as the percent increase over the resting level of $[Ca^{++}]_i$.

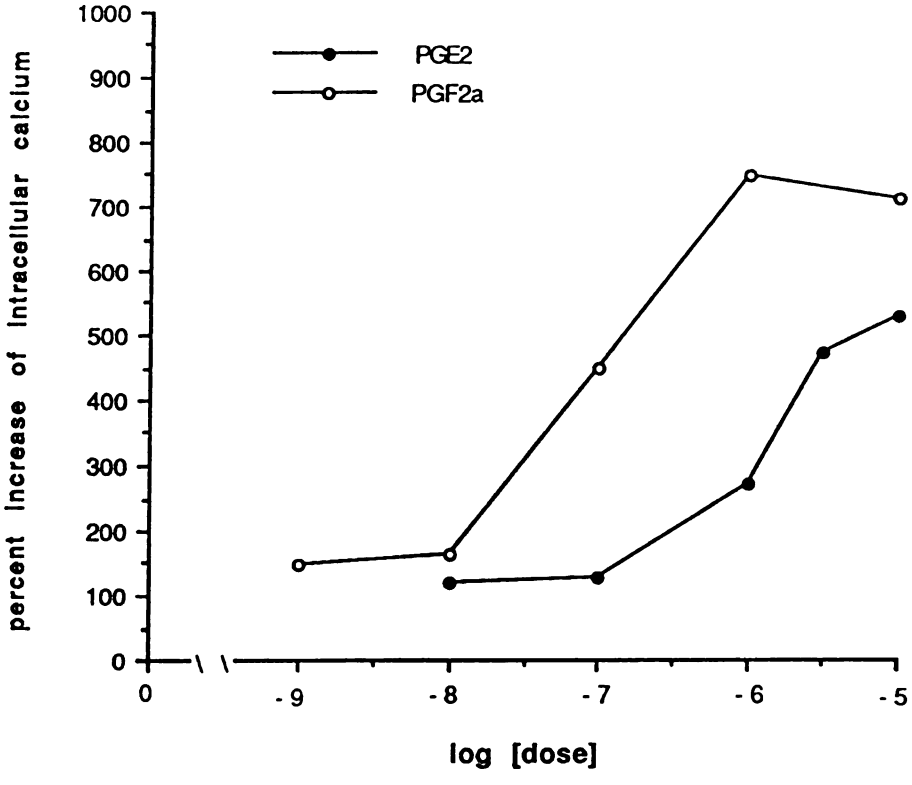
percent increase of intracellular calcium
1000
900
800
700
600
500
400
300
200
100
0
0
-9
-8
-7
-6
-5
log [dose]
PGE2
PGF2a

Figure 14. The non-additive effect of maximal doses of PGE_2 and $PGF_{2\alpha}$ on Ca^{++} mobilization and IPs formation in PKC-depleted Swiss 3T3 cells. (A). The Ca^{++} traces of cells challenged with $5x10^{-5}$ M PGE_2, 10^{-5} M $PGF_{2\alpha}$, and a combination of $5x10^{-5}$ M PGE_2 and 10^{-5} M $PGF_{2\alpha}$. (B). The effect of $5x10^{-5}$ M PGE_2, 10^{-6} M $PGF_{2\alpha}$, and a combination of $5x10^{-5}$ M PGE_2 and 10^{-6} M $PGF_{2\alpha}$ on IPs formation.

B

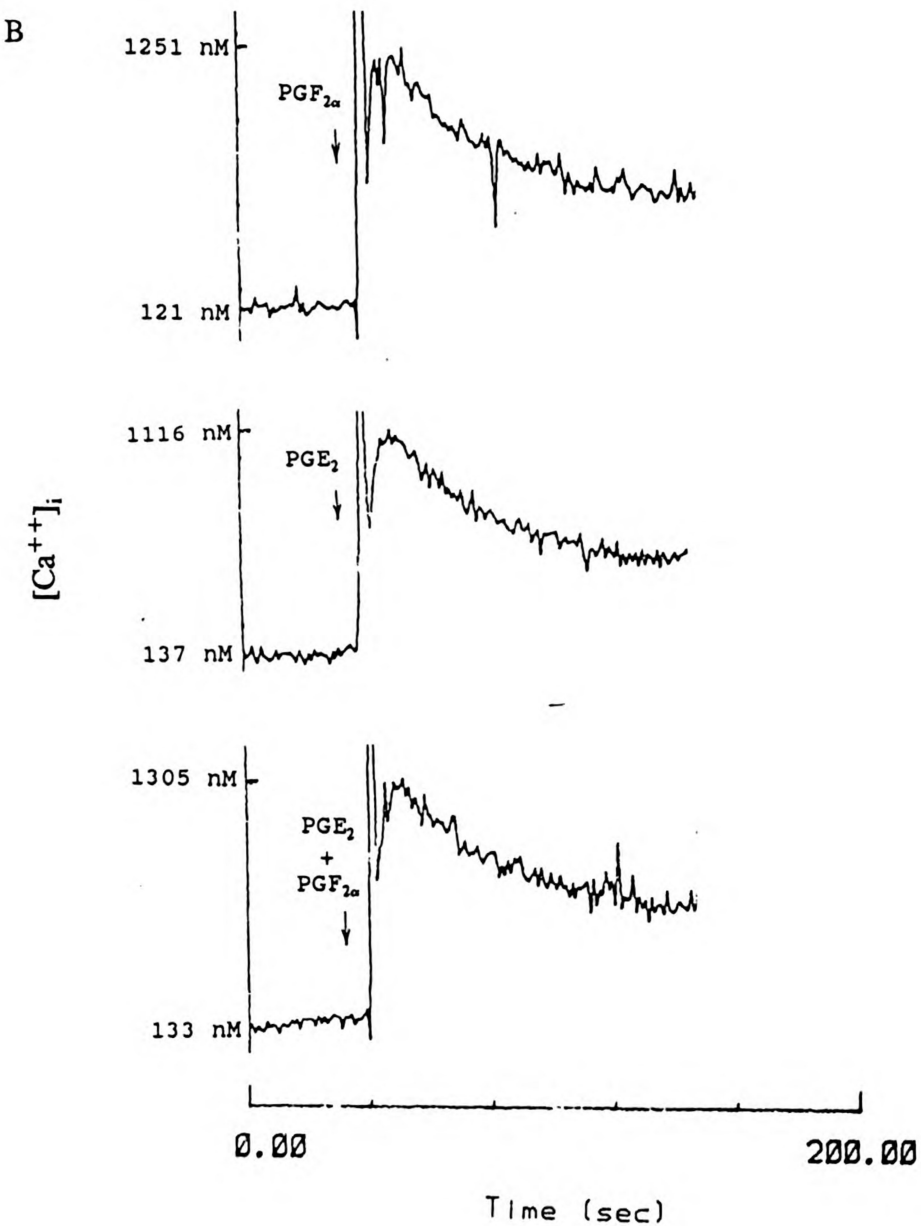
1251 nM
PGF2α
121 nM
1116 nM
PGE2
137 nM
1305 nM
PGE2
+
PGF2α
133 nM
[Ca++]i
0.00
200.00
Time (sec)

A

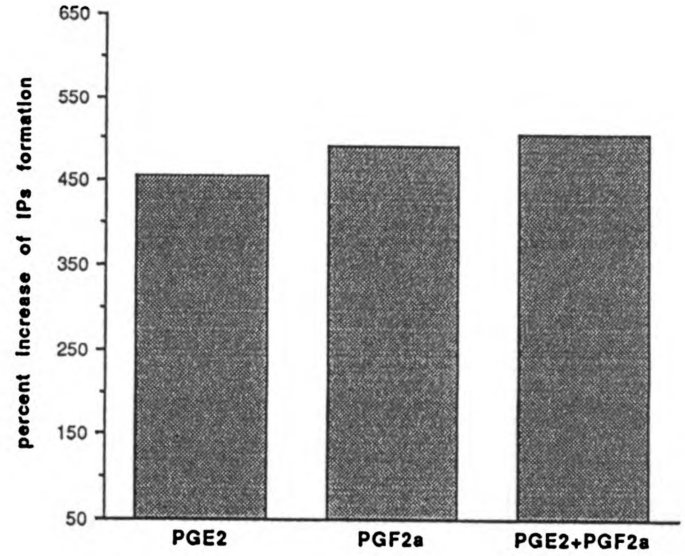
650
550
450
350
250
150
50
percent increase of IPs formation
PGE2
PGF2a
PGE2+PGF2a

Figure 15. Effect of pretreatment with $PGF_{2\alpha}$ on Ca^{++} mobilizationin in confluent quiescent 3T3 cells. Cells were prereated with 10^{-5} M $PGF_{2\alpha}$ and the subsequent responses to challenges by (A) 10^{-5} M $PGF_{2\alpha}$ and (B) 10^{-5} M PGE_2 and 10^{-5} M bombesin were measured.

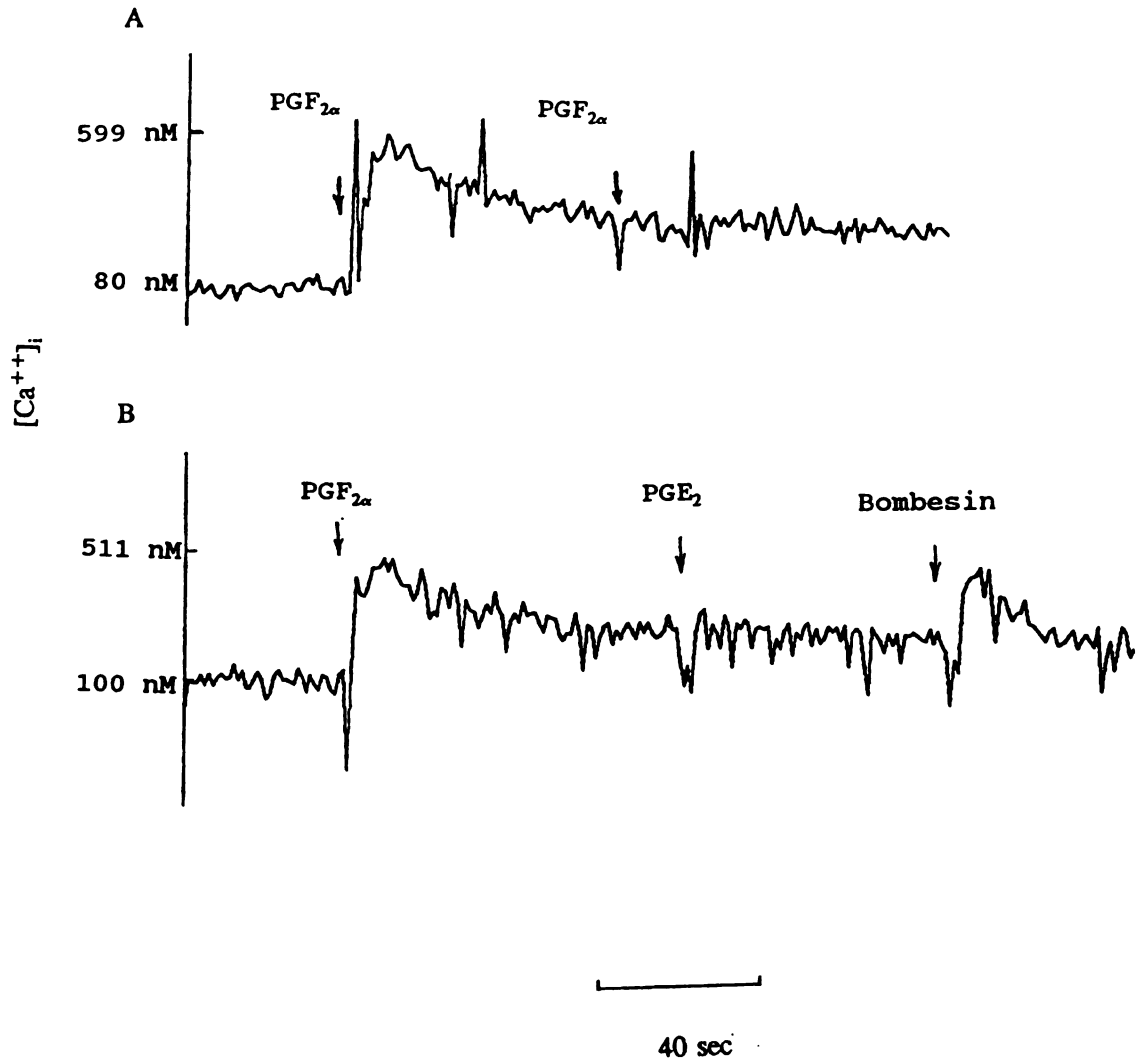
A
599 nM
80 nM
PGF2α
PGF2α
[Ca++]i
B
511 nM
100 nM
PGF2α
PGE2
Bombesin
40 sec

DISCUSSION

Proliferation of cultured fibroblasts can be induced by a number of hormones that stimulate PIP_2 hydrolysis (9,10). $PGF_{2\alpha}$ is known to be a mitogen that elicits its effects through the PLC pathway (4,5). Compared to $PGF_{2\alpha}$, PGE_2 is much less potent in stimulating cell growth. In the presence of a low concentration of insulin that does not by itself initiate DNA synthesis, PGE_2 induces cell proliferation. It was reported previously that PGE derivatives increase cAMP formation in Swiss 3T3 cells, and this was believed to be the basis of the synergistic effect of PGEs on initiation of DNA synthesis. The present study demonstrated that PGE_2, as well as $PGF_{2\alpha}$, can induce PIP_2 hydrolysis and subsequent Ca^{++} release from intracellular stores. This may be a mechanism by which PGE_2 exerts its synergistic effect on cell growth.

PGEs stimulate adenylate cyclase in a variety of cells. PGEs and PGFs can also activate the PLC system in cells such as MDCK cells, UMR-106 cells, and bovine adrenal chromaffin cells (11,12,13). PKC is activated by diacylglycerol generated through the PLC pathway and acts as a negative regulator of this pathway (14). Therefore, when the negative effect of PKC was withdrawn by depletion of PKC, a potentiation of responses

derived from PLC pathway are expected. The mechanism by which PKC inhibits phosphoinositide hydrolysis in response to mitogens remains to be established. PKC-mediated phosphorylation of receptors, G-proteins, and PLCs were all well documented (15,16 17). It is possible that the inhibitory effect of PKC on IPs formation results from phosphorylation at multiple targets in the PLC pathway. TPA-induced down-regulation of PKC has been observed in various cell line, the extent of which differs from cell line to cell line (18). In Swiss 3T3 cells, it was shown that PKC was not immunologically detectable after 40 hours of treatment with 300 ng/ml TPA.

Numerous examples have been reported of a guanine nucleotide requirement in receptor activation of PLC in cell-free preparations or in permeabilized cells (19,20). The direct evidence that G proteins are involved in PLC activation are from Sternweis, who reported recently that an antibody of G_q attenuated the stimulation of PLC by a number of hormones (21). Both PTX-sensitive and PTX-insensitive G proteins involved in activating PLC are found in different types of cells. For instance, chemotactic peptide (f-Met-Leu-Phe)-stimulated PLC activity in neutrophils is abolished by PTX treatment (22). However, in Swiss 3T3 cells, there is only a partial inhibition by PTX of IPs formation in response to vasopressin and bombesin (27% and 23%, respectively) among various mitogens (23). In our study, overnight incubation with high concentration of PTX (1000 ng/ml) caused a partial loss

of responsiveness in IPs formation to PGE_2. There might be two possibilities for this observation. One possibility is that PG receptor can interact with more than one type of G protein coupled to PLC, and that not all of these G proteins are substrates for PTX-catalysed ADP ribosylation. Another possibility is that PG receptor interacts with one G protein coupled with PLC, and this G protein is only poorly ADP-ribosylated by PTX.

PGE_2 and $PGF_{2\alpha}$ are structurally related compounds, which can cross-react with different receptors. It has been found that in some cases, a single tissue contains more than one type of PG receptor, which accounts for the fact that different PGs exert totally different physiological effect on this tissue; while in some cases, there exist only one type of receptor interacting with different PGs with different affinity. For instance, in $PGF_{2\alpha}$-sensitive tissues such as the rat colon and dog iris (20,21), it has been suggested that PGE_2 and PGD_2 exert their effect by interacting with a single $PGF_{2\alpha}$ receptor. In the rat UMR-106 cell line, however, evidence has been obtained indicating that PGE_2 and $PGF_{2\alpha}$ stimulate PIP_2 hydrolysis and release of intracellular Ca^{++} release by acting through separate receptors (12). Recently, a radioligand binding study using Swiss 3T3 cells (22) revealed a specific binding site for $PGF_{2\alpha}$. It was shown that $PGF_{2\alpha}$ was 100 fold more potent than PGE_2 in competing with the

[^{3}H]-$PGF_{2\alpha}$ for its binding site. Consistent with this finding, results from our experiments suggested that PGE_2 activates PLC pathway through a $PGF_{2\alpha}$ receptor. This conclusion is based on two observations. First, the effects of PGE_2 and $PGF_{2\alpha}$ on IPs formation and Ca^{++} mobilization are not additive. Secondly, pretreatment of maximal dose of $PGF_{2\alpha}$ rendered cells refractory to subsequent stimulation of maximal dose of $PGF_{2\alpha}$ and PGE_2, but did not affect the response to bombesin, which also mobilizes Ca^{++} via mediating IP_3 formation. The unaffected responsiveness to bombesin in $PGF_{2\alpha}$ desensitized cells demonstrated that the IP_3-sensitive pool of Ca^{++} was not depleted by the maximal dose of $PGF_{2\alpha}$. Therefore, the desensitization of cells to PGE_2 by $PGF_{2\alpha}$ did not result from depletion of the Ca^{++} pool, but probably resulted from desensitization of a single receptor. Another piece of evidence suggesting that this receptor is a $PGF_{2\alpha}$ receptor is that PGE_2-induced IPs formation was not inhibited by AH6809, an EP1-selective antagonist. PGE can act through a PGE EP1 receptor to induce Ca^{++} mobilization, but this receptor does not appear to be present in Swiss 3T3 cells.

REFERENCES

1. Samuelsson, B., Goldyne, M., Granstrom, E., Hamberg, M., Hammarstrom, S. and Malmsten, C. (1978) Annu. Rev. Biochem. 47, 997-1029.
2. Powles, T. J., Bockman, R. S., Honn, K. V. and Ramwell, P. (1982) In: The Prostaglandins and Rested Lipids. Alan R. Liss, Inc., New York.
3. Smith, W. L. (1989) Biochem. J. 259.
4. Jimenez de Asua, L., Otto, A. M., Lindgren, J. A. and Hammarstrom, S. (1983) J. Biol. Chem. 258, 8774-8780.
5. Macphee, C. H., Drummond, A. H., Otto, A. M. and Jimenez de Asua, L. (1984) J. Cel, Physiol. 119, 35-40.
6. Rozengurt, E., Collins, M. K. L. and Keehan, M. (1983) J. Cell Physiol. 116, 379-384.!
7. Grynkiewicz, G., Poenie, M. and Tsien, R. (1985) J. Biol. Chem. 260, 3440-3450.
8. Brown, K. D., Littlewood. C. J., Blakeley, D. M. (1990) Biochem. J. 270, 557-560.
9. Vicentini, L.M., Villereal, M.L. (1989) Life Sci. 262, 2269-2276).
10. Tilly, B.C., Moolenar, W.H. (1989) In: Inositol Lipids and Cell Signalling (Michell, R., Drummond, A.H. and Down, C.P., eds), pp. 485-494, Academic Oress, London

11. Aboolian, A., Vandermolen, M., Nord, E. P. (1988) Am. J. Physiol. 256, F1135-F1143.

12. Yamaguchi, D. T., Hahn, T. J., Beeker, T. G., Kleeman, C. R., Mullem, S. (1988) J. Biol. Chem. 263, 10745-10753.

13. Yokohama, D. T., Tanaka, T., Ito, S., Negishi, M., Hayashi, H., Hayaishi, O. (1988) J. Biol. Chem. 263, 1119-1122.

14. Kikkawa, U., Kishimoto, A., Nishizuka, Y. (1989) Annu. Rev. Biochem. 58, 31-44.

15. Sibley, D.R., Benovic, J.L., Cron, M.G., Lefkowitz, R.J. (1988) Endocr. Rew. 9, 38-56.

16. Katada, T., gilman, A.G., Watanabe, Y., Bauer, S., Jacobs, K.H. (1985) Eur. J. Biochem. 151, 431-437.

17. Rhee, S.G., Suh, P.-G., Ryu, S.-H., Lee, S.Y. (1989) Science 244, 546-550.

18. Adams, J.C., Gullick, W.J. (1989) Biochem. J. 257, 905-911.

19. Cattaneo, M.G., Vicentini, L.M. (1989) Biochem. J. 262, 665-667.

20. Cockcroft, S., Gomperts, B.D. (1985) Nature 314, 534-536.

21. Gutowski, S., Smrcka, A., Mowak, L., Wu, D., Simon, M., Sternweis, P.C. (1991) J. Biol. Chem. 266, 20519-20524.

22. Strnad, C. F., Parente, J. E. and Wong, K. (1986) FEBS Lett. 206, 20-24.

23. Taylor, C. W., Blakeley, D. M., Corps, A. N., Berridge, M. J. and Brown, K. D. (1988) Biochem. J. 249, 917-920.

24. Coleman, R.A., Humphrey, P.P.A., kennedy, I., Lumley, P. (1984) Trends Pharmacol. Sci. 5, 303-306.

25. Eglen, R.M., Whiting, R.L. (1989) Br. J. Pharmacol. 98, 1335-1343.

26. Lawrence, R.A., Woodward, D.F. in manuscript.

CHAPTER FOUR

EXPRESSION CLONING OF A 14-3-3 PROTEIN THAT POTENTIATES Ca^{++} MOBILIZATION IN *XENOPUS* OOCYTES IN RESPONSE TO PROSTAGLANDIN E_2

The purification of membrane-bound receptors is generally difficult because they are present in low abundance and are difficult to stabilize following solubilization. The first full purification of an adenylate cyclase stimulatory receptor, the β-adrenergic receptor was achieved by Lefkowitz et al (1), which led to subsequent molecular cloning of the cDNA for this receptor (2). For other receptors whose protein purification had not been achieved, cDNA cloning was not possible since no partial protein sequence was available for making oligonucleotide probes for classical cloning methods. This had greatly hindered the progress of receptor studies until 1987, when an innovative approach was developed by Masu et al.(3), who succeeded in cloning the substance K receptor by expressing its activity in *Xenopus laevis* oocyte. This expression cloning method made it possible to clone receptors without information about their protein sequence. The use of expression cloning has resulted in the isolation of cDNAs encoding a large number of receptors, most of which belong to

the G protein-coupled receptor family.

The cloning strategy of Masu et al.(3) is conceptually straightforward (Fig.1). Briefly, a cDNA library is constructed in a lambda phage expression vector containing SP6 or/and T7 promoters for use in *in vitro* transcription. mRNAs are synthesized from the mixture of cDNAs ligated into the expression vector, and they are then injected into oocytes which translate the mRNA. Functional assays are performed on injected oocytes to test for the presence of the receptor mRNA. A cDNA pool that contains the specific mRNA is identified and this pool can be taken through a series of fractionation steps until a functional defined single clone is obtained.

In our attempt to clone a prostaglandin E_2 receptor using the *Xenopus* oocyte expression system, we isolated a clone that potentiated mobilization of intracellular Ca^{++} in response to PGE_2 in oocytes. Surprisingly, sequence analysis of this cDNA showed that it is highly homologous to the 14-3-3 proteins, a family of acidic proteins highly expressed in mammalian brain; but is not homologous to members of the G protein-coupled receptor family.

MATERIALS AND METHODS

Materials. Dulbecco's modified Eagle medium, fetal calf serum (FCS) were purchased from GIBCO. *Xenopus laevis* were from Nasco (Fort Atkinson, WI). SP6 and T7 RNA polymerases, RNasin ribonuclease inhibitor, and rabbit reticulocyte lysate *in vitro* translation kit were obtained from Promega. ^{7}mG(-5')pppG was from Phamacia. RNase free DNase I, Not I were from Mannheim Boehringer. Sequenase DNA sequencing kit was purchased from United States Biological Company. [α-^{32}P]dCTP was from Du Pont-New England Nuclear. ^{35}S-methionine was from Amersham Corp. PGE_2 was purchased from Cayman Chemicals. Serotonin was obtained from Sigma. The cDNA for 5-$HT1_c$ serotonin receptor (4) was a generous gift from Dr. D. Julius, College of Physicians and Surgeons, Columbia University.

Construction of cDNA Library. A mixture of complementary DNAs (cDNAs) was synthesized from NIH 3T3 polyA(+) RNA (mRNA) using a specific 30mer oligonucleotide as primer: 5'-CGAGGCCATGGCGGCCGCTTTTTTTTTTTT-3'. This primer contains the rare Not I and Sfi I restriction sites next to the poly(dT) tail so that following incorporation of the cDNA into the lambda ZAP phage vector, cleavage of one of the sites can be used to terminate the subsequent *in vitro* transcription of cDNA immediately after the poly(A) tail. After synthesis of

single- and double- strand cDNAs, the cDNA mixture was modified with EcoRI methylase, and EcoR I linkers were blunt-end ligated to both ends. Following cleavage with EcoRI, the resulting cDNAs were inserted into the EcoR I sites located downstream of the SP6 or T7 promoters (they could be ligated in either orientations) in the lambda ZAP vector. Finally, the lambda cDNAs were packaged to yield a cDNA library containing 1.85×10^4 clones. Most of the above reaction were performed by protocols described by Maniatis (5).

In vitro synthesis of RNA. The lambda DNA mixture was isolated and extracted using the method described by Maniatis (5), and cleaved with Not I restriction enzyme. The resultant cDNA mixture was then transcribed *in vitro* using SP6 and T7 RNA polymerases (which initiated transcriptions from inserts oriented in either direction). The reaction mixture contained: 10 μl 5X transcription buffer (200 mM Tris-HCl, pH 7.5, 30 mM $MgCl_2$, 10 mM spermidine, and 50 mM NaCl), 5.0 μl 0.1 M DTT, 2.0 μl RNasin ribonuclease inhibitor, 5.0 μl 5 mM each ATP, CTP, UTP; 0.5 mM GTP, 5.0 μl ^{7}mG(-5')pppG, 5.0 μl (10-20 μg) linear DNA template and add H_2O to a final volume of 50 μl. RNA transcripts were then extracted with phenol:$CHCl_3$ and then with $CHCl_3$ alone, and precipitate with ethanol. The pellet was resolved in DEPC water at a concentration of 1 μg/ml.

Expression of synthesized RNAs in oocytes. Ovarian lobes of oocytes were taken from *Xenopus laevis* and oocytes were isolated under a dissection microscope. The oocytes were then

allowed to sit in MBS (modified Barth's solution) overnight at 18°C. Intact oocytes were selected the next day for injection. RNA (50 ng in 50 nl of water) was injected into each oocyte using a micropipette and a micromanipulator under a dissection microscope. The injected oocytes were incubated in MBS for about 40 hours before being assayed for Ca^{++} mobilization in response to PGE_2.

Measurement of intracellular Ca^{++} mobilization in oocytes. The injected oocytes were loaded with the fluorescence dye Fura-2, by incubation in MBS containing 10 μM fura-2/AM at 19 degrees with constant shaking for 40-60 min. Dye-loaded oocytes were then washed and kept in MBS until use. Change of fluorescence within the oocytes was monitored with a dual excitation wavelength SPEX spectrofluorometer. Samples containing five oocytes were allowed to stand in the bottom of a crystal spatula inserted into a mini-cuvette, and challenged by the addition of 5 μM PGE_2. During each trace, the oocytes were excited at wavelengths of 340 nm and 380 nm, and the emission was monitored at 505 nm. The fluorescence ratio was obtained by dividing the fluorescence intensity resulting from excitation at 340 nm by the fluorescence intensity resulting from excitation at 380 nm. This value was used to estimate the $[Ca^{++}]_i$ (6).

Subfractionation of cDNA pools. The original cDNA library contained 1.85×10^4 clones. After determining that cDNAs from this pool was able to confer the PGE_2-induced Ca^{++}

mobilization on oocytes, this pool of clones was subdivided into several smaller pools. After a series of subdivisions, a single clone responsible for the Ca^{++} mobilizing response to PGE_2 was obtained.

Sequencing of cDNA. The cDNA responsible for the Ca^{++} mobilizing activity of PGE_2 was named GING. GING was inserted into the EcoR I sites of M13mp18 and M13mp19 bacteria phage DNA. Single stranded sequencing of both strands of cDNA was performed using the method of Sanger et al. (7). A universal oligonucleotide primer from the vector was used as the first primer for the initial sequencing. Subsequently, a 17mer was synthesized from the known sequence of the cDNA and used as the primer for downstream sequencing. Four primers were used to complete the sequencing of the entire cDNA.

In vitro translation of GING RNA. Template RNAs were heated at 67°C for 10 min and immediately cool on ice. This increases the efficiency of translation by destroying secondary structures. Reticulocyte translation reaction mixture were composed of 17.5 µl lysate, 0.5 µl 1 mM amino acid mixture (minus methionine), 2.0 µl ^{35}S-methionine (1,200Ci/mmole) at 10 mCi/ml, 2.2 µl H_2O, 0.5 µl RNasin ribonuclease inhibitor (40u/µl), and 1.0 µl RNA substrates (0.5-1 µg/µl) in H_2O. The reaction mixture was incubated at 37°C for 60 min and then loaded to SDS gel.

Transfection of COS-1 cells. To determine if GING can be

functionally expressed in mammalian cells (e.g. COS-1 cell), GING was subcloned into the expression vector pSVT7 in two orientations. G(+) is the plasmid in which GING was inserted with its apparent translation start site downstream of the SV40 promoter; G(-) is the plasmid in which GING was inserted in the opposite orientation to serve as a negative control. ST(+) is the plasmid in which the cDNA for 5-HT_1 serotonin receptor was inserted; this later vector served as a positive control. The DEAE-dextran method as described by Shimokawa et al. (9) was used to transfect COS-1 cells. DMEM containing DEAE-dextran (7.5 mg/ml) was filtered and plasmid DNA was added to reach a final concentration of 5 μg/ml. COS-1 cells at 70-80% confluence in the wells of 12 well-tissue culture plates were incubated with 1 ml of media containing a pSVT7-cDNA plasmid at 37 degrees for one hour. Then 2.3 ml of DMEM/FCS containing 52 μg of chloroquine/ml was added to each well. the samples were incubated for another 5 hours. At the end of transfection period, the cells were washed extensively, and then incubated for 40-48 hours in DMEM containing 10% FCS in a water saturated 7% CO_2 atmosphere at 37 degrees.

Measurement of inositol phosphate. As described in the method section of chapter two.

Measurement of Ca^{++} mobilization in single cells. As described in the method section of chapter two.

RESULTS

Expression cloning. An initial pool of 1.85×10^4 lambda ZAP recombinant clones was subfractionated until a pool of 20 cDNA clones was obtained that conferred upon oocytes the ability to mobilize Ca^{++} in response to PGE_2 (Fig.2). Single clones were picked from this pool and RNA transcripts from each clone were checked individually. One clone containing a 1.7 kb cDNA insert was identified as responsible for the response to PGE_2 in oocytes.

Based on restriction enzyme analysis, this cDNA, designated GING, was found to be inserted into the lambda ZAP vector with its 5'end next to the SP6 promoter, and its 3'end next to the T7 promoter (Fig.3A). Therefore, SP6 RNA polymerase would be expected to generate a sense transcript, while T7 RNA polymerase should generate an anti-sense transcript (which could serve as a negative control). To obtain sense and anti-sense transcripts, the cDNA was cut out of the vector at the flanking Spe I restriction site (Fig.3B), and RNA transcripts were synthesized using SP6 and T7 polymerase respectively. When the sense (SP6) and anti-sense (T7) transcripts were injected into oocytes separately, the sense transcript rendered oocytes responsive to PGE_2, whereas the anti-sense one did not (Fig.4).

Sequence analysis of GING. Sequence analysis showed that GING contains 1650 nucleotides (Fig.5). Its longest open reading frame extends from an ATG at position 19 to a stop codon at position 720, encoding a polypeptide of 233 amino acids, with a predicted molecular weight of 26,096. The polyadenylation signal AAATAAAA is found at position 1594. The NotI site, CGGCCGCC, which was inserted into the 30mer primer for the synthesis of the cDNA library, was found near the 3′ end of GING.

The deduced amino acid sequence of GING is shown in Fig.6. The hydropathy plot does not show any prominent hydrophobic domains characteristic of transmembrane spanning regions. In fact, the hydropathy profile suggested that GING encodes a hydrophilic soluble protein.

A search of the GenBank Database indicated that the predicted amino acid sequence of the GING protein is 62% identical (73% similar) to the bovine 14-3-3 protein (Fig.7). This protein is a cytosolic protein that is highly rich in brain, but also widely distributed in other tissues (6).

Northern blot analysis. As shown in Fig.8, a single 2.0 Kb species was done by Northern blot hybridization of GING with mRNA prepared from 3T3 cells, treated with or without 1 mM PGH synthase inhibitor aspirin. The pretreatment of aspirin did not change the mRNA level of GING.

In vitro translation of GING. A rabbit reticulocyte lysate was used for *in vitro* translation of the RNA

transcribed from GING. The translation was performed in both the presence and absence of canine pancreatic microsomal membranes (MM), which can process newly translated proteins. The processing by MM includes glycosylation, signal peptide cleavage, and membrane translocation. Fig.9 shows the SDS gel of the translated products derived from RNA synthesized from GING and from three other control RNAs, with and without the addition of MM. In the presence of MM, (a) α-factor became glycosylated and the mobility of the radioactive products increased from 18.6 Kd to 32.0 Kd; (b) β-lactamase had its signal peptide cleaved and the mobility ofthe product deceased from 31.5 Kd to 28.9 Kd; and (c) Brome Mosaic Virus (BMV) protein was not processed so that the mobility of the products of 20 Kd, 35 Kd, and 110 Kd were unchanged. The RNA from GING gave rise to a radioactive band of 28 Kd, the mobility of which was not altered by the addition of MM. The observed molecular weight is close to the predicted value of 26 Kd. This experiment established that RNA from GING can be translated, and that the translated product is not membrane associated and is not subject to processing by microsomal membranes.

Functional expression of GING in COS-1 cells. Plasmids G(+), G(-) and ST(+) containing cDNAs for sense and anti-sense transcription of GING and sense transcription of the 5-HT_1 serotonin receptor (Fig.10) were used to transfect COS-1 cells. After expression for 40-48 hours, the transfected cells

were examined for Ca^{++} mobilization in response to various agonists at the single cell level. Of ten transfection experiments, five showed significant increases in responses to PGE_2 in G(+) transfected cells compared to G(-) transfected cells. In the other five experiments, no positive results were observed. It is not known whether the negative results were due to the failure of COS-1 cells to express the GING cDNA, or to the lack of an endogenous factor (e.g. an endogenous receptor) present in various batch of cells that is necessary for the function of GING. The results of the five positive transfection experiments are summarized in Table 4. In control COS-1 cells that were transfected with Ging(-), only $7\pm1\%$ (n=413) of cells responded to 10 μM PGE_2 and $10\pm2\%$ (n=413) of cells responded to 10 μM serotonin; in contrast $32\pm4\%$ (n=409) of COS-cells transfected with G(+) responded to 10 μM PGE_2, and $41\pm1\%$ (n=172, from three of these five experiments) of COS-1 cells transfected with G(-) responded to 10 μM serotonin. A transfection efficiency of 20-30% is close to that Segre et al. reported about the average transfection efficiency of COS-7 cells transfected with a parathyroid hormone (PTH) receptor cDNA (10). Fig.11 shows the traces of transfected cells in response to serotonin, PGE_2 and bradykinin, an agonist which induces an endogenous response in COS-1 cells.

To examine if GING is a factor specific for Ca^{++} mobilization in response to PGE_2 or a general factor for Ca^{++}

mobilization in response to other hormones, a series of agonists including $PGF_{2\alpha}$, CHA, isoproterenol, PTH and serotonin were tested in G(-) and G(+) transfected cells. None of these agents seemed to potentiate Ca^{++} mobilization in G(+) transfected cells except serotonin. In six of ten experiments, there was a moderate increase of responsiveness to serotonin in G(+) transfected cells compared with G(-) transfected cells. As summarized in Table 5, 11±4% (n=528) of cells responded to 10 μM serotonin in G(-) transfected cells, whereas 26±4% (n=590) of cells responded in G(+) transfected cells.

The following experiments were formulated to determine if GING protein potentiates Ca^{++} mobilization in response to PGE_2 and serotonin by causing inositol phosphates (IPs) formation. COS-1 cells were transfected with G(-), G(+), and ST(+). IPs were measured as described in method section. As shown in Fig.12, 10 μM serotonin induced a small background increase (<30%) of IPs turnover in G(-), as well as G(+) transfected cells; whereas a significant increase (630%) occurred in response to serotonin in ST(+) transfected cells. PGE_2 did not induce IPs formation in either G(-) or G(+) transfected cells. Thus, no effect of GING protein on IPs formation was detected. Surprisingly, when G(+) and ST(+) were introduced into COS-1 cells simultaneously, it was found that IPs formation in response to serotonin was inhibited, compared with control cells transfected with G(-) and ST(+)

(Fig.13).

The preliminary results of transient expression in COS-1 cell suggest that GING protein potentiates Ca^{++} mobilization in response to PGE_2 and serotonin in mammalian cells as well as in oocytes. Its action did not seem to involve an increase in IPs formation.

Figure 1. The sib-selection cloning strategy using the oocyte expression system.

Synthesis of cDNA

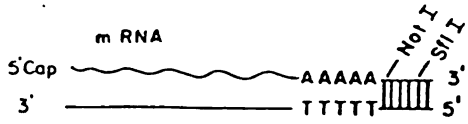

Addition of Linker

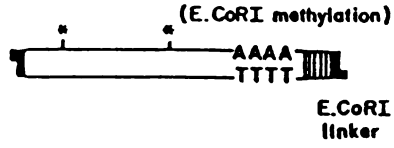

Ligation to vector

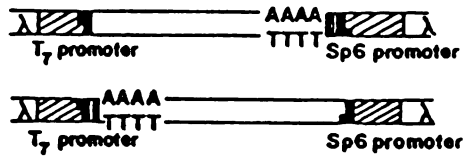

Linearization and Transcription

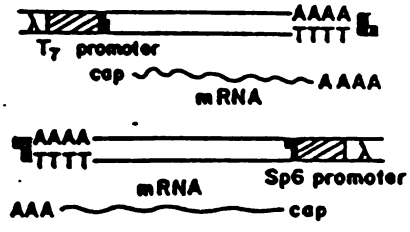

Injection of oocyte with cDNA transcripts and measure $[Ca^{++}]$ in

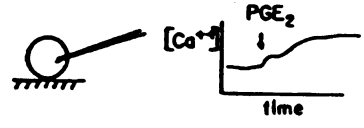

Sib selection to yield a specific cDNA clone

Figure 2. Ca^{++} mobilization in response to PGE_2 by oocytes injected with (A). water, and (B). RNA synthesized from a positive pool of cDNA containing 20 clones. Ca^{++} mobilization was measured by spectrofluorometer as described in the text. The spikes in the traces were caused by opening of the shutter.

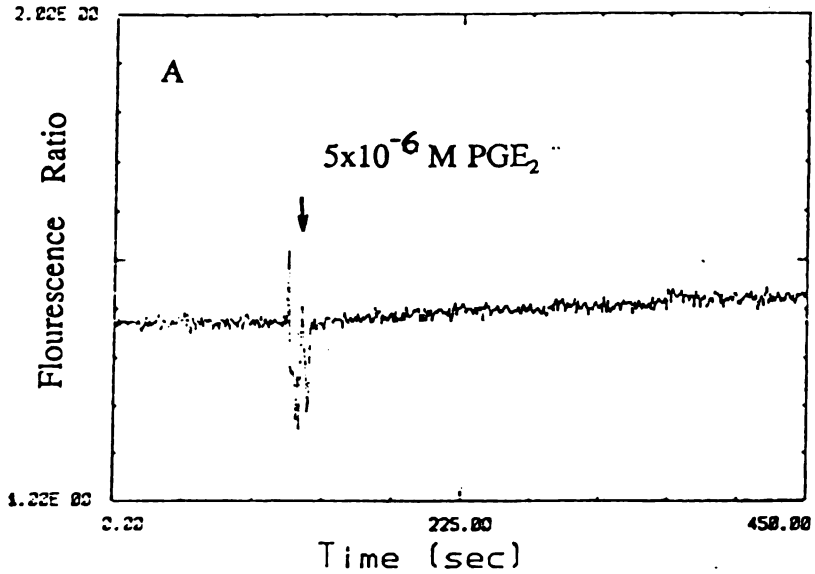
A
5x10⁻⁶ M PGE₂
Flourescence Ratio
225.00
450.00
Time (sec)

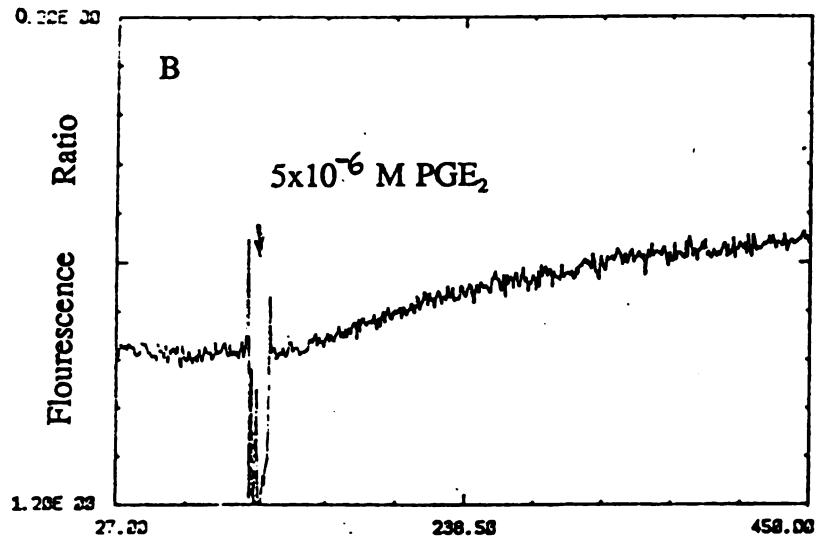
B
5x10⁻⁶ M PGE₂
Flourescence Ratio
450.00

Figure 3. (A). The SPE I fragment from lambda ZAP-GING containing SP6 and T7 promoters at the two ends of the cDNA. (B). Agarose gel of RNA transcripts from the SPE I fragment. Lane 1, synthesized by T7 polymerase; Lane 2, synthesized by SP6 polymerase.

A

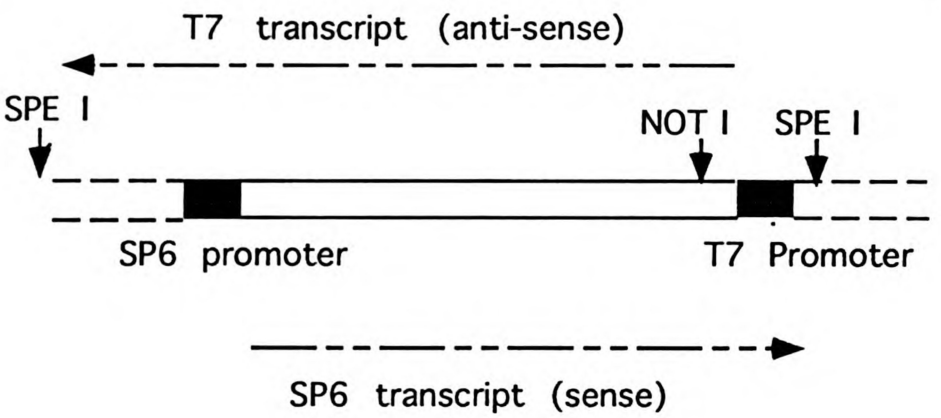
T7 transcript (anti-sense)
SPE I
NOT I
SPE I
SP6 promoter
T7 Promoter
SP6 transcript (sense)

B

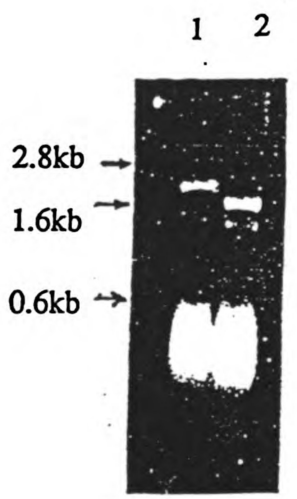
1
2
2.8kb
1.6kb
0.6kb

Figure 4. Traces of Ca^{++} mobilization in response to PGE_2 in oocytes injected with (A). transcripts synthesized by SP6 polymerase (G_+), and (B). transcripts synthesized by T7 polymerase (G_-). Ca^{++} mobilization was measured by spectrofluorometer as described in the text.

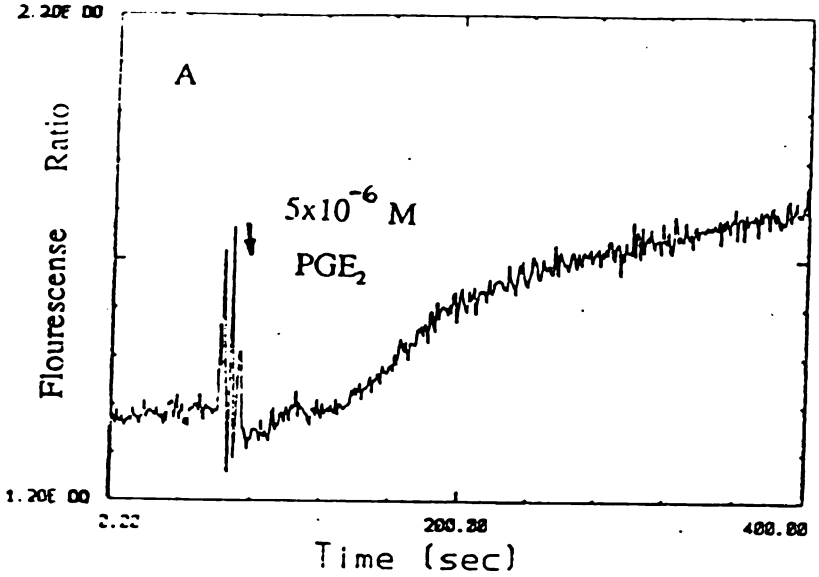
A
Flourescense Ratio
5x10^{-6} M
PGE$_2$
Time (sec)

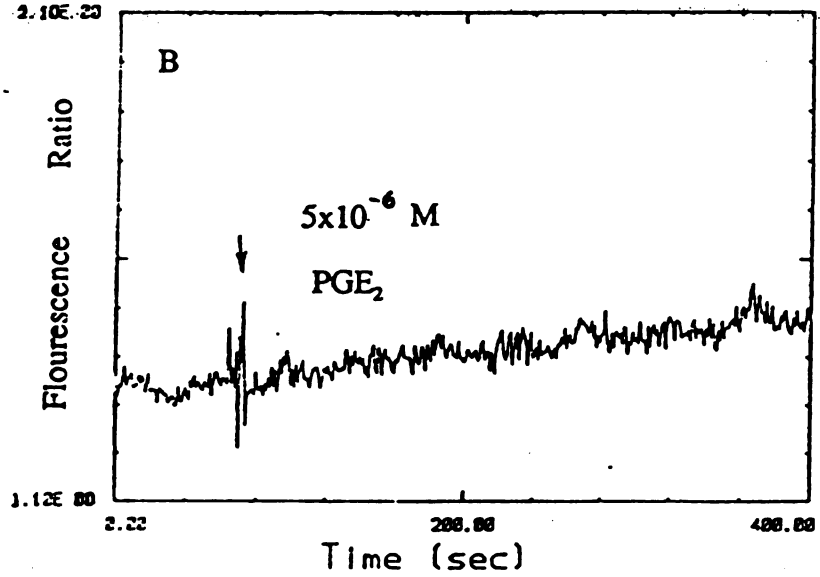
B
Flourescence Ratio
5x10^{-6} M
PGE$_2$
Time (sec)

Figure 5. The nucleotide sequence of GING.

```
   1  CAGTGAATTC CGGACGAAAT GGTGGAATCA ATGAAGAAAG TAGCAGGGAT
  51  GGACGTGGAG CTGACAGTTG AAGAACGAAA CCTTTTATCT GTTGCATATA
 101  AAAATGTGAT TGGAGCCAGA AGAGCATCCT GGAGAATAAT CAGCAGCATT
 151  GAACAGAAGG AAGAAAACAA GGGAGGAGAG GACAAATTAA AGATGATTCG
 201  GGAGTACCGG CAAATGGTTG AAACTGAGCT CAAGTTAATC TGTTGTGACA
 251  TTCTGGATGT ACTGGACAAA CACCTCATTC CAGCAGCTAA CACTGGCGAG
 301  TCCAAGGTTT TCTATTATAA AATGAAAGGG GACTACCACA GGTATCTGGC
 351  TGAGTTTGCC ACAGGAAATG ACAGGAAGGA GGCAGCAGAG AACAGCCTCG
 401  TGGCTTACAA AGCTGCTAGT GACATTGCGA TGACAGAACT TCCTCCAACG
 451  CACCCCATTC GTTTAGGTCT TGCTCTCAAC TTTTCCGTAT TCTACTATGA
 501  AATTCTTAAT TCCCCCGACC GTGCCTGCAG GTTGGCAAAA GCAGCTTTTG
 551  ATGACGCAAT TGCAGAACTG GACACGCTGA GTGAAGAAAG CTATAAGGAC
 601  TCTACGCTCA TCATGCAGCT GCTACGTGAT AACCTGACGC TGTGGACCTC
 651  AGACATGCAG GGTGATGGTG AAGAGCAGAA TAAAGAAGCG CTGCAGGATG
 701  TGGAAGATGA GAATCAGTGA GACGAAATAA AAGCCAACAA GAGAAACCAT
 751  CTCTGACTAC CCCTTCCCCC CCTCCCCTTG GAAGTTCCCC ATTGTCACTG
 801  AGAACCACCA AATTTGACTT TCACATTTGG TCTCAGAATT TAGGTTCCTG
 851  CCCTGTTGTT TTTCTTTCTT TTTCTTTTTT TTTTTTCTCC CCTCCCCTTT
 901  TTTAAAACAA ACAAACAAAC AAACAGTTTT CAGAAGTTCT TAAGGCAAGA
 951  GTGAATTTCT GTGGATTTTA CTGGTCCAGC TTTAGGTTCT TTACGACACT
1001  AACAGGACTG CATAGAGGCT TTTTCAGCAT TACTGTATTG TCTCCGGCCA
1051  CACTGGCAAG ATCATCATTA GAAATGGAAA TGACATTTGA AAGCCATTAG
1101  ACTTCTAGGT GATGCATCTA AGAAAGATTA ATCACACAAT AGAGGCATAT
1151  GCGCTGTCAT TTTTCCTTTT TTTAATTGTT AAATTGAATT TTATACCAAT
1201  GTTTAAACTT AAATTGGGTG TTAGCTTGAG GTGTTTTGGG GGAGTTTGTT
1251  GTAATGGTTT TGCTGTAAAC TGTGTTTGGA ACTCTGCTGA AGTGTTGCTG
1301  AAAAGCATGG TGCTGGTAAC AGTTCAACAA TCCGTGGCTG CTCATTCTTG
1351  CCGACTCCTC CCCCTCTGAA GCAGGTTAGC ATTGAAGGTG GTATGGAAGC
1401  CTGCATGCGT GTTCAACTCT GTTCCTCCTC CCTCCTCCTC GGCCTCCCTC
1451  CTCCCCTCCT TCGCTCGCTC AACCTCTTTT GTTCAGTACG TGTAACTTGA
1501  AGCTAATTTG TACTACTGGA TATCTGACTG GAGCCGCAGG TACAGATCTG
1551  TATTGTTCTT ACTGAAACAC AGCATGGAAT TAACATTAAA CTTAAATAAA
1601  ACAAACCTAA ATTAAAAATG CCAAAAAAAA AAAAAGCGGC CGCCATCGGA
```

Figure 6. (A). The predicted amino acid sequence of the longest open reading frame of GING. (B). Hydropathicity profile of GING. The averaged hydropathicity index of a nonadecapeptide composed of amino acids residue i-9 to i+9 is plotted against i, and i represents amino acid number.

A.

```
  1  MVESMKKVAG MDVELTVEER NLLSVAYKNV IGARRASWRI ISSIEQKEEN
 51  KGGEDKLKMI REYRQMVETE LKLICCDILD VLDKHLIPAA NTGESKVFYY
101  KMKGDYHRYL AEFATGNDRK EAAENSLVAY KAASDIAMTE LPPTHPIRLG
151  LALNFSVFYY EILNSPDRAC RLAKAAFDDA IAELDTLSEE SYKDSTLIMQ
201  LLRDNLTLWT SDMQGDGEEQ NKEALQDVED ENQ
```

B.

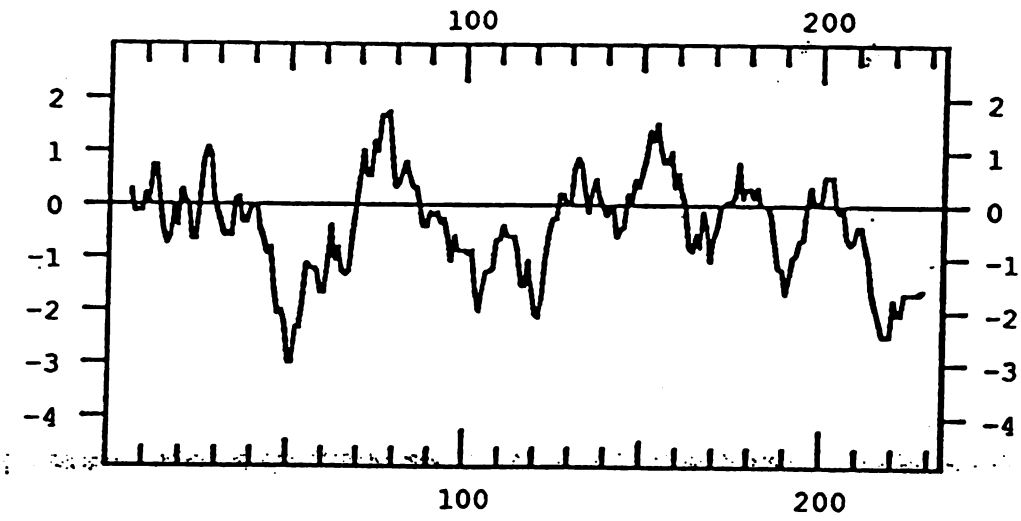

Figure 7. Alignment of the amino acid sequence of bovine 14-3-3 protein (top) and GING protein (bottom). Pairs of identical residues are connected with two dots. Pairs of similar residues are connected with one dot.

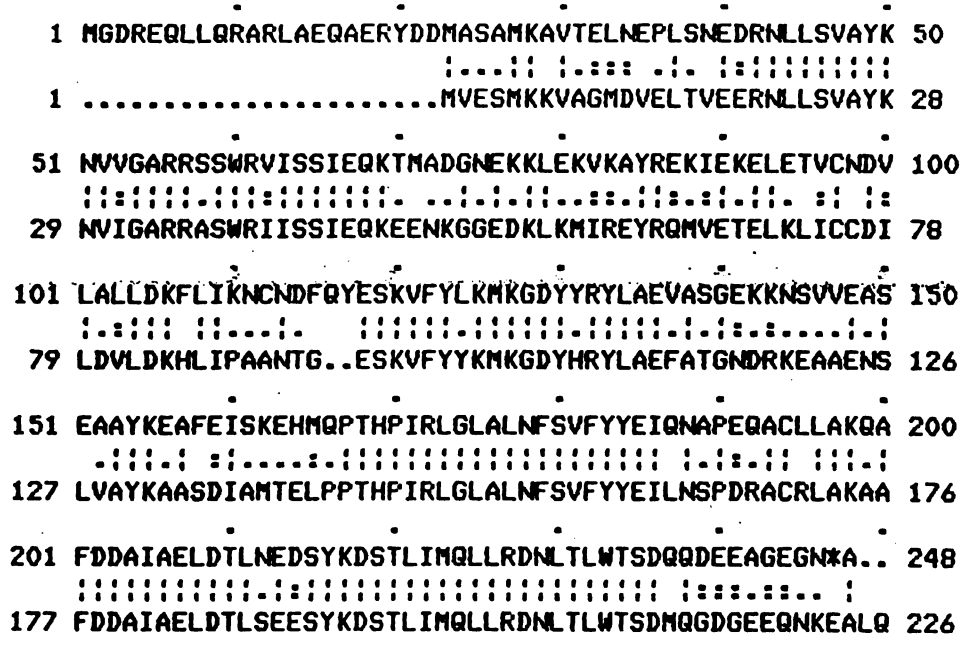

Figure 8. Northern blot of ^{32}P labeled GING hybridized with poly(A)$^+$ RNA isolated from lane 1: NIH 3T3 cells; lane 2: NIH 3T3 cells treated with 1 mM aspirin for overnight. 5-10 μg mRNA were used for each lane. The full-length fragment of GING was used as the probe.

3T3
3T3/aspirin
2.0 Kb

Figure 9. ^{35}S-Met labeled products translated *in vitro* from RNAs by a rabbit reticulocyte lysate system. Each RNA was translated in the presence (indicated by "+") or absence (indicated by "-") of microsomal membrane. Lane 1, no RNA; lanes 2 and 3, Brome Mosaic Virus RNA (BMV); lanes 4 and 5, GING RNA; lanes 6 and 7, α-factor RNA; lane 8 and 9, β-lactamase RNA.

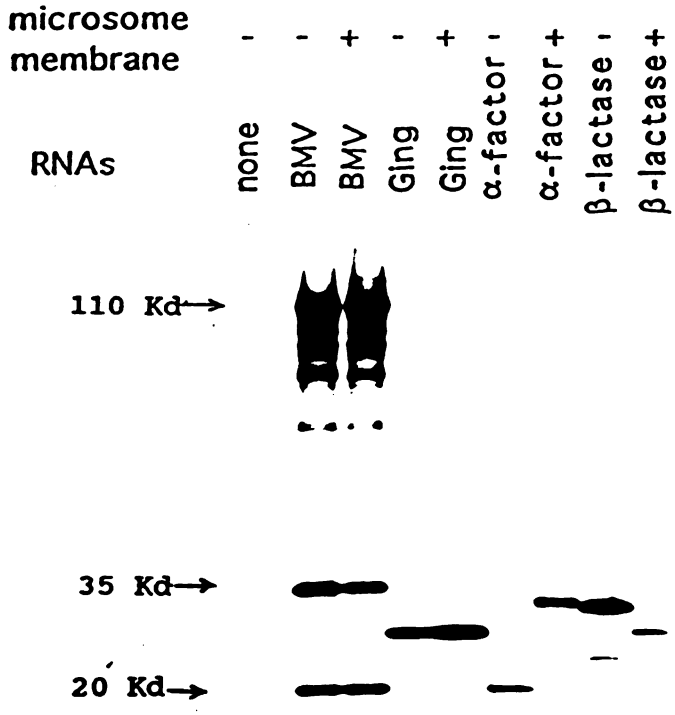
microsome membrane
- - + - + - + -
RNAs
none BMV BMV Ging Ging α-factor α-factor β-lactase β-lactase
110 Kd
35 Kd
20 Kd

Figure 10. Plasmids containing GING and a cDNA for the 5-HT_1 serotonin receptor. G(+): GING was inserted into pSVT7 with the transcription start site downstream of SV40 promoter. G(-): GING was inserted into pSVT7 in the orientation opposite to that of G(+). ST(+): cDNA for 5-HT_1 receptor was inserted into pSVT7 with the transcription start site downstream of SV40 promoter.

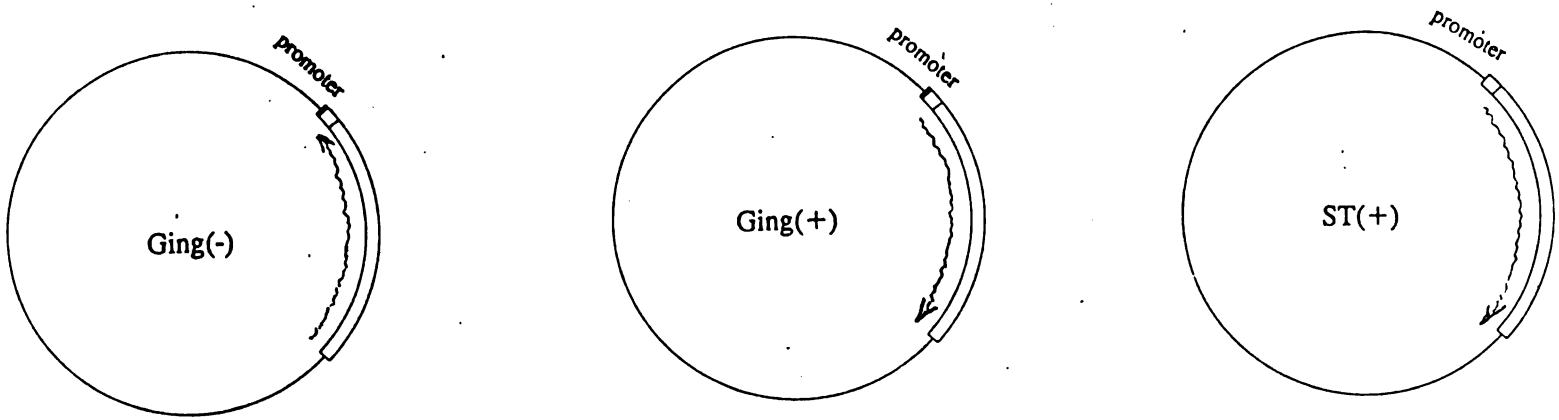
promoter
Ging(-)
promoter
Ging(+)
promoter
ST(+)

Figure 11. Traces of Ca^{++} mobilization in response to agonists by transfected COS-1 cells. (A). G(-) transfected cells challenged by 10^{-5} M serotonin (ST) and 10^{-5} M bradykinin (BK) consecutively. (B). ST(+) transfected cells challenged by 10^{-5} M ST. (C). G(-) transfected cells challenged by 10^{-5} M PGE_2 and 10^{-5} M BK consecutively. (D). G(+) transfected cells challenged by 10^{-5} M PGE_2 and 10^{-5} M BK consecutively. Ca^{++} mobilization was measured at the single cell level using an interactive laser cytometer as described in the text. Each panel represents traces of cells from one scanned field.

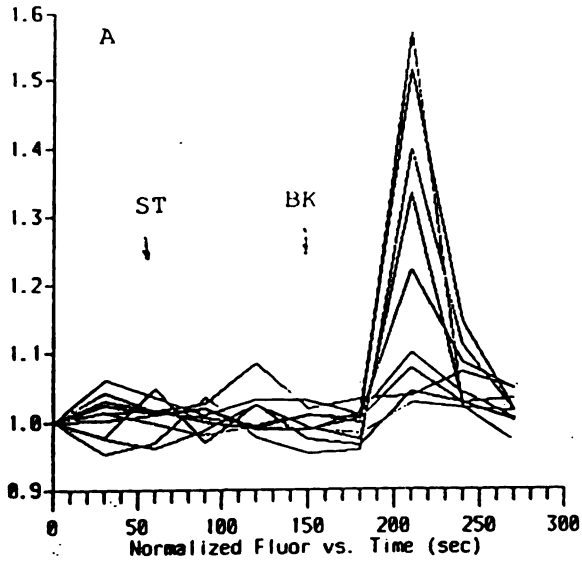
A
ST
BK
1.6
1.5
1.4
1.3
1.2
1.1
1.0
0.9
0 50 100 150 200 250 300
Normalized Fluor vs. Time (sec)

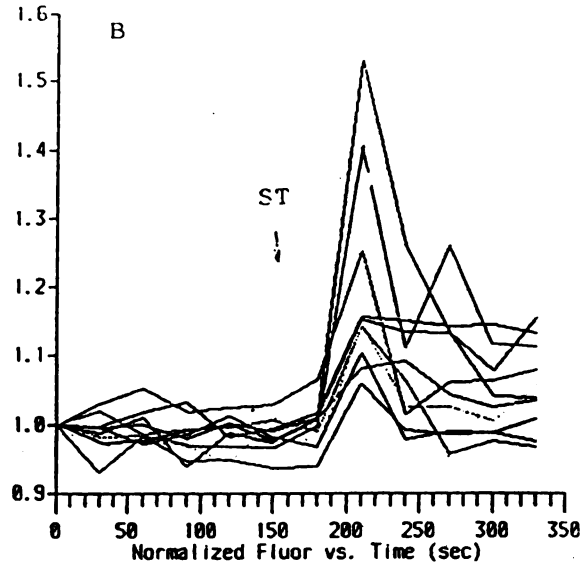
B
ST
1.6
1.5
1.4
1.3
1.2
1.1
1.0
0.9
0 50 100 150 200 250 300 350
Normalized Fluor vs. Time (sec)

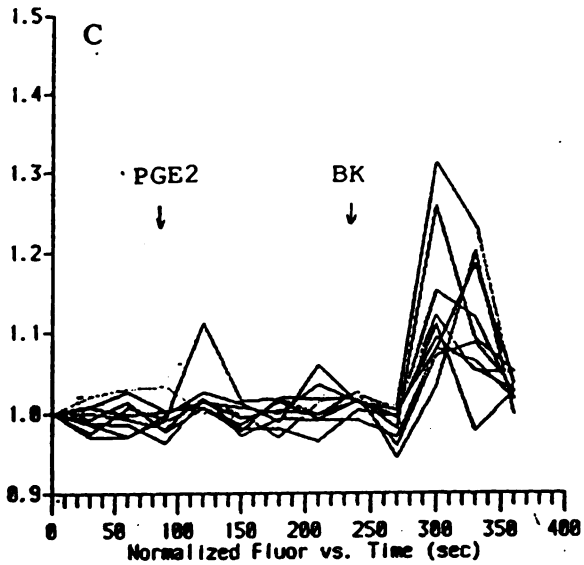
C
PGE2
BK
1.5
1.4
1.3
1.2
1.1
1.0
0.9
0 50 100 150 200 250 300 350 400
Normalized Fluor vs. Time (sec)

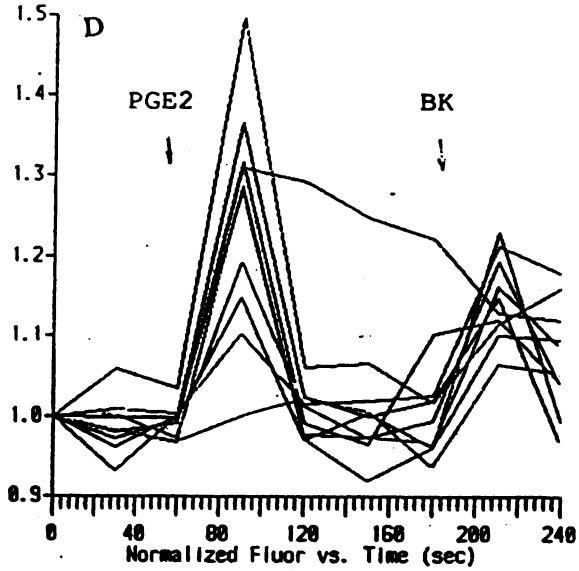
D
PGE2
BK
1.5
1.4
1.3
1.2
1.1
1.0
0.9
0 40 80 120 160 200 240
Normalized Fluor vs. Time (sec)

Table 4. Ca^{++} mobilization in response to PGE_2 and serotonin in transfected COS-1 cells. COS-1 cells were transfected with plasmids G(-), G(+) or ST(+) as described in the text. After incubating at 37 degrees for 40-48 hours, cells were loaded with 10 μM fluo-3/AM and examined for increases in $[Ca^{++}]_i$ when challenged by 10 μM PGE_2 or serotonin. Cells with $\geq$ 10% increases of fluorescence intensity were defined as responsive cells. n is the number of cells examined in five experiments for G(-), G(+) transfected cells, and in three of the five experiments for ST(+) transfected cells. Results were expressed as percentage of cells that respond (mean$\pm$S.E.).

	PGE_2	Serotonin	
GING(-)	7$\pm$ 1%	10$\pm$ 2%	n=413
GING(+)	32$\pm$ 4%	N.D.	n=409
ST(+)	N.D.	41$\pm$ 1%	n=172

Figure 12. Formation of inositol phosphates (IPs) in response to PGE_2 and serotonin (ST) in G(-), G(+) and ST(+) transfected COS-1 cells. IPs formation was measured as described in the text after transfected cells were stimulated with 10^{-5} M agonists for 30 min. The results are expressed as percent increase of in total IPs versus control cells treated with vehicle alone.

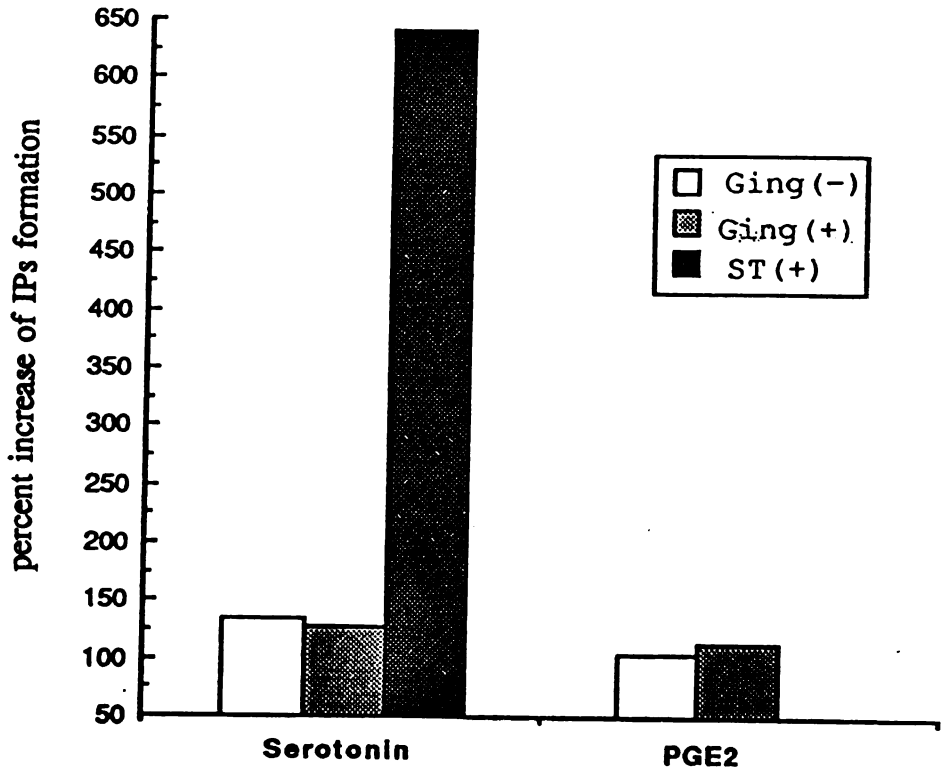
percent increase of IPs formation
650
600
550
500
450
400
350
300
250
200
150
100
50
Ging (-)
Ging (+)
ST (+)
Serotonin
PGE2

Figure 13. The effect of GING protein on IPs formation in response to serotonin in ST(+) and G(-)/G(+) cotransfected cells. COS-1 cells were cotransfected with 5 μg G(-) and 5 μg ST(+) or 5 μg G(+) and 5 μg ST(+) as described in the text. Total IPs formation was measured as described after transfected cells were stimulated with the indicated concentrations of serotonin for 30 min.

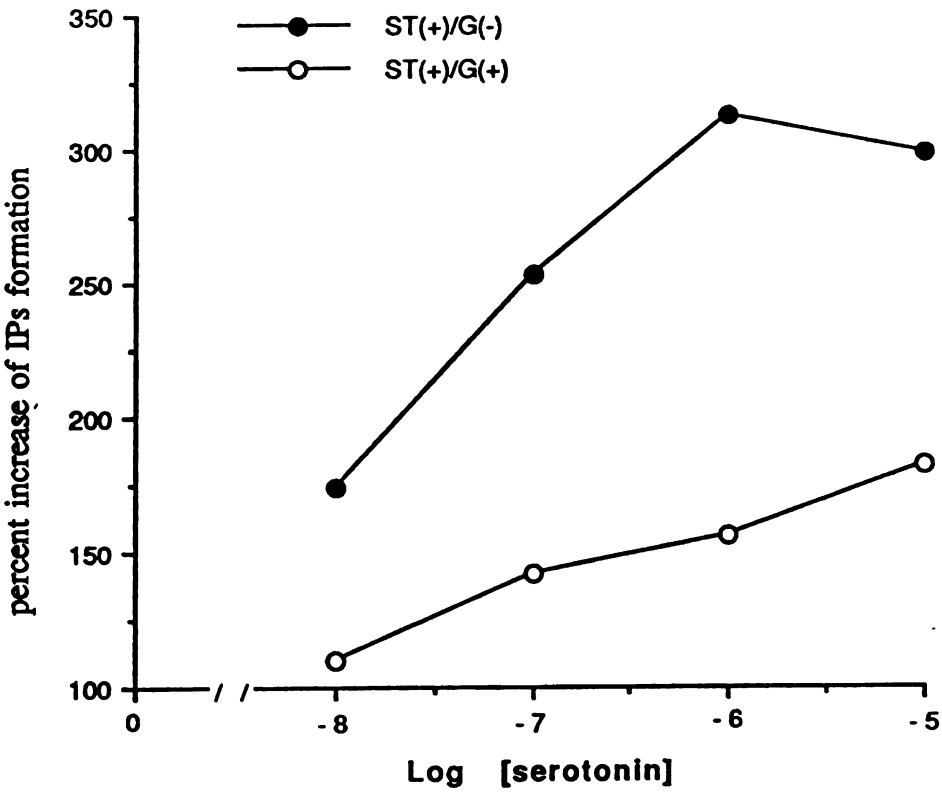
ST(+)/G(-)
ST(+)/G(+)
percent increase of IPs formation
350
300
250
200
150
100
0
-8
-7
-6
-5
Log [serotonin]

DISCUSSION

Xenopus oocytes have been extensively used for efficient translation of foreign mRNAs, including mRNAs encoding receptors and ion channels (10, 11). The *de novo* synthesis of proteins from their mRNAs generate biochemically functional end products, which can be detected by various biochemical and electrophysiological methods. This makes the oocyte an excellent system for expression cloning.

In attempting to clone a receptor for PGE_2 with this system, we used the *Xenopus* oocyte system and employed Ca^{++} mobilization as our functional assay. We obtained a clone which does not encode a typical G protein-linked receptor, but rather a cytosolic protein belonging to the family of 14-3-3 proteins. PGE_2 is an autacoid that elicits effects by interacting with membrane receptors, triggering a series of biochemical events. The fact that GING protein is not a receptor suggests that there exist an endogenous PGE_2 receptor in oocytes and that GING can potentiate a downstream effect of receptor activation leading to an increase of $[Ca^{++}]_i$.

In fact, a PGE receptor coupled to activation of adenylate cyclase has been reported to be present in the membranes of follicular cells that surround the oocyte (12). There exist gap junction contacts between oocyte and

follicular cells that allow passage of some molecules (13). It was shown that K^+ channels can be activated by PGE_2 in a cAMP-mediated manner (12), indicating that PGE_2 stimulates an increase in cAMP in follicular cells, which then leads to phosphorylation of the K^+ channels. Phosphorylation of enzymes or ion channels usually involves more than one type of protein kinase, including cAMP-dependent protein kinase, Ca^{++}/phospholipid-dependent protein kinase, and Ca^{++}/calmodulin-dependent protein kinase type II.

14-3-3 protein was first isolated by Grasso and Perez (14) from bovine brain as a "brain-specific" protein (12). Later, Boston et al. (15,16) purified the human homolog of the bovine 14-3-3 protein, and localized it to neurons in the human cerebral cortex. Using a radioimmunoassay, they showed that although human brain has the highest concentration of 14-3-3, other tissues also synthesized considerable amounts of this protein (16). No biological function had been assigned to the 14-3-3 protein until Ichimura et al.(17) isolated a group of bovine 14-3-3 proteins and cloned the cDNA for the η chain from a bovine cerebellum cDNA library. They demonstrated that the purified η chain could activate tyrosine and tryptophan hydroxylase activity *in vitro*, in the presence of Ca^{++}/calmodulin-dependent protein kinase II. Later, they found that the distribution of 14-3-3 proteins in vertebrate and bovine tissues correlates with the distribution of Ca^{++}-

dependent protein kinases (18). More recently, Alastair et al.(19) isolated a group of acidic proteins from sheep brain and found that these proteins inhibit Ca^{++}/phospholipid-dependent protein kinase C. These acidic proteins were found to be homologous to the bovine 14-3-3 proteins. Last year, an intracellular phospholipase A_2 was cloned from a human placental cDNA library; the phospholipase A_2 was also shown to be a member of the 14-3-3 family (20). Obviously, this family of proteins is widely involved in various cellular activities. Now, our discovery of an effect of a 14-3-3 protein on Ca^{++} mobilization in response to PGE_2 adds another example of a potential the role for 14-3-3 proteins. The observation by Ichimura et al.(18) that the distribution of 14-3-3 proteins correlates with the distribution of Ca^{++}-dependent protein kinases suggested that 14-3-3 proteins may participate in processes involving Ca^{++}-dependent protein kinases. Based on this observation and the finding that PGE_2 increases cAMP formation in follicular cells of oocytes, one explanation for the effect of the GING protein in our system is that GING activates a Ca^{++}/phospholipid-dependent protein kinase, which coupled with the effect of PGE_2 to stimulate cAMP-dependent protein kinase, leading to the phosphorylation and activation of certain components (i.e. enzymes or Ca^{++} channels) involved in the pathway for the release of intracellular Ca^{++} or influx of extracellular Ca^{++}.

The last question I would like to discuss here is the oocyte system used for expression cloning. Since GING protein is not a receptor that initiates the response to PGE_2, but rather is involved downstream of the receptor to potentiate the response, its effect will largely depend on the level of endogenous receptor. If the level of endogenous receptor is low, there will not be enough receptor to activate the pathway to initiate the response, thus no effect of GING protein will be observed. According to this assumption, the poor reproducibility of functional assay in oocytes encountered in our cloning work may be due to the large variations of levels of endogenous receptors in different batches of oocytes. In fact, background responses were observed in 15-20% of oocytes not injected with RNA. Accordingly, the responses to PGE_2 between control oocytes and RNA-injected oocytes within those batches could not be resolved due to the limited sensitivity of the system. The situation is similar when GING is *in vitro* expressed in mammalian cells. The type of cells used for expression of GING has to possess a certain level of endogenous receptors so that the potentiating effect of GING protein in response to the corresponding hormones could be observed. Cos-1 cells used in our case for GING expression seems to possess a PGE receptor coupled to adynylate cyclase, too, since a small backgrond increase of cAMP can be observed when stimulated with 10^{-5} M PGE_2 (21). The presence of this native receptor may account for the potentiating effect of

GING on Ca^{++} mobilization in response to PGE_2 observed in G(+) transfected COS-1 cells. It is possible, therefore, that the lack of responses to PGE_2 in some batches of G(+) transfected cells is due to the lack of enough endougenous PGE receptors mediating cAMP formation.

REFERENCE

1. Shorr, R.G., Lefkowitz, R. J., and Caron, M.G. (1981) J. Biol. Chem. 256, 5820-5826.
2. Dixon, R.A.F. et al. (1986) Nature 321, 75-79.
3. Masu, Y., Nakayama, K., Tamaki, H., Harada, Y., Kuno, M., and Nakanishi, S. (1987) Nature 329, 836-838.
4. Julius, D., MacDermott, A.B., Axel, R., Jessell, T.M. (1988) Science 241, 558-564.
5. Maniatis, T., Fritch E.F., Sambrook, J. (1982) In: Molecular Cloning, Cold Spring Harbor Laboratory, Cold Spring Harbor, NY.
6. Grynkiewicz, G., Poenie, M., Tsien, R.Y., (1985) J. Biol. Chem. 260, 3440-3450.
7. Sanger, F., Nicklen, S. and Coulson, A.R., (1977) Proc. Natl. Acad. Sci. USA 74, 5463-5467.
8. Shimokawa, T., Smith, W.L. (1992) J. Biol. Chem. 267, 12387-12392.
9. Juppner, H. et al. (1991) Science 254, 1024-1026.
10. Meyerhof, W., Morley, S., Schwarz, J., Richiter, D. (1988) Proc. Natl. Acad. Sci. USA 85, 714-717.
11. Gundersen, C.B., Miledi, R., Parker, I. (1984) Nature 308, 421-424.
12. Mori, K., Oka, S., Tani, A., Ito, S., Watanabe Y. (1989)

Biolchem. and Biophy. Res. Comm. 162, 1534-1540.

13. Woodward, R.M., Miledi, R. (1987) Proc. Natl. Acad. Sci. USA 84, 4135-4139.
14. Grasso, A., Roda, G., Hogue-Angeletti R.A., Moore, B.W., and Perez V.J. (1977) Brain Res. 124, 497-507.
15. Boston, P.F., Jackson, P., Kynoch, P.A.M., Thompson, R.J. (1982) J. Neurochem. 38, 1466-1474.
16. Boston, P.F., Jackson, P., Thompson, R.J. (1982) J. Neurochem. 38, 1475-1482.
17. Ichimura,T., Isobe, T., Okuyama, T., Takahashi, N., Araki, K., Kuwano, R. and Takahashi Y. (1988) Proc. Natl. Acad. Sci. USA 85, 7084-7088.
18. Ichimura T., Sugano, H., Kuwano, R., Sunaya T., Okuyama T. and Isobe T. (1990) J. Neurochem. 56, 1449-1451.
19. Aitken, A., Ellis, C.A., Harris, A., Sellers, L.A., Toker. A. (1990) Nature 344, 594.
20. Zupan, L.A., Steffens, D.L., Berry, C.A., Landt, M., Gross, R.W. (1992) J. Biol. Chem. 267, 8707-8710.
21. Honda, A., Sugimoto, Y., Namba, T., Wataba, A., Irie, A., Negishi, M., Narumiya, S. and Ichikawa, A. (1993) J. Biol. Chem. 268, 7759-7762.